

# Report of the Workshop on BEV/NUCLEON COLLISIONS OF HEAVY IONS - HOW AND WHY

November 29-December 1, 1974

Bear Mountain, New York

Supported by  
NATIONAL SCIENCE FOUNDATION  
and  
NEVIS LABORATORIES, COLUMBIA UNIVERSITY

Organizing Committee  
A. KERMAN, L. LEDERMAN, T.D. LEE, M. RUDERMAN, J. WENESER

Scientific Reporters  
LAWRENCE E. PRICE, JAMES P. VARY

PUBLISHED BY

BROOKHAVEN NATIONAL LABORATORY  
ASSOCIATED UNIVERSITIES, INC.

UNDER CONTRACT NO. E(30-1)-16 WITH THE  
UNITED STATES ENERGY RESEARCH AND DEVELOPMENT ADMINISTRATION

## N O T I C E

This report was prepared as an account of work sponsored by the United States Government. Neither the United States nor the United States Energy Research and Development Administration, nor any of their employees, nor any of their contractors, subcontractors, or their employees, makes any warranty, express or implied, or assumes any legal liability or responsibility for the accuracy, completeness or usefulness of any information, apparatus, product or process disclosed, or represents that its use would not infringe privately owned rights.

Printed in the United States of America  
Available from  
National Technical Information Service  
U.S. Department of Commerce  
5285 Port Royal Road  
Springfield, VA 22161  
Price: Printed Copy, Domestic \$4.75;  
Foreign \$7.25; Microfiche \$1.45

October 1975

500 copies

## INTRODUCTION AND SUMMARY

The history of physics teaches us that profound revolutions arise from a gradual perception that certain observations can be accommodated only by radical departures from current thinking. This Workshop addressed itself to the intriguing question of the possible existence of a nuclear world quite different from the one we have learned to accept as familiar and stable.

T.D. Lee and Gian-Carlo Wick brought up the question by pointing out that, with reasonable assumptions on the form of the mediating mesonic interactions between nucleons, one is led to the prediction of a superdense phase of nuclear substance that either is stable or has an appreciable isomeric lifetime.

They were led to this question by a desire to "do something" about the apparent violations of discrete symmetries which have been buffeting particle physics over the past 15 or so years. An enlarged system – a complex vacuum – could restore the missing symmetry, and it was as a means of exciting the new variables that collisions between large amounts of nuclear matter were suggested.

The interest had already been well advanced in collisions between heavy nuclei as a means of studying the modes of motion of large masses of nuclear matter. Astrophysicists were concerned with the properties of neutron stars. The possibility that superdense matter might be produced in very energetic heavy-ion collisions provided a new interest.

We recognized in these problems an ideal opportunity to break conventional divisions and collect together particle and nuclear theorists, astrophysicists, chemists, nuclear and particle experimentalists, accelerator experts, and generally wise men.

The conference lasted two days. Its success is only partially conveyed in this report. Personal interactions were strong. It is, of course, our hope that future experimental and theoretical advances will be traceable to the subtle stimulation provided at Bear Mountain in November 1974.

The discussions on the possibility of achieving the abnormal phase in nuclear matter may perhaps be summarized by noting that the parameters describing this phase are very far from the ones operating in ordinary nuclei. It is therefore not easy to extrapolate from the present state of nuclear knowledge; instead it is useful to ask whether there are any signs or tokens hinting at the final answer in the regions nearer to normal nuclear matter.

The possibility of pion condensates in near-normal nuclear matter as well as in the regions of high density reached in the astrophysical domain has been the subject of speculative theoretical calculation. The critical review by Gerry Brown, bringing to bear the methods and ideas of nuclear many-body theory, indicates that such pion condensates cannot occur at densities near normal. Neutron star densities may well reach values some 10 times normal. As pointed up in the talks of Mal Ruderman and of Ray Sawyer, the equations of state and some more detailed properties may well be sensitive to pion condensates, and this is an area being given active thought. There is, however, no definitive conclusion at this time.

Relativistic heavy ions may well provide the means in the laboratory to study high density nuclear phenomena. Such work is now beginning, based on the capa-

bilities of the Bevalac as well as on the means provided by a Higher Authority in cosmic rays. These explorations, described and analyzed in the papers of Harry Heckman and of Herman Feshbach, show characteristic phenomena that do not appear, however, to be outside the bounds of present nuclear knowledge. Relativistic heavy-ion interactions will clearly form a field of study interesting in its own right as well as a particular tool for achieving abnormal conditions of nuclear matter. Walter Greiner discusses this latter aspect, and, on the basis of nuclear hydrodynamics, predicts shock-wave phenomena and the achievement of high densities.

Is it possible that superdense nuclei have been created somewhere in the process of evolution of the universe and survived to the present? John Schiffer describes a clever but negative experiment designed to show a characteristic signal of the natural presence in very small quantities of such creatures. Buford Price and Larry Price each describe early steps in accelerator-based investigations.

An ambitious program of calculation that would span both normal nuclear calculations and the very different superdense region is outlined by Arthur Kerman. A key ingredient in all thoughts on the existence of a superdense phase is the qualitative and quantitative form of the mesonic interaction with the nucleon. Can we read these out of the already familiar? Informal discussion throughout the Workshop meeting was concerned with different forms of this question. The answer that seemed to emerge from the meeting was "no," that the superdense region is just too far away, and only a direct assault promises a definitive answer. The most promising avenue appears to be via the collisions between energetic heavy ions and heavy targets.

Can the accelerator builders produce the means? Herman Grunder, Guisseppe Cocconi, Arie van Steenbergen, and Milt White all gave very positive indications.

Finally, absorbing glimpses of the applications of abnormal matter were given in a round table discussion.

LEON LEDERMAN  
JOSEPH WENESER

## CONTENTS

### Session I. CHAIRMAN: R. Serber

A Possible New Form of Matter at High Density.....	T.D. LEE	1
Nuclear Physics Questions Posed by Relativistic Heavy Ions.....	H. FESHBACH	13
Current Knowledge of the Interactions of Relativistic Heavy Ions.....	H.H. HECKMAN	14

### Session II. CHAIRMAN: J. Weneser

Pion Condensates.....	G.E. BROWN	18
Comments on Charged Pion Condensation in Dense Matter.....	G. BAYM	34
Nuclear Matter Calculations of Finite and Infinite Nuclear Systems From Relativistic Field Theory.....	A.K. KERMAN	36
On the Possibility of Nuclear Shock Waves in Relativistic Heavy-Ion Collisions.....	J. HOFMANN, H. STÖCKER, W. SCHEID, AND W. GREINER	39
Shock Waves in Colliding Nuclei.....	P. J. SIEMENS	48
Astrophysical Implications for Nuclear Interactions.....	M. RUDERMAN	50
Astrophysical Implications of Pion Condensation.....	R. SAWYER	52

### Session III. CHAIRMAN: L.M. Lederman

Round Table Discussion of Speculative Properties of Heavy Isomers, Abnormals, Superheavies, etc., and Their Applications.....		
.....O. CHAMBERLAIN, M. GOLDHABER, L.N. HAND, A. TURKEVICH, AND G.H. VINEYARD		59

### Session IV. CHAIRMAN: J.P. Schiffer

Search for Stable Strange Nuclei.....	J.P. SCHIFFER	61
Search for Ultradense Nuclei in Collisions of GeV/Nucleon Ar + Pb.....	P.B. PRICE	67
Ultrahigh Momentum Transfer Scattering of Protons by Heavy Nuclei.....	L.E. PRICE	71

### Session V. CHAIRMAN: H.G. Blosser

The Bevalac, a High-Energy Heavy-Ion Facility – Status and Outlook.....	H.A. GRUNDER	72
Developments at CERN.....	G. COCCONI	78
Heavy-Ion, $A > 200$ , Acceleration in the AGS.....	K. PRELAC AND A. VAN STEENBERGEN	79
The PPA as a Relativistic Heavy-Ion Accelerator.....	M.G. WHITE	86
Participants.....		91



# A Possible New Form of Matter at High Density\*

T.D. LEE

*Columbia University, New York, New York 10027*

## I. INTRODUCTION

In this talk, I would like to discuss some of my recent theoretical speculations, made in collaboration with Gian-Carlo Wick. Over the past year, we have tried to investigate the structure of the vacuum. It is through this investigation that the possibilities of vacuum excitation states and abnormal nuclear states have been suggested. Before coming to the main topic, whether or not there may be the possibility of a new form of matter at high density, perhaps I should first digress on questions related to the vacuum.

In physics, one defines the vacuum as the lowest energy state of the system. By definition, it has zero 4-momentum. In most quantum field-theoretic treatments, quite often the vacuum state is used only to enable us to perform the mathematical construct of a Hilbert space. From the vacuum state, we build the one-particle state, then the two-particle state, . . . ; hopefully, the resulting Hilbert space will eventually resemble our universe. From this approach, different vacuum state means different Hilbert space, and therefore different universe.

Nevertheless, one may ask: What is this vacuum state? Does it have complicated structure? If so, can a part of this structure be changed? Ever since the formulation of relativity, after the downfall of the classical aether concept, one learns that the vacuum is Lorentz invariant. At least, one knows that just running around and changing the reference system won't alter the vacuum. However, Lorentz invariance alone does not insure that the vacuum is necessarily simple. For example, the vacuum can be as complicated as the product or sum of any scalar field or other scalar object at the zero 4-momentum limit:

$$\text{vacuum} \sim \phi^n \quad \text{or} \quad (\bar{\psi}\psi)^m \quad \text{at} \quad k_\mu = 0. \quad (1)$$

From Dirac's hole theory, one knows that the vacuum, though Lorentz-invariant, can be rather complicated. That this complicated structure of the vacuum may in part be changeable is suggested by the large variety of broken symmetries, found especially over the past two decades.

If we consider symmetry quantum numbers such as the isospin  $\mathbf{I}$ , the strangeness  $S$ , the parity  $P$ , . . . , we find

$$\frac{d}{dt} \left\{ \begin{array}{c} \mathbf{I} \\ S \\ P \\ C \\ CP \\ \vdots \\ \vdots \end{array} \right\}_{\text{matter}} \neq 0. \quad (2)$$

---

\*This research was supported in part by the U.S. Atomic Energy Commission.

Since we are interested in the long wavelength limit of the field, the scalar field  $\phi(x)$  is used only as a phenomenological description. It can be any kind of 0+ resonance between particles. The details of its microscopic structure do not concern us, nor is the renormalizability an important factor. All we are interested in is that its zero 4 momentum limit exists; once such a limit exists, then the expectation value  $\langle \phi \rangle$  becomes automatically and inextricably connected to the description of the vacuum and the question of vacuum excitations.

In (9), we require the constant  $c > 0$  so that  $U$  has a lower bound, and  $a \geq \frac{1}{2}b^2/c > 0$  so that the absolute minimum of  $U$  is at  $\phi = 0$ , in accordance with our convention (5). Since we are interested only in a slowly varying field over a large volume, we may neglect both the surface energy and the energy due to  $(\partial\phi/\partial x_\mu)^2$ . Therefore, the classical description of  $\phi(x)$  should be a reasonably good approximation. The energy density of the field is then simply  $U(\phi)$ .

### A. Constant Source

Let us now introduce an external source  $J(x)$ . As a first example, we consider the simplest case that  $J$  is a constant inside a large volume  $\Omega$ , but zero outside. The energy of the system becomes

$$[U(\phi) + J\phi]\Omega.$$

The graphs in Figure 2 illustrate how in the lowest energy state, inside  $\Omega$

$$\bar{\phi} = \langle \phi(x) \rangle \quad (10)$$

can be changed under the influence of a constant  $J$ .

In case (i), as  $J$  increases, there is a critical value at which  $\bar{\phi}$  makes a sudden jump. Once a domain of an abnormal value of  $\bar{\phi}$  is created, if  $J$  is subsequently removed, in case (i),  $\bar{\phi}$  will return to 0; but in case (ii), depending on the magnitude of the abnormal value produced, even if  $J$  is removed  $\bar{\phi}$  may not return immediately to 0.

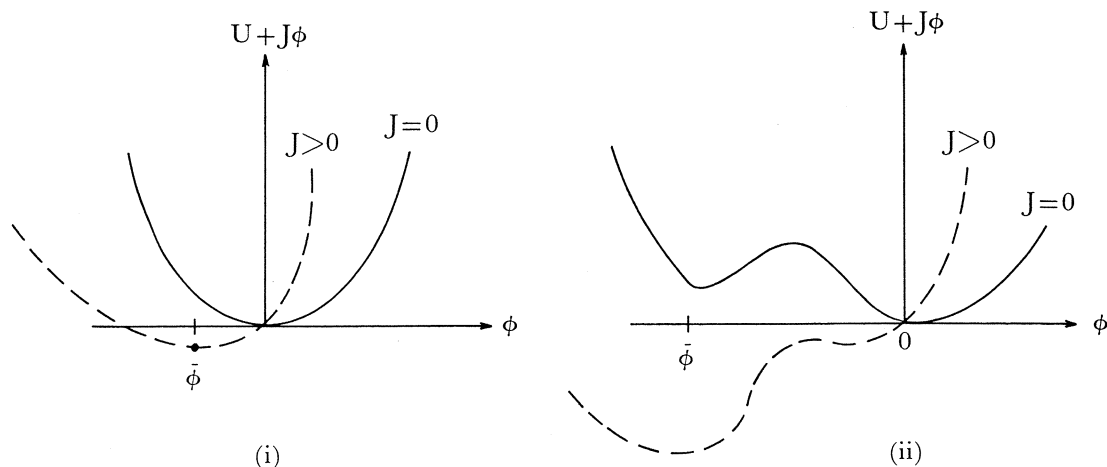


Figure 2.

## B. Matter Source

Let us consider the more realistic case that the source is not a constant, but consists of, say, some physical fermions, represented by a Dirac field  $\psi$ . (Of course, if one wishes, one can also use bosons instead of fermions.) For our later discussions on abnormal nuclear states,  $\psi$  is the nucleon field; for other purposes such as the “bag model,”  $\psi$  can be the quark field. The Lagrangian density becomes

$$\mathcal{L} = \mathcal{L}_\phi - \psi^\dagger \gamma_4 [\gamma_\mu (\partial/\partial x_\mu) + (m + g\phi)] \psi \quad (11)$$

where  $\mathcal{L}_\phi$  is given by (8),  $m$  is the mass of the free fermion, and  $g$  is the coupling constant. An important feature is that if  $\phi$  is a constant  $\neq 0$  over a large volume  $\Omega$ , then inside  $\Omega$  the effective mass of the fermion becomes

$$m_{\text{eff}} = m + g\bar{\phi}. \quad (12)$$

Thus, by measuring  $m_{\text{eff}}$ , one can detect whether there is any change in  $\bar{\phi}$ . In the above Lagrangian, so far as the fermion field is concerned, there is an equivalence between

$$m \rightarrow m + \delta m \quad \text{and} \quad \phi \rightarrow \phi - (\delta m/g). \quad (13)$$

Up to a point, this transformation resembles both the gauge invariance in electrodynamics

$$\psi \rightarrow e^{i\theta} \psi, \quad A_\mu \rightarrow A_\mu - \frac{1}{e} \frac{\partial \theta}{\partial x_\mu}, \quad (14)$$

and the equivalence between gravitation and acceleration in general relativity. However, in both electromagnetism and gravitation, because of the zero mass of photon and graviton we have exact symmetries. Here, because there is no spin 0 particle of zero mass, transformation (13) is not an exact symmetry in the physical world. (It would, of course, be disastrous if it were, since the inertia mass would then become a non-observable.) As we shall see, this transformation can be used to produce changes in  $m$  and  $\phi$ . Thereby, it may lead to a new form of matter at high density.

## III. ABNORMAL NUCLEAR STATES

Let the volume  $\Omega$  be filled with nucleons of density  $n$ ,

$$n \equiv \Omega^{-1} \int (\psi^\dagger \psi) d^3r. \quad (15)$$

As we shall see, if the nucleon density  $n$  is sufficiently high, the system may exist in an “abnormal nuclear state,” in which the effective nucleon mass becomes zero, or nearly zero (instead of the free nucleon mass  $m_N$ ). The simplest way to see why such an abnormal state may develop is to examine the quasi-classical solution.

Let us assume that the nucleons form a Fermi gas of a uniform density and  $\phi$  is a classical field. In such a quasi-classical treatment, the lowest energy state is one in which  $\phi$  is a constant and the Fermi gas is completely degenerate. The corresponding energy density  $\xi(n)$  is given by

$$\xi(n) = U(\phi) + \frac{2}{\pi^2} \int_0^{k_F} (k^2 + m_{\text{eff}}^2)^{1/2} k^2 dk \quad (16)$$

where  $m_{\text{eff}}$  is the effective mass of the nucleon, related to  $m_N \cong 940$  MeV by

$$m_{\text{eff}} = m_N + g\phi, \quad (17)$$

and  $k_F$  is the Fermi momentum given by

$$k_F = (3\pi^2 n/2)^{1/3}. \quad (18)$$

For simplicity, we assume the nuclear matter to be composed of half protons and half neutrons. We shall also assume  $\Omega$  to be sufficiently large that the surface energy can be neglected.

Throughout our discussion, we define the *normal nuclear state* to be one in which  $m_{\text{eff}} \cong m_N$  and the *abnormal nuclear state* to be one in which  $m_{\text{eff}} \cong 0$ . As  $n$  increases, the Fermi-sea contribution to the energy becomes increasingly more important. Thus, independent of the detailed form of  $U(\phi)$ , in the high-density limit one finds

$$\lim_{n \rightarrow \infty} \phi = - (m_N/g) \quad \text{and} \quad \lim_{n \rightarrow \infty} m_{\text{eff}} = 0; \quad (19)$$

i.e., the state becomes abnormal. On the other hand, in the low-density limit, because of (5), one must have

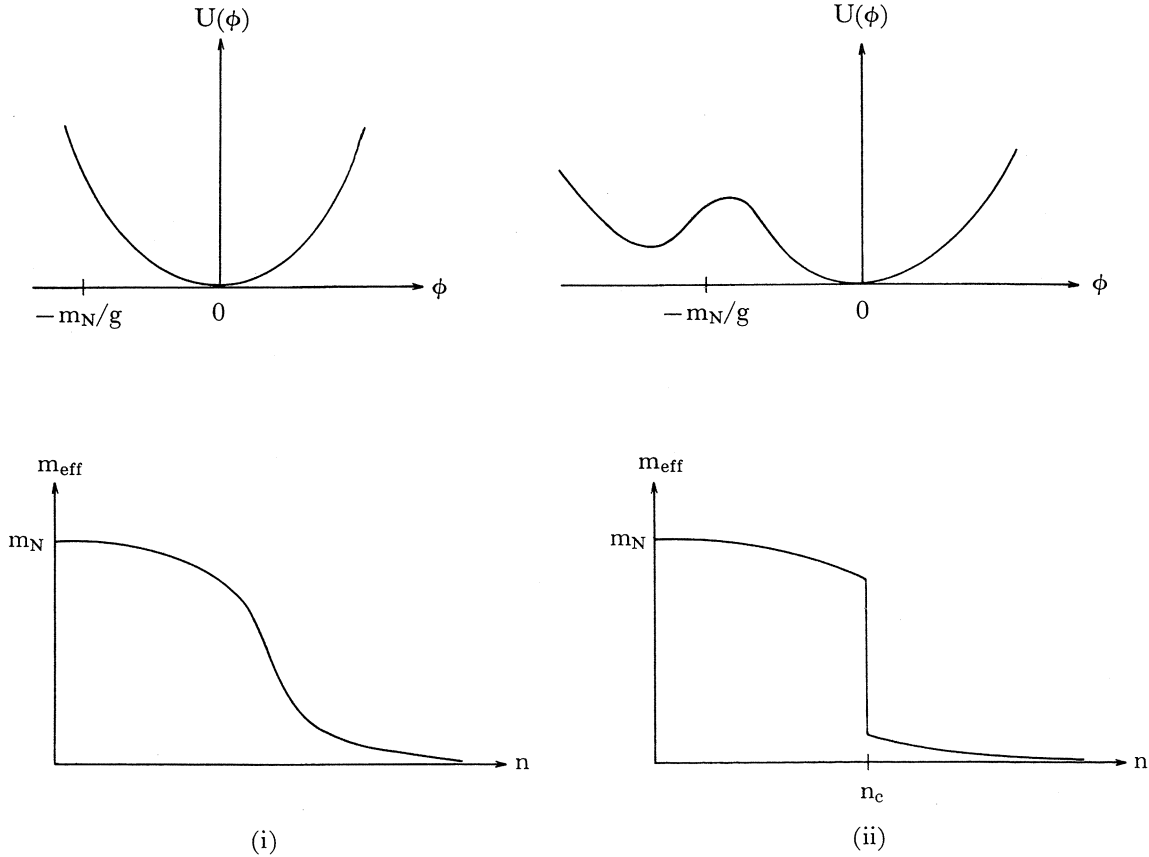


Figure 3.

$$\lim_{n \rightarrow 0} \phi = 0 \quad \text{and} \quad \lim_{n \rightarrow 0} m_{\text{eff}} = m_N; \quad (20)$$

i.e., the state is normal. As illustrated in Figure 3, depending on the parameters in the theory, the transition from the low-density "normal" solution ( $m_{\text{eff}} \approx m_N$ ) to the high-density "abnormal" solution ( $m_{\text{eff}} \approx 0$ ) may or may not be a continuous one. The mechanism of the transition is similar to that in the case of a constant  $J$  discussed before. There is however one important difference: because the nucleon energy depends only on  $(m_N + g\phi)^2$ , its minimum occurs at  $\phi = -m_N/g$ . Hence,  $\lim \phi = -m_N/g$  as  $n \rightarrow \infty$ , while in the case of a constant  $J$  one has  $\lim \phi = -\infty$  as  $J \rightarrow \infty$ .

#### IV. $\sigma$ -MODEL

A particularly interesting example of a discontinuous transition is the well-known  $\sigma$ -model. For a fairly wide range of the parameters, the critical density  $n_c$  for the transition is found to be approximately given by

$$n_c \approx 11.6 \left( \frac{m_\sigma}{m_N} \right)^2 \left( \frac{g^2}{4\pi} \right)^{-1} n_0 \quad (21)$$

where

$$n_0^{-1} = \frac{4}{3} \pi (1.2 \text{ fm})^3,$$

and  $m_\sigma$  is the  $\sigma$ -meson mass. In Figure 4, we map out the region in  $g^2/4\pi$  and  $m_\sigma$  for  $n_c \leq 2n_0$ .

At present, there are no reliable data on either  $m_\sigma$  or  $g^2$ . If we identify  $\sigma$  to be the broad  $2\pi$  resonance, then

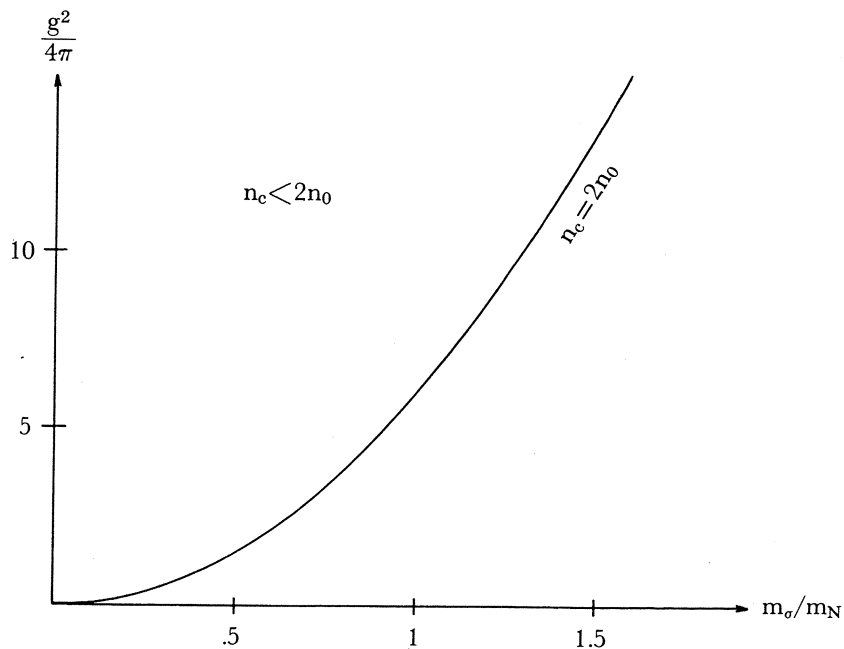


Figure 4.

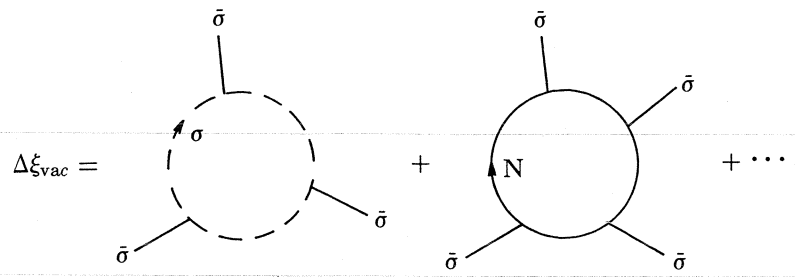


Figure 5.

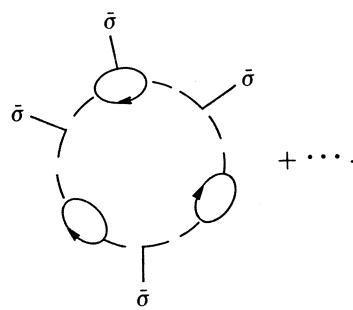


Figure 6.

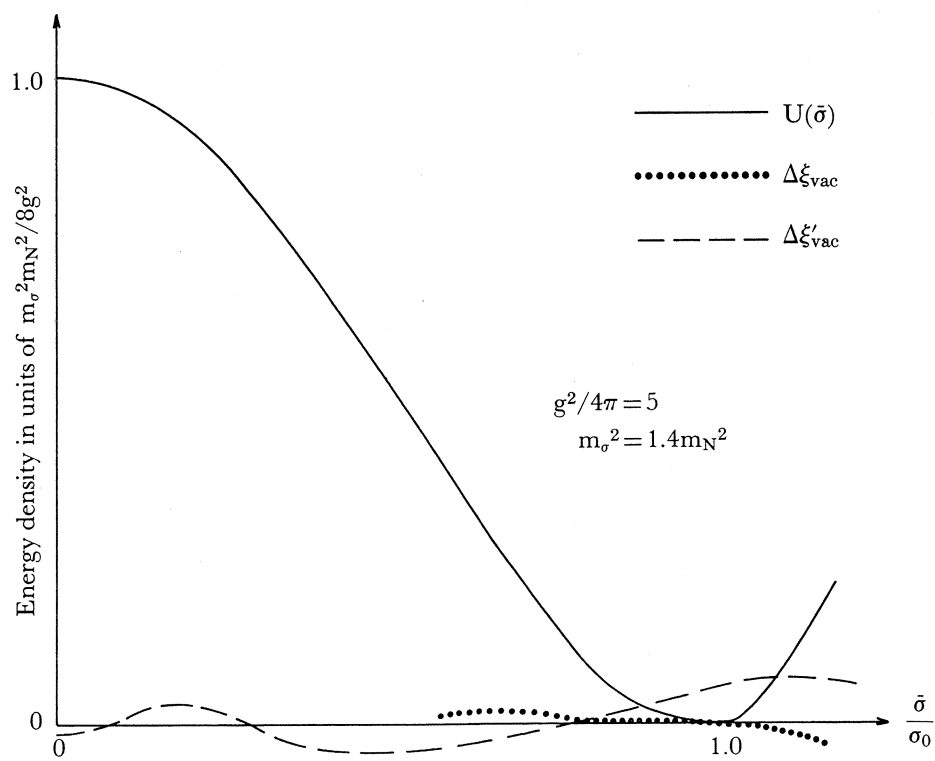


Figure 7.

$$m_\sigma \sim 700 \text{ MeV}. \quad (22)$$

Extensive calculations have been made in the literature to fit the central attractive part of the nuclear forces from such a  $2\pi$  exchange. Depending on the assumption of repulsive forces (due to vector meson exchanges), different authors obtained different coupling constants for the  $0+$  channel:

$$g^2/4\pi \text{ varies from 2.5 to 15.} \quad (23)$$

Even with such a wide range of estimated values, it seems possible that the physical reality may be located at the left of the curve  $n_c = 2n_0$ . Thus, by doubling the present nucleon density one may produce the abnormal nuclear state.

So far all our discussions are carried out only in the so-called tree approximation. One may wonder about the higher-order loop diagrams. This problem has been systematically investigated recently. All the one-loop and two-loop diagrams have been explicitly calculated; in addition, some of the three- and more-than-three-loop diagrams have also been evaluated by one of my students, Mr. M. Margulies. Figure 5 gives the result of all one-loop diagrams for  $m_\sigma^2 = 1.4 m_N^2$  and  $g^2/4\pi = 5$ . For the  $\sigma$ -model

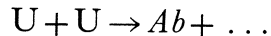
$$U(\sigma) = \frac{m_\sigma^2 m_N^2}{8g^2} \left[ 1 - \left( \frac{\sigma}{\sigma_0} \right)^2 \right]^2 \quad (24)$$

where  $\sigma_0 = m_N/g$ , and  $\bar{\sigma} = \sigma_0$  in the vacuum state.

$\Delta\xi_{\text{vac}}$  is the sum of all one-loop diagrams (Figure 5); and  $\Delta\xi'_{\text{vac}}$  includes also the diagram shown in Figure 6. At  $\bar{\sigma}^2 < \frac{1}{3}\sigma_0^2$ ,  $\Delta\xi_{\text{vac}}$  becomes complex; one must use  $\Delta\xi'_{\text{vac}}$  instead (see Figure 7). Because the meson-loop diagrams and the nucleon-loop diagrams are always of opposite sign, large cancellations may occur, especially when  $m_\sigma^2 \cong 1.4 m_N^2$ . This explains why even for  $g^2/4\pi = 5$ ,  $\Delta\xi_{\text{vac}}$  and  $\Delta\xi'_{\text{vac}}$  (calculated for  $n = 6n_0$ ) are both rather small.

## V. PRODUCTION AND DETECTION

In order to produce the abnormal nuclear state, we must consider reactions in which (i) a large number of nucleons are involved, so that the surface energy can be neglected, and (ii) the nucleon density can be increased by a significant factor  $\sim 2$ . One is, therefore, led to considerations of high energy collisions between heavy ions, say



where  $Ab$  denotes the abnormal nuclear state. If  $Ab$  is produced, what are its characteristics? How can it be detected?

Because of the high density involved, the equation of state of the abnormal state depends sensitively on the short-range repulsive force. For definiteness, we may assume it to be a simple hard-sphere repulsion. Let  $d$  be the diameter of the hard spheres. In Figure 8, we plot the (volume) binding energy per nucleon,

$$\text{b.e.} \equiv m_N - (\xi/n), \quad \text{versus} \quad d \equiv \text{hard-sphere diameter.}$$

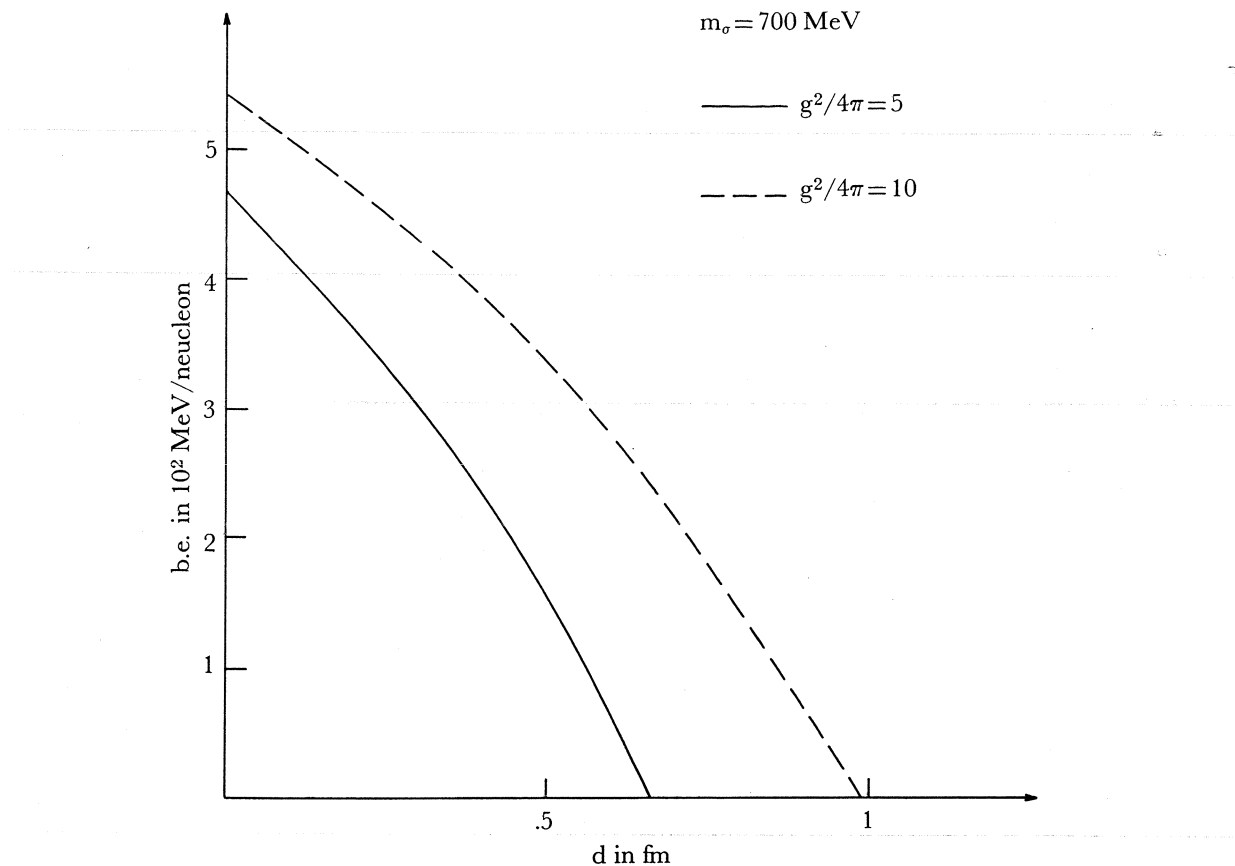


Figure 8.

As an example, we may assume  $m_\sigma = 700$  MeV,  $g^2/4\pi = 5$ , and  $d = 2/m_\omega \approx 0.5$  fm where  $m_\omega = \omega^0$  meson mass. In this case, per nucleon the kinetic energy is  $\sim 490$  MeV and the  $\sigma$ -field energy is  $\sim 300$  MeV; therefore, one has a binding energy  $\sim (940 - 490 - 300) \sim 150$  MeV/nucleon for the abnormal state. The nuclear radius is  $\sim (0.9 \text{ fm})A^{1/3}$ . If one neglects both the surface energy and the Coulomb energy, the abnormal nuclear state is *stable!* (For a pure neutron system, the kinetic energy is much higher because of the exclusion principle; in addition, because of  $\rho^0$ -exchange, one expects the repulsive force between neutrons to be greater than that between neutron and proton. Consequently, most likely, the abnormal state of a pure neutron system is unstable.)

A clear signal of reaction (24) is the detection of a stable (or metastable) nucleus of very large baryon number  $A$ , say,  $\sim 400$ . For a charge  $Z \sim 200$ , the Coulomb energy is not important; therefore, we expect  $Z \sim \frac{1}{2}A$ . Once an abnormal state is produced, through successive neutron absorption one may hope to increase its  $A$  and  $Z$  gradually. When  $Z$  increases, Coulomb energy becomes important; furthermore, the abnormal state can create  $e^+e^-$  pairs. The  $e^+$  will be sent to infinity, but a fair fraction of the  $e^-$  will be kept within the abnormal nucleus. As  $Z$  increases, the number of  $e^-$  also increases. The interplay between the added Fermi energy of  $e^-$  and the Coulomb energy may eventually bring the abnormal state to the point of instability when  $A$  reaches  $\approx 10^4$ .

There remains the problem of the production mechanism of the abnormal state. Only a brief discussion will be given, since we are not able to evaluate the various complexities involved. Let us consider reaction (24) at  $\sim 1/2$  to 1 GeV/nucleon in the center-of-mass system.

(i) *Penetration problem:* Although the mean free path of a nucleon inside the nuclear matter is relatively short, because of the high energy, in most of the nucleon-nucleon collisions one expects the two final nucleons to move more or less along their initial general direction, with about 1 or 2 soft mesons created per nucleon-nucleon collision. Thus, provided the impact parameter is small, these two U nuclei should penetrate each other, and thereby increase the nuclear density from its normal value  $n_0$  to  $\sim 2n_0$ . In addition, there is a large number of soft mesons produced which carry away a large part of the excess energy.

(ii) *Response time:* The collision time of (24) is about

$$\tau_{\text{coll}} \sim 10^{-12} \text{ cm}/c$$

where  $c$  is the velocity of light (provided that the energy is not very high so that Lorentz contraction can be neglected). The order of magnitude of the response time of the meson field is about

$$\tau_{\text{resp}} \sim \left( \frac{h}{m_\phi c} \right) / c \sim 3 \times 10^{-14} \text{ cm}/c.$$

This follows from the simple Klein-Gordon equation for a scalar field  $\phi$ :

$$- \frac{\partial^2}{\partial x_\mu^2} \phi + m_\phi^2 \phi = -gn_S + \dots$$

where  $\dots$  denotes the nonlinear part of the meson-meson force and  $n_S = (\psi^\dagger \gamma_4 \psi)$ . Since

$$\tau_{\text{resp}} \ll \tau_{\text{coll}},$$

as  $n_S$  changes, the value of the meson field responds almost adiabatically. When  $n_S$  reaches  $\sim m_\phi^2 m_N/g$ , the meson field becomes  $\phi \sim -m_N/g$ , which forms the abnormal state.

(iii) *Potential barrier:* After the two U nuclei penetrate each other, and  $\phi$  develops the abnormal value, there is still the question: would the nucleons keep on moving away from each other, so that the whole system becomes separated? We note that as the meson field assumes the abnormal value  $\phi \sim -m_N/g$ , the effective nucleon mass becomes zero. The energy of each nucleon is  $|\mathbf{p}|$  inside the nucleus, but  $(\mathbf{p}^2 + m_N^2)^{1/2}$  outside. Thus, there is a potential barrier  $B$  holding the nucleons together in the abnormal state. So long as  $|\mathbf{p}|$  is  $\lesssim m_N$ , most of the nucleons will collide with the barrier and remain inside. Through such collisions, additional mesons will be emitted, and the nucleons may gradually readjust their wave functions to those of the abnormal state.

While an accurate calculation of the production probability is difficult, from the above discussion one sees that, in order to produce  $Ab$ , the collision energy of the heavy ions should not be small; otherwise penetration becomes difficult. The collision energy should also be not too high; otherwise the collision time  $\tau_{\text{coll}}$  may become too

small because of Lorentz contraction, and the barrier  $B$  becomes  $\sim \frac{1}{2} |\mathbf{p}|^{-1} m_p^2$ , which may also be too low to hold the nucleons together. The best value may perhaps be  $\approx 100$  to several hundred MeV/nucleon in the center-of-mass system.

## VI. REMARKS

The question whether we live in a “medium” or in a “vacuum” dates back to the beginning of physics. From relativity, we know that the “vacuum” must be Lorentz-invariant. As remarked before, Lorentz invariance by itself does not mean that the “vacuum” is simple. From Dirac’s hole theory, one has learned that the vacuum, though Lorentz-invariant, can be rather complicated. However, so long as all of its properties cannot be changed, so long as, e.g., the value of vacuum polarization cannot be modified, then it is purely a question of semantics whether the vacuum should be called a medium or not.

What we try to suggest is that if we do indeed live in a medium, then there should be ways through which we may change the properties of that medium.

It may be worth while to emphasize once again how limited have been our experiences in either nuclear physics or particle physics. So far almost all our nuclear physics experiments have been restricted to nuclei at a constant density. We have never really ventured out to study nuclear physics at any densities other than the normal one. Likewise, in particle physics, we have a similar tradition in specializing along a fairly narrow direction. Take, for example, high energy physics. Hitherto, we have concentrated only on experiments in which we distribute a higher and higher amount of energy into a region with smaller and smaller dimensions. In order to study the question of “vacuum,” or the possibility of the abnormal states, we must turn to a different direction; we should investigate some “bulk” phenomena by distributing high energy or high nucleon density over a relatively large volume. *The fact that such directions have never been explored should, by itself, serve as an incentive for doing such experiments.* As we have discussed, there are possibilities that abnormal states may be created, in which the nucleon mass may be very different from its normal value. It is conceivable that inside the volume of the abnormal state some of the symmetry properties may become changed, or even that the usual roles of strong and weak interactions may become altered. If indeed the properties of the “vacuum” can be transformed, we may eventually be led to some even more striking consequences than those that have been discussed in this lecture.

# Nuclear Physics Questions Posed by Relativistic Heavy Ions

HERMAN FESHBACH

*Massachusetts Institute of Technology, Cambridge, Massachusetts 02139*

It is too early to give definitive statements regarding what insights into nuclear structure can be obtained from collisions of relativistic heavy ions with nuclei. Our present problem is to understand the reaction mechanism involved and the nuclear parameters upon which the mechanisms depend.

As an example we consider the fragmentation of the relativistic heavy-ion projectile by the target. These experiments will be discussed by Heckman in the next paper. The major experimental results are (1) the distribution of the fragments of a particular species in the projectile rest frame is spherical, (2) the momentum distribution is a Gaussian whose width is a simple function of  $A_p$  and  $A_f$ , the mass numbers for the projectile and the fragment, independent of the target properties, (3) the cross section shows a weak dependence on  $A_T$ , the target mass number,  $\sigma \sim A_T^{0.256}$ , and (4) the cross section for the production of a particular fragment is  $\sigma_{pT} \gamma^{(f)} / \gamma$ , with  $\gamma = \sum_f \gamma^{(f)}$ . The last result is consistent with the data, though it has been emphasized by Vary that it is not a unique interpretation. Results (1) and (3) are interpreted as indicating that the collision is peripheral, the projectile receiving a nuclear force pulse on passing the target and then disintegrating downstream. Randomization of the impulse transmitted to the projectile is suggested by (4), which is equivalent to the Bohr independence hypothesis. Result (2) is explained by a statistical hypothesis which states that the momentum distribution is proportional to the probability of forming a fragment by choosing  $A_f$  nucleons at random from the projectile considered as a Fermi gas, the sum of the momenta  $p_i$  of the fragments adding to zero. Assuming the momentum distribution of a given fragment to be Gaussian with a width given by  $\langle P_i^2 \rangle = A_i \langle p^2 \rangle$ , where  $\langle p^2 \rangle$  is the average of the momentum squared of a nucleon in the projectile, substantial agreement with the data is obtained. However, there are fluctuations away from the average predicted curve for a particular fragment, although independence of the target properties remains.

A dynamical theory of the nuclear pulse exerted by the target on the projectile is developed. The linear dimension of the target of importance to the pulse is the nuclear surface thickness,  $a$ , reduced by the Lorentz contraction, an effect that depends weakly on the target properties. The effective time scale is given by the edge thickness ( $\sim \sqrt{aR}$ , with  $a$ =surface thickness and  $R$ =target radius) divided by  $\gamma$  ( $\equiv 1/\sqrt{1-v^2/c^2}$ ) and the particle velocity  $v$ . The corresponding energy ( $\hbar$ /time  $\sim \hbar v / \sqrt{aR}$ ) is about 400 MeV for  $^{16}\text{O}$ . The effective frequency range of importance is determined by the intersection of the spectrum of the pulse and the level density in the projectile. Making a rough estimate of this effect we find that the cross section varies as  $A_T^{1/6}$ , roughly independent of energy.

Coulomb fragmentation was also discussed. The frequency cutoff for the virtual photon spectrum is  $\gamma \hbar v / R$ , which is  $\sim 1/2R$  (fm) GeV for the Berkeley experiment, so that the energy cutoff is of the order of a few hundred MeV. Coulomb fragmentation ( $A_f \geq 2$ ) does not seem to play a significant role in the experimental cross sections. It would lead to a cross section varying as  $Z^2$ .

# Current Knowledge of the Interactions of Relativistic Heavy Ions

HARRY H. HECKMAN

*Lawrence Berkeley Laboratory, Berkeley, California 94720*

I hope to do justice to the rather presumptuous title of my talk by reviewing some experimental results that have given us some key information on the interactions of relativistic heavy ions. My topics are (1) the nucleus-nucleus interaction in nuclear track emulsions, (2) target fragmentation studies, (3) particle production in heavy-ion collisions, and (4) fragmentation of relativistic  $^{12}\text{C}$  and  $^{16}\text{O}$  nuclei.

## I. NUCLEAR EMULSION EXPERIMENTS<sup>1</sup>

Measurements of the mean free paths (MFP) for interactions in emulsion have led to the following conclusions: (1) The MFPs are independent ( $\sim \pm 10\%$ ) of kinetic energy in the interval  $0.2 < E < 30$  GeV/nucleon. (2) The interaction cross sections are consistent with the Bradt-Peters (geometrical) relation

$$\sigma = \pi r_0^2 (A_T^{1/3} + A_P^{1/3} - b)$$

where  $r_0 = 1.20$  to  $1.26$  fm,  $b \approx 0.5$ ,  $A_T$  = target mass number, and  $A_P$  = projectile mass number.

Emulsion experiments have been carried out at the Bevatron to measure the projected angular distributions for  $Z=1$  and  $2$  secondaries produced by the fragmentation of  $^{12}\text{C}$ ,  $^{14}\text{N}$ , and  $^{16}\text{O}$  nuclei at  $2.1$  GeV/nucleon. At angles  $< 5^\circ$ , the distributions show a strong forward peaking that corresponds to a transverse momentum width  $\sigma_{P_\perp} \sim 80$  MeV/c for  $Z=1$  secondaries and  $\sim 140$  MeV/c for  $Z=2$  secondaries. The (projected) angular distribution for  $Z=1$  particles exhibits a broad tail, indicative of the presence of pions and protons with large transverse momenta.

Cosmic-ray studies of the low-energy alpha fragments produced in heavy-ion collisions (incident ions:  $Z \geq 3$ ,  $E \geq 100$  MeV/nucleon) have shown that the alpha spectra cannot be accounted for by conventional evaporation theory. Increased nuclear temperatures, suppressed Coulomb barriers, and recoil-velocity effects of evaporating residual nuclei cannot account for the high-energy tail,  $E \geq 50$  MeV. Some 28% of helium nuclei appear to be produced in other than evaporation processes.

By examining the net momentum of the  $\alpha$ -particle evaporation products from target nuclei (where the incident cosmic-ray heavy ions are  $3 \leq Z \leq 26$  at  $E > 1.7$  GeV/nucleon), emulsion measurements have shown that the mean forward velocity of the residual target nucleus is  $\langle \beta \rangle = 0.022$  ( $\langle P_{\parallel} \rangle = 21$  MeV/c per nucleon, the distribution of  $P_{\parallel}$  being Gaussian in form, with  $\sigma \sim 90$  MeV/c per nucleon).

Similar measurements have been made with beams of  $4.5$ -GeV/c  $\pi^-$  and protons  $9 < E < 25$  GeV, and it is found that  $\langle \beta \rangle = 0.01$  to  $0.02$  in all cases. The recoil velocities (momenta?) of the evaporating nucleus thus appear to be insensitive, to within a factor of two, to the energy and mass of the incident projectile.

## II. FRAGMENTATION OF HEAVY TARGET NUCLEI<sup>2</sup>

The production of light nuclei (He through O) by bombardment of U and Au targets with beams of protons (4.9 and 5.5 GeV) and of <sup>4</sup>He and <sup>12</sup>C nuclei (2.1 GeV/nucleon) have been studied by solid-state particle-identifier and plastic-detector techniques. A comparison of the energy spectra from  $\alpha$ -particle and proton-induced reactions shows that the alpha-induced spectra for the secondary nuclei He, Li, Be, and B are emitted from systems that exhibit higher nuclear temperatures and lower effective Coulomb barriers. As an example, the parameters required to fit the spectra of <sup>7</sup>Li to evaporation-type spectra are as shown in Table 1.

Table 1

	Beam	
	Proton (4.9 GeV)	<sup>4</sup> He(2.1 GeV/nucleon)
Temperature*	10–15 MeV	12–19 MeV
Coulomb barrier	18.6 MeV	15.4 MeV
Velocity of emitting nucleus, $\langle \beta \rangle$	0.005	$<0.01$

\*Higher temperature necessary to fit high-energy tail.

Preliminary experiments with Lexan plastic detectors used to measure the differential cross sections for the production of fragments with  $5 \leq Z \leq 9$  in reactions of 2.1-GeV/nucleon <sup>12</sup>C ions with Au target nuclei show strikingly enhanced production of B and C fragments at energies  $> 150$  MeV. Above this energy the spectrum changes from roughly exponential in energy and isotropic in a forward-moving frame to an approximate power-law in energy of the form  $N(E) \propto E^{-n}$ . The negative exponent increases with  $Z$  of the fragment, e.g.,  $\sim -2.7$  for B to  $\sim 5.0$  for O.

In general, the conclusion from experiments on target fragmentation is that it is not possible to fit the angular and energy distributions of fragments with  $E \geq 150$  MeV by using “thermal” models. Also, the kinematics of quasi-elastic processes cannot fit the data. The emission of energetic fragments from heavy target nuclei is a nonthermal process, strongly dependent upon the mass of the projectile.

## III. PRODUCTION OF NUCLEI $A \leq 3$ AND NEGATIVE PIONS IN HEAVY-ION COLLISIONS<sup>3</sup>

Preliminary results from experiments on particle production at 2.5 deg (lab) from collisions of protons, deuterons, alphas, and <sup>12</sup>C nuclei with targets of Be, C, Cu, and Pb have led to the following conclusions:

a. The rapidity distributions of the secondary nuclear fragments are peaked at the rapidity of the incident beam. The rapidity variable is

$$y = \frac{1}{2} \ln[(E + P_{\parallel})/(E - P_{\parallel})].$$

b. The momentum spectra of secondary nuclear fragments and their production cross sections are independent of energy, 1.05 to 2.1 GeV/nucleon, which is indicative of limiting fragmentation.

c. The relative cross sections of the secondary fragments are independent of the target nucleus, consistent with the hypothesis of factorization.

d. The cross sections for high-momentum proton production in  $d$ - and  $\alpha$ -nucleus collisions and for  $\pi^-$  production in  $\alpha$ -nucleus collisions have a  $\sigma \propto A_T^{1/3}$  dependence, which suggests that the production process is a peripheral one.

e. The invariant cross sections for  $\pi^-$  production by protons ( $1.05 < E < 4.1$  GeV) and alphas ( $E = 1.05$  and 2.1 GeV/nucleon) on Be targets form "universal" functions when plotted as a function of the scaling variable  $K_{\parallel}^*/K_{\parallel}^* (\text{max})$ . The quantity  $K_{\parallel}^*$  is the longitudinal momentum of the outgoing pion in the overall center-of-mass system.

The cross sections for  $\pi^-$  production above  $T_{\pi^-} \approx 415$  MeV at 15 deg (lab) by 0.52-GeV/nucleon  $^{14}\text{N}$  ions appear to be greater than can be accounted for by Fermi motion, with use of reasonable forms of projectile momentum distributions

#### IV. FRAGMENTATION OF $^{12}\text{C}$ AND $^{16}\text{O}$ AT RELATIVISTIC ENERGIES<sup>4</sup>

On-going experiments on the 0-deg fragmentation of  $^{12}\text{C}$  ( $E = 1.05$  and 2.1 GeV/nucleon) and  $^{16}\text{O}$  ( $E = 2.1$  GeV/nucleon) nuclei in targets H, Be, C, Al, Cu, Ag, and Pb are yielding information that pertains to the mechanisms of projectile fragmentation, the transverse and longitudinal momentum distributions of fragmentation products in the projectile frame, the production cross sections for all isotopes and the dependence of the cross sections on beam energy and mass of the target nucleus. On the basis of a partial analysis of the experimental data, the characteristic features of projectile fragmentation at beam energies 1.05 and 2.1 GeV/nucleon are as follows:

a. The velocities of the beam fragments are approximately equal to the velocity of the incident ion. The momentum/nucleon values of the fragments are  $\sim 0.1$  to 0.5% less than that of the incident projectile, depending on the mass of the fragment.

b. The momentum distributions of the secondary fragments are Gaussian in the projectile frame.

c. The widths of the Gaussian distributions,  $\sigma_{P_{\parallel}}$  and  $\sigma_{P_{\perp}}$ , vary from about 90 to 180 MeV/c in the projectile frame.

d. Qualitatively,  $\sigma_{P_{\parallel}} \propto [F(P - F)/P]^{1/2}$ , where  $P$  and  $F$  are the masses of the projectile and the fragment, respectively. Systematic deviations from this relation indicate an (unknown) dependence of  $\sigma_{P_{\parallel}}$  on the mass of the fragment  $F$ .

e.  $|\langle P_{\parallel} \rangle| \simeq \frac{1}{3} \sigma_{P_{\parallel}}$ .

f.  $\sigma_{P_{\parallel}}$  and  $\langle P_{\parallel} \rangle$  are independent of target nucleus and energy in the range 1.0 to 2.1 GeV/nucleon.

g. The modes of fragmentation and the cross sections are independent of target mass  $A_T$  and beam energy for fragments  $A_F \leq A_P - 2$ , i.e., when two or more nucleons are removed from the projectile.

h. Assuming the cross sections factor according to  $\sigma_{PT}^F = \gamma_P^F \gamma_T$ , where the target factor is assumed to be of the form  $A_T^n$ , the cross sections for the production of fragments  $2 \leq A_F \leq A_P - 2$  can be expressed as  $\sigma_{PT}^F \simeq \gamma_P^F A_T^{1/4}$  where  $\gamma_P^F$  is the cross section for the production of fragment  $F$  by projectile  $P$  on hydrogen nuclei. A satisfactory fit to the data can also be obtained by assuming a geometrical model of the form  $\sigma_{PT}^F = \gamma_{PT}^F \gamma_T^P$ , where  $\gamma_T^P = r_0(A_T^{1/3} + A_P^{1/3} - b_1)$ , and  $r_0 = 1.26$  fm and  $b_1 = 1.88$ .

i. Coulomb dissociation via the giant dipole resonance is observed for  $A_F = A_P - 1$  fragments, i.e., for single nucleon loss. The magnitude of this cross section can be accounted for by the Weizsäcker-Williams theory for the virtual photon field of the target nucleus.

## REFERENCES

1. Cosmic-ray work done at University of Lund and University of Minnesota; accelerator work done at the Bevatron at Lawrence Berkeley Laboratory and at the Princeton-Pennsylvania Accelerator by the group from the Naval Research Laboratory.
2. Work at Lawrence Berkeley Laboratory by A. ZEBELMAN, A. POSKANZER, J.D. BOWMAN, R.G. SEXTRO, AND V. VIOLA; at the University of California at Berkeley by F.S. CRAWFORD, P.B. PRICE, L. STEVENSON, AND J.N. WILSON.
3. Work at Lawrence Berkeley Laboratory by J. JAROS, J. PAPP, L.S. SCHROEDER, J. STAPLES, H. STEINER, AND A. WAGNER; at the Princeton-Pennsylvania Accelerator by W. SCHIMMERMANN, K.G. VOSBURGH, K. KOEPKE, AND W. WALES.
4. Work at Lawrence Berkeley Laboratory by F.S. BIESER, B. CORK, D.E. GREINER, H.H. HECKMAN, AND P.J. LINDSTROM.

# Pion Condensates

G.E. BROWN\*

*NORDITA, Copenhagen, Denmark*

*and*

*State University of New York at Stony Brook, Stony Brook, New York 11790*

The possible existence of pion condensates was proposed by A.B. Migdal,<sup>1</sup> and independently by Sawyer and Scalapino.<sup>2</sup> Not only did this provide interesting possibilities for a change in the equation of state for dense matter, but the idea of a condensate of pseudoscalar particles, necessarily in a state of finite momentum, which could, so to say, be created out of the vacuum, posed many new and interesting conceptual problems. My main claim to expertise in this field is that I have had more correspondence than anyone else with the participants. I hope to be able to synthesize the developments to date and to give a broad view, not without personal prejudices

## I. DEVELOPMENT

For those who have not worked on this subject, a brief restatement of the original work of Sawyer and Scalapino<sup>3</sup> relating to neutron matter may be helpful. The coupling between nucleons and  $\pi^-$  mesons can be described as

$$\delta H = \frac{ifk\sqrt{2}}{m_\pi} [\bar{p}(\mathbf{p} + \mathbf{k})\sigma_3 n(\mathbf{p})\phi_{\pi^-} + \text{h.c.}] \quad (1)$$

where all  $\pi^-$  mesons are assumed to be in a running wave of momentum  $-\mathbf{k}$ . Given  $\rho$  nucleons per unit volume ( $\rho = 2\omega\phi^2$ ), let us assume the proportion of neutrons which have changed into protons and  $\pi^-$  mesons to be  $X$ , so that

$$2\omega_c\phi_{\pi}^2 = \rho X \quad (2)$$

where  $\omega_c$  is the condensate frequency. Introducing quasi-particles, which are mixtures of neutrons and protons,

$$u(\mathbf{p}) = \sqrt{1-X}n(\mathbf{p}) + i\sqrt{X}\sigma_3 p(\mathbf{p} + \mathbf{k}), \quad (3)$$

one finds, taking the expectation value of  $\delta H$  in this quasi-particle representation, the interaction energy per nucleon to be

$$\frac{E_{\text{int}}}{\text{nucleon}} = -\sqrt{\rho X} \frac{2fk}{m_\pi \sqrt{\omega_c}} \sqrt{X(1-X)}. \quad (4)$$

Neglecting nucleon recoil energies, we find the total energy per nucleon to be

$$\frac{E}{\text{nucleon}} = X\omega_c - 2\sqrt{\rho} \frac{f}{m_\pi} \frac{k}{\sqrt{\omega_c}} X \sqrt{1-X}. \quad (5)$$

Condensation is possible when the second term on the right-hand side is larger in magnitude than the first term. With increasing density this will necessarily occur

---

\*Work supported in part by AEC Contract At(11-1)-3001.

because of the  $\sqrt{\rho}$  in the coefficient of the second term. One obtains a solution at densities  $\rho_c$  a little higher than nuclear-matter density,  $\rho_c = \rho_0 = 0.17 \text{ fm}^{-3}$ .

Various effects have been left out in this first, simple treatment.

A. Effects that tend to lower the densities at which condensation occurs:

1. Inclusion of a small admixture of  $\pi^+$  mesons.
2. Inclusion of the  $\Delta_{33}(1236)$  isobar.
3. Higher-order effects of the one-pion-exchange potential in the nucleon-nucleon interaction.

B. Effects that tend to raise the densities:

1. The short-range repulsion in the nucleon-nucleon force.
2. The role of  $\rho$ -meson exchange in cutting down pionic effects.
3. The  $S$ -wave interaction between  $\pi^-$  mesons and the neutrons.

C. Self-energy interactions of the particle and hole; it is not clear which way these will go.

In order to discuss all these effects, it is more convenient to go over to a general formalism introduced by Baym.<sup>4</sup>

## II. FORMALISM

The first result<sup>4</sup> we need, one familiar from the theory of superfluidity, is that the condensate wave function  $\langle \phi(\mathbf{r}, t) \rangle$  must vary in time as  $\exp(-i\mu_\pi t)$ ; i.e.,  $\omega_c = \mu_\pi$ . This can be obtained by minimizing the free energy, as a function of  $\langle \phi \rangle$  and its conjugate momentum, at constant pion density. Here  $\langle \phi \rangle$  is the expectation value of the pion wave function. For the pseudoscalar  $\phi$  to have an expectation value, of course the symmetry of the vacuum must be broken. This will occur for a certain minimum amount of neutron or nuclear matter, the threshold density necessary for pion condensation.

The second result we need follows from thermodynamic equilibrium. Since, in neutron stars,

$$n \rightleftharpoons p + \pi^-$$

is an equilibrium process, one has the following equality between chemical potentials:

$$\mu_\pi = \mu_n - \mu_p . \quad (6)$$

Once there is critical density of neutron matter, the equation

$$(\mu_\pi^2 - m_\pi^2 + \nabla^2) \langle \phi(\mathbf{r}) \rangle = J(\mathbf{r}) , \quad (7)$$

which can be derived directly from Hamilton's equations of motion, will have a solution. Remember, again, that  $\langle \phi \rangle$  is a pseudoscalar, and therefore existence of a solution demands broken symmetry. In Eq. (7),  $J(\mathbf{r})$  is the pionic current, which would be

$$J(\mathbf{r}) = \frac{\sqrt{2}f}{m_\pi} \nabla \cdot (\bar{p} \sigma_3 n) + \text{h.c.} \quad (8)$$

in our simple example, see Eq. (1). Later on we must generalize  $J$  to include pieces involving the  $\Delta_{33}(1236)$  isobar. Of course,  $J$  is a pseudoscalar. Expanding  $J(\mathbf{r})$  to first order in  $\langle \phi(\mathbf{r}') \rangle$  and using

$$\frac{\delta J(\mathbf{r})}{\delta \langle \phi(\mathbf{r}') \rangle} = \pi(\mathbf{r}, \mathbf{r}'; \omega = \mu_\pi) \quad (9)$$

to obtain the  $\pi^-$  self-energy in the medium, we see that the  $\pi^-$  condensation threshold is the point where

$$D^{-1}(\omega = \mu_\pi) \langle \phi \rangle = 0, \quad (10)$$

i.e., where the pion Green's function  $D$ , for  $\langle \phi \rangle = 0$ , develops a pole at  $\omega = \mu_\pi$ .

Since

$$D(\mathbf{r}', \mathbf{r}; t) = \langle [\phi(r', t) \phi(r, 0)]_+ \rangle \quad (11)$$

where the lower suffix indicates time ordering, using Eq. (7),

$$D_0^{-1} D D_0^{-1} = \langle [J(\mathbf{r}', t), J(\mathbf{r}', 0)]_+ \rangle + D_0^{-1} \quad (12)$$

where  $D_0$  is the Green's function for free propagation [with  $\pi(\mathbf{r}, \mathbf{r}'; \omega) = 0$ ]. The  $D_0^{-1}$  introduce poles only at the kinematics for non-interacting pions. Consequently, the nontrivial poles of the  $\langle J, J \rangle$  correlation function, which depends only on  $k$  and  $\omega$  for an infinite system, comes at  $\omega = \mu_\pi$  to the collective state of pion condensation

In the theory of collective states in many-body systems, we are quite used to this sort of formalism. As shown in Figure 1, we can think of an excitation being started off by the absorption of a pion in neutron matter. This excitation then develops in time, through all virtual particle-hole, isobar-hole, etc., excitations having the quantum numbers of the pion. For a sufficiently high neutron density  $\rho_c$ , it is possible that the energy  $\omega$  of the state comes down to  $\mu_\pi$ .

The situation of  $\pi^0$  condensation in nuclear matter may be easier to visualize here. Since

$$n \rightleftharpoons \pi^0 + p$$

and the system is in equilibrium, the chemical potential  $\mu_{\pi^0} = \mu_n - \mu_p = 0$ . Thus  $\omega_c = 0$ , the static situation. We are then confronted with the very familiar case of a collective particle-hole excitation coming down to zero energy, the system then mak-

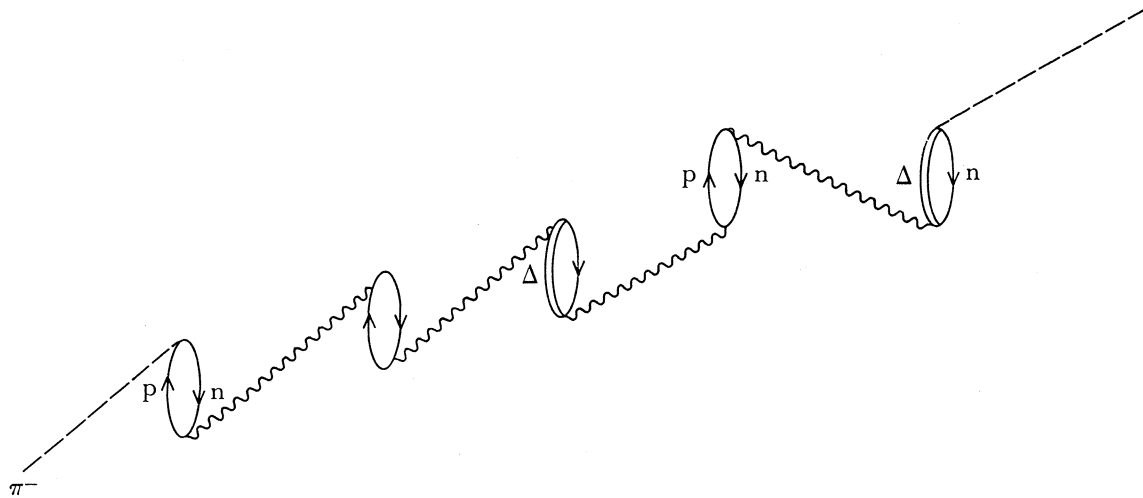


Figure 1. Graphical description of particular processes giving rise to the spin-isospin wave corresponding to a pion condensate. The wavy lines are the full interactions between the relevant hadrons.

ing a phase transition so that for higher densities, spin, isospin density waves are built into the ground state.

Summing the geometrical series\* (Figure 1) for the  $\langle J, J \rangle$  correlation function with only nucleon-particle, nucleon-hole excitations (no isobars), one finds

$$\langle J, J \rangle = \frac{-2f^2k^2U(k, \omega)}{1 - \frac{2f^2k^2}{m_\pi^2 + k - \omega^2} U(k, \omega)} \quad (13)$$

where  $U(k, \omega)$  is the Lindhard function. With neglect of nucleon recoil, one has

$$U(k, \omega) = \rho / \omega \quad (14)$$

so that the condition that the  $\langle J, J \rangle$  correlation function has a pole at  $\omega = \mu_\pi$  is just that

$$1 - \frac{2f^2k^2}{m_\pi^2 + k^2 - \mu_\pi^2} \frac{\rho}{\mu_\pi} = 0. \quad (15)$$

Bertsch and Johnson<sup>6</sup> show that the requirement that the denominator of (13) vanish for  $\omega = \mu_\pi$  is the same condition that the denominator have a double pole in  $\omega$ . Solution of

$$1 - \frac{2f^2k^2}{m_\pi^2 + k^2 - \omega^2} \frac{\rho}{\omega} = 0 \quad (15.1)$$

for a double pole is trivial algebraically, and gives

$$\begin{aligned} \omega_c &= \left( \frac{k_c^2 + m_\pi^2}{3} \right)^{1/2}, \quad k_c = \sqrt{2} m_\pi; \\ \rho_c &= \frac{1}{3\sqrt{3}f^2} \frac{(k_c^2 + m_\pi^2)^{3/2}}{k_c^2} \cong 0.17 \text{ fm}^{-3}. \end{aligned} \quad (15.2)$$

This  $\rho_c$  is just equal to  $\rho_0$ , nuclear matter density.

Before closing this section, we write explicitly the relation of the  $\langle J, J \rangle$  correlation function to the pion Green's function, the latter being used by Bertsch and Johnson. Note that the  $\langle J, J \rangle$  correlation function (13) can be written

$$\langle J, J \rangle = \frac{-(\omega^2 - m_\pi^2 - k^2)2f^2k^2U(k, \omega)}{\omega^2 - m_\pi^2 - k^2 + 2f^2k^2U(k, \omega)} \quad (16)$$

and noting that

$$(\omega^2 - m_\pi^2 - k^2) = D_0^{-1}(k, \omega), \quad (16.1)$$

$$2f^2k^2U(k, \omega) = -\Pi_P(k, \omega) \quad (16.2)$$

with the pion self-energy coming from  $P$ -wave propagation.

### III. A LIGHT (RATHER THAN DENSE) DIVERSION

In the work both of Baym and Flowers<sup>7</sup> and of Migdal et al.,<sup>8</sup> pion condensation in neutron stars begins at a much lower density than  $\rho_0$ . With assumptions simi-

\*See G.E. Brown<sup>5</sup> for a simple way of carrying out isospin sums; the spin sum can be carried out in the same way.

lar to those of Sawyer and Scalapino, except that a few percent of protons are present because of the small number of electrons present in mainly neutronic matter, Baym and Flowers find condensation at

$$\rho_c = 0.058 \text{ fm}^{-3} \quad (k_c = 1.1 \text{ fm}^{-1}), \quad (17)$$

that is, at a third of the density found with Sawyer and Scalapino's simplest model.

This looks exciting, at first glance, but (a) condensation at such low densities seems to disappear when short-range correlations between nucleons are introduced,<sup>9</sup> and (b) the condensate at such low densities cannot have large amplitude, because it depends on the 2 or 3% protons present.

Let us develop this latter point a bit. What keeps a neutron from going over into a proton and  $\pi^-$  at low densities is that the energy to be gained by the new interaction [see Eq. (4)] is insufficient to balance the energy needed to create the  $\pi^-$  meson,  $\omega_{\pi^-} = (k^2 + m_{\pi^-}^2)^{1/2}$ . However, if a few protons are around, a proton can be changed into a neutron, the new neutron-particle, proton-hole pair having the quantum numbers of the  $\pi^-$ . For low neutron densities, with low  $\mu_n$ , the energy needed for this is  $\ll m_{\pi^-} c^2$ . Thus, the neutron-particle, proton-hole pair is like a low-energy  $\pi^-$ . The "pion condensate" is, indeed, rather a two-particle, two-hole state in which one neutron particle is correlated with the proton hole, and a proton particle is correlated with a neutron hole, the latter as in the Sawyer and Scalapino condensate discussed earlier. Migdal et al.<sup>8</sup> erroneously call these correlated two-particle, two-hole excitations a  $\pi^+$  condensate, erroneously because the charge in the condensed pion field is always negative.\* Aside from the (important) inclusion of  $\Delta$ -isobars, the work of Migdal et al.<sup>8</sup> is equivalent to that of Baym and Flowers, although the language is different.

#### IV. SHORT-RANGE NUCLEON-NUCLEON CORRELATIONS

In all detail, the one-pion exchange term is

$$\begin{aligned} V_{\text{OPEP}}(k, \omega) &= -\frac{f^2}{m_{\pi}^2} \frac{\boldsymbol{\sigma}_1 \cdot \mathbf{k} \boldsymbol{\sigma}_2 \cdot \mathbf{k}}{k^2 + m_{\pi}^2 - \omega^2} \\ &= -\frac{f^2}{m_{\pi}^2} \left\{ \frac{[\boldsymbol{\sigma}_1 \cdot \mathbf{k} \boldsymbol{\sigma}_2 \cdot \mathbf{k} - \frac{1}{3} \boldsymbol{\sigma}_1 \cdot \boldsymbol{\sigma}_2 k^2]}{k^2 + m_{\pi}^2 - \omega^2} + \left[ \frac{1}{3} (\boldsymbol{\sigma}_1 \cdot \boldsymbol{\sigma}_2) \right] - \left[ \frac{1}{3} \frac{(\boldsymbol{\sigma}_1 \cdot \boldsymbol{\sigma}_2)(m_{\pi}^2 - \omega^2)}{k^2 + m_{\pi}^2 - \omega^2} \right] \right\}. \quad (18) \end{aligned}$$

These three terms represent:

$$\begin{aligned} \text{(i) tensor:} \quad & -\frac{8}{3} m_{\pi}^2 \frac{f^2 k^2}{(k^2 + m_{\pi}^2 - \omega^2)}, \\ \text{(ii) } \delta\text{-function:} \quad & -\frac{4}{3} \frac{f^2}{m_{\pi}^2}, \\ \text{(iii) Yukawa:} \quad & +\frac{4}{3} m_{\pi}^2 \frac{f^2 (m_{\pi}^2 - \omega^2)}{(k^2 + m_{\pi}^2 - \omega^2)}, \end{aligned} \quad (19)$$

\*I am indebted to Gordon Baym for this comment.

where we have labeled the terms on the right-hand side of Eq. (19) by the dependence they would have in configuration space and in the order in which they occur on the right-hand side of Eq. (18).

Suppose, now, as is commonly thought, that the nucleons have strong short-range repulsions, which keep them apart; i.e., in terms of a nucleon-nucleon correlation function

$$\langle \rho(1)\rho(2) \rangle = g(|\mathbf{r}_1 - \mathbf{r}_2|), \quad (20)$$

we ask only that

$$g(0) = 0. \quad (20.1)$$

Then the  $\delta$ -function part of the  $V_{OPEP}$  will be cut out, so that Eq. (15.1) is modified to\*

$$1 - \frac{2f^2k^2}{m_\pi^2 + k^2 - \omega^2} \frac{\rho}{\omega} + \frac{2}{3} \frac{f^2\rho}{\omega} = 0. \quad (21)$$

In the case of  $\pi^0$  condensates, Barshay and Brown<sup>10</sup> found that such a minimal effect of the nucleon-nucleon interaction raised the critical density  $\rho_c$  to the point where condensation probably would not occur in this model (without isobars).

\*Going over to nonzero  $\omega$ , only the *static*  $\delta$ -function piece should be taken out.

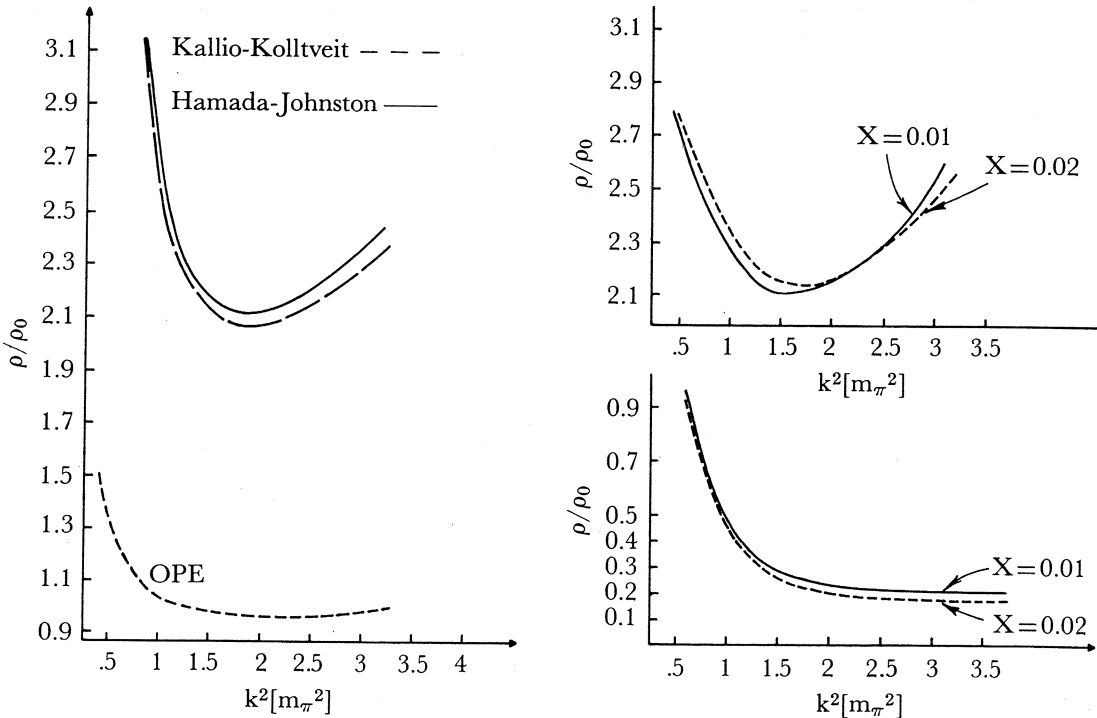


Figure 2. The threshold density  $\rho_c$  as a function of  $k^2$  in units of the nuclear matter density  $\rho_0 = 0.17 \text{ fm}^{-3}$ . (Left) For pure neutron matter (double pole threshold condition) as calculated with a Kallio-Kolltveit force (broken line) and a Hamada-Johnston potential (solid line). The dotted line at the bottom is obtained with a pure OPEP interaction. (Right) For neutron-star matter supplemented by a small fraction  $X$  of protons, using the threshold condition of Baym<sup>4</sup> as calculated with a Hamada-Johnston potential (upper curves) and OPEP only (lower curves). Solid lines:  $X = 0.01$ ; broken lines:  $X = 0.02$ . From Weise and Brown.<sup>9</sup>

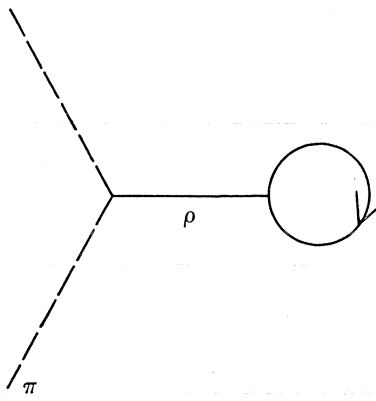


Figure 3. *S*-wave pion-nucleon self-energy.

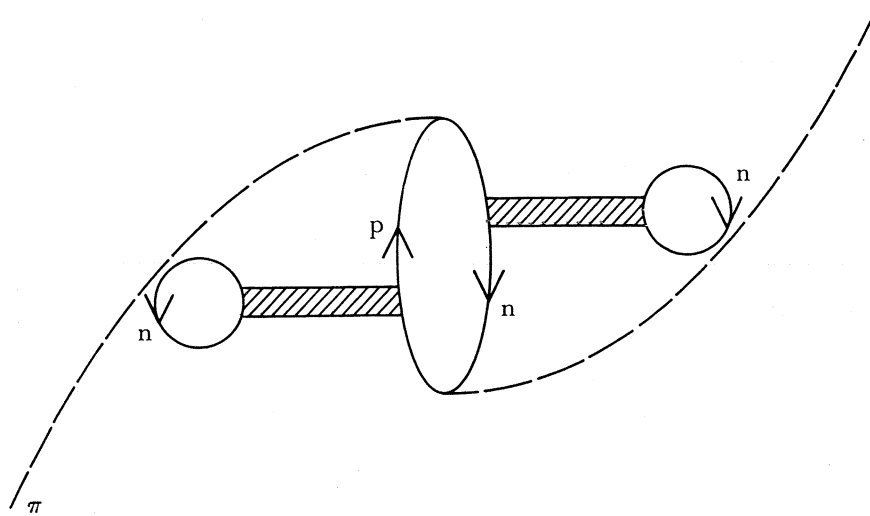


Figure 4. Nucleon self-energy insertions into a typical bubble in the  $\langle J, J \rangle$  correlation function. Here the crosshatched rectangle represents all possible interactions with the neutron sea.

In the case of  $\pi^-$  condensation in neutron stars, Weise and Brown<sup>9</sup> found the results shown in Figure 2. In the curves shown here, pieces of the nucleon-nucleon interaction other than hard core are included.\* The main points we wish to make with these curves are that (a) inclusion of short-range repulsions increases the critical density for pion condensation considerably, and (b) such inclusion removes the differences between condensations with and without a small number of protons initially present.

Removal of the  $\delta$ -function is completely equivalent to the Lorentz-Lorenz correction of Ericson and Ericson<sup>11</sup> to the pion self-energy.

\*Baym and Flowers,<sup>7</sup> for a model corresponding to the curves on the right in Figure 2, find with "minimal nuclear forces," e.g., simply removal of the  $\delta$ -function, that  $\rho_c \approx 1.1 \rho_0$ ,  $k_c = 1.60$  fm<sup>-1</sup>.

## V. INCLUSION OF THE S-WAVE PION-NUCLEON INTERACTION

The *S*-wave pion-nucleon interaction can be characterized by a Hartree potential  $V_S$  or by a pion self-energy\*

$$V_S = \frac{1}{2m_\pi} \pi_S(k, \omega) = 40 \frac{\omega}{m_\pi} \frac{\rho}{\rho_0} \text{ MeV} \quad (22)$$

(see Figure 3). Again,  $\sigma_0 = 0.17 \text{ fm}^{-3}$  is the nuclear matter density.

The *S*-wave interaction is trivially included by adding this  $\pi_S$  to  $\pi_P$ , Eq. (16.2), in the denominator of the  $\langle J, J \rangle$  correlation function. The isospin dependence of  $\pi_S$ , which comes into play when some  $\pi^+$  mesons are present, is properly included in that  $\omega \rightarrow -\omega$  when  $\pi^-$ 's are replaced by  $\pi^+$ 's (crossing symmetry).

## VI. NUCLEON SELF-ENERGIES

It might be thought that nucleon self-energies (see Figure 4) would play a large role, since a proton at rest is bound by  $\sim 50$  MeV more than a neutron for neutron densities  $\sim \rho_0$ . Much of this additional binding comes from higher-order effects of the tensor interaction, which are suppressed by Pauli and dispersion corrections in going to higher densities, and the momentum dependence of the proton-neutron interaction cuts down the interaction for protons with the relatively large momenta occurring in pion condensates. Estimates made by G.E. Brown and S.O. Bäckman with the Reid and Hamada-Johnston nucleon-nucleon interactions indicate that for  $\rho \approx \rho_0$  the proton and neutron self-energies are roughly equal. Bertsch and Johnson, in a preprint, seem to come to similar conclusions.

\*This *S*-wave interaction can be thought of as proceeding through  $\rho$ -meson exchange between pions and neutrons.

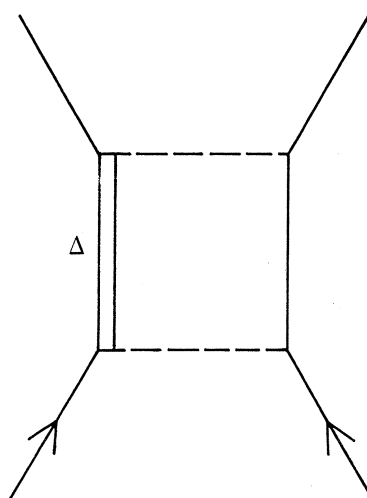


Figure 5. Mechanism of Green and Haapakoski for the attraction in the neutron-neutron interaction.

This whole question has to be reopened, because of the developments of Green and Haapakoski<sup>12</sup> pointing out that most of the attraction in the neutron-neutron interaction comes from intermediate  $\Delta_{33}(1236)$  isobars (see Figure 5). In the many-body system this will be suppressed, in going to higher densities, by the same mechanisms that suppress higher-order tensor interactions in the neutron-proton system. Since this suppression makes the neutrons less bound, it increases the neutron chemical potential  $\mu_n$  and, consequently, also the condensation frequency  $\omega_c = \mu_\pi = \mu_n - \mu_p$ .

## VII. OTHER EFFECTS FROM THE NUCLEON-NUCLEON INTERACTION

Extensive calculations with inclusion of current nucleon-nucleon interactions are being done by S.O. Bäckman. Some results have been reported in preprints by Bäckman and Weise and by Bertsch and Johnson. We discuss here only qualitative points.

As noted in Figure 1, the wavy lines represent the complete nucleon-nucleon interaction. This is often approximated by the nucleon-nucleon  $G$ -matrix.\* With such an approximation, the  $\langle J, J \rangle$  correlation function is

$$\langle J, J \rangle = -\frac{2f^2 k^2 U(k, \omega)}{1 + G(k, \omega) U(k, \omega)}. \quad (23)$$

Splitting  $G$  into spin, isospin channels, one has

$$G = \frac{1}{4}(G^{11} + G^{00} - G^{10} - G^{01}) \quad (24)$$

where the upper indices represent  $S$  and  $T$ . With tensor components, this becomes more complicated. A reasonable approximation<sup>13</sup> is to take

$$G(k, \omega) \cong V_{\text{OPEP}}(k, \omega) + [G(k, 0) - V_{\text{OPEP}}(k, 0)] = V_{\text{OPEP}}(k, \omega) + \tilde{G}(k) \quad (25)$$

where  $V_{\text{OPEP}}(k, \omega)$  is given by Eq. (18). The thinking behind Eq. (25) is that contributions to  $G(k, \omega)$  from exchange of mesons heavier than the pion will have  $\omega$ -dependencies like  $(k^2 + m^2 - \omega^2)$  where  $m$  is the mass of the relevant meson. For large  $m$  the  $\omega^2$  is relatively unimportant.

To understand Eq. (24), let us consider the interaction  $G^{10}$ , the one entering into the deuteron. If the interaction is attractive in the  $T=1, S=0$  state, then it makes the denominator of Eq. (23) more positive, hindering condensation. This comes about because in order to make a spin-isospin wave which has  $T=1, S=1$ , we must turn the spin of one of the particles in the  $S=0$  state so as to make the  $S=1$  state. If the two particles are more bound in  $S=0$  states, it costs energy to turn the spin around. The kinetic energy also increases.

It might then appear that the tensor force, whose second- and higher-order effects bind the deuteron, would work against condensation. Here, however, a new effect<sup>14</sup> brought about by the finite wave vector for pion condensation enters. This is

---

\*The  $G$ -matrix is nuclear terminology for what is often called the  $t$ -matrix, with standing-wave boundary conditions.

Table 1

Threshold Values for  $\pi^-$  Condensation in Neutron Matter  
 With Only Nucleons (No Isobars) Present  
 (Nucleon-nucleon correlations are included. The critical density is in units  
 of normal nuclear matter density,  $\rho_0 = 0.5m_\pi^3$ .)

	$\rho_c/\rho_0$	$\omega_c[m_\pi]$	$k_c[m_\pi]$
No S-wave interaction	2.0	1.1	2.7
S-wave int. included	$\gg 3$	—	—

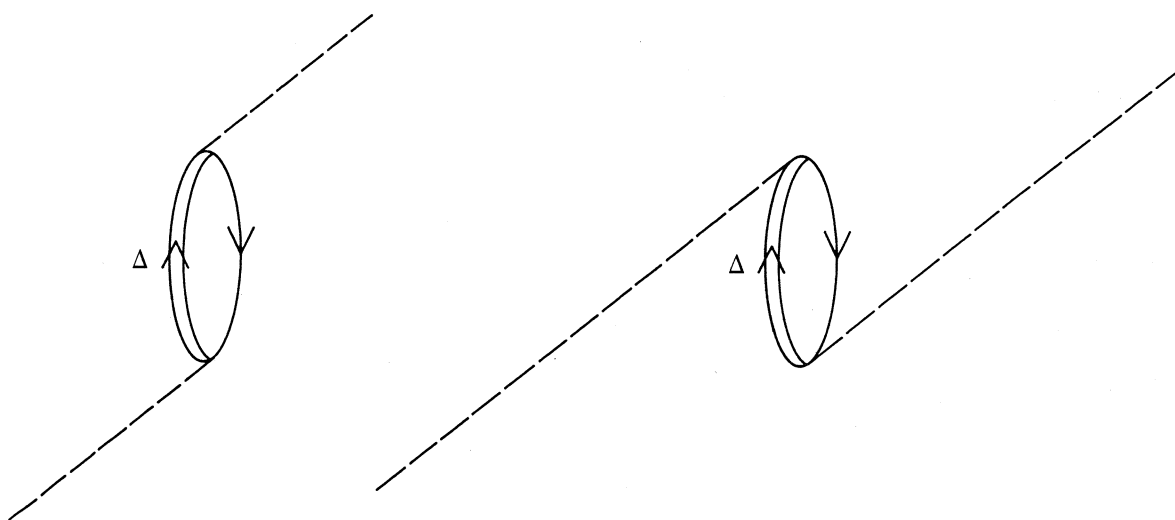


Figure 6. Contribution of the  $\Delta_{33}(1236)$  isobar to the pion self-energy.

the effect of off-diagonality of the  $G$ -matrix elements which, for large momentum transfer ( $\gtrsim m_\pi c$ ) gives repulsive matrix elements.

In Table 1 we show the results of Bäckman and Weise,<sup>13</sup> including the nucleon-nucleon force,  $S$ -wave pion-nucleon interaction, but leaving out the  $\Delta_{33}(1236)$  isobars. These calculations assumed an initial mixture of 2.5% protons. Chemical potentials  $\mu_n$  and  $\mu_p$  were taken from Sjöberg.<sup>15</sup> The chief difference from the free Fermi gas chemical potentials is that  $\mu_p$  is large and negative.

### VIII. ROLE OF ISOBARS

The final chapter in our (production) drama\* might be entitled, "Can the Isobar Save Fair Lady Condensate From Her Deep Compression Chamber?" Remembering the role that the isobar plays in the pion self-energy in pion scattering (Figure 6), one sees that the isobar is the only agency which can bring the condensate down to low densities. Indeed, in the work of Migdal and collaborators, who include

\*The Russian version<sup>8</sup> of the ending is a happy one.

the S-wave pion-nucleon interaction and their version of hard-core repulsions between nucleons, inclusion of the isobar brings  $\rho_c$  well below  $\rho_0$ .

Within the framework of Chew-Low theory, the contribution of the isobar to the pion self-energy is, for  $\pi^-$  mesons in a neutron medium,

$$\pi_\Delta^{(-)} = \frac{8}{3} f^2 \rho k^2 \left[ \frac{1}{\omega - \omega_\Delta} - \frac{1}{3} \frac{1}{\omega + \omega_\Delta} \right] \quad (26)$$

with the isobar energy  $\omega_\Delta = 2.1 m_\pi c^2$ . From crossing symmetry, the self-energy for  $\pi^+$  mesons can be obtained as

$$\pi_\Delta^{(+)}(k, \omega) = \pi_\Delta^{(-)}(-k, -\omega).$$

In nuclear matter, from isospin invariance, the self-energy for  $\pi^{(0)}$  mesons is

$$\pi_\Delta^{(0)}(k, \omega) = \frac{1}{2} [\pi_\Delta^{(+)}(k, \omega) + \pi_\Delta^{(-)}(k, \omega)]. \quad (27)$$

In pion mass units  $\rho_0 = \frac{1}{2}$  (i.e.,  $\rho_0 = \frac{1}{2} m_\pi^3$ ), so that

$$\pi_\Delta^{(0)}(k, 0) = \frac{16}{9} f^2 \frac{\rho k^2}{\rho_0} \frac{1}{\omega_R} \cong 0.83 \frac{\rho}{\rho_0} k^2. \quad (27.1)$$

On the face of it, this is the overwhelming contribution to the pion self-energy, so we must be careful to treat it in the most accurate way possible.

It is amusing to consider that the pion propagator, with isobar self-energy, in nuclear matter would be

$$D(k, 0) = \frac{1}{k^2 + m_\pi^2 - 0.83 k^2} \cong \frac{6}{k^2 + m_\pi^2/6} \quad (27.2)$$

so that the effective Yukawa interaction would become

$$V_{\text{OPEP}}(r) = \frac{f^2}{m_\pi^2} (\sigma_1 \cdot \nabla) (\sigma_2 \cdot \nabla) \exp\left(\frac{-m_\pi r}{\sqrt{6}}\right). \quad (27.3)$$

The above simple treatment neglects the fact that there are forces other than that from one-pion exchange in the  $S=1$ ,  $T=1$  channel. Within the nomenclature of Fermi-liquid formalism, these would be vertex corrections in the self-energy, as explained in Figure 7. It is clear that there are vertex corrections; in fact, the well-known Lorentz-Lorenz correction is the example of one.\*

More specifically, we need to know the interactions between nucleons and isobars, as reinterpreted in Figure 8 in the particle-particle channel.

We first consider the matrix element Figure 8a. We know already that pion exchange contributes to the interaction. Whereas the isospin  $T=0$   $\omega$  meson cannot contribute to the transition between nucleon and isobar, which requires a change of  $\Delta T=1$ , the nucleons certainly can exchange  $\omega$  mesons before pion exchange, and if the commonly accepted view that the  $\omega$  meson is coupled to the hypercharge current is adopted, then the nucleon and isobar have the same repulsive interaction from  $\omega$ -exchange as two nucleons. Thus, we can say that something similar to a hard-core repulsion exists between all particles.

---

\*Barshay et al.<sup>16</sup> describe it in a way in which the connection is clear.

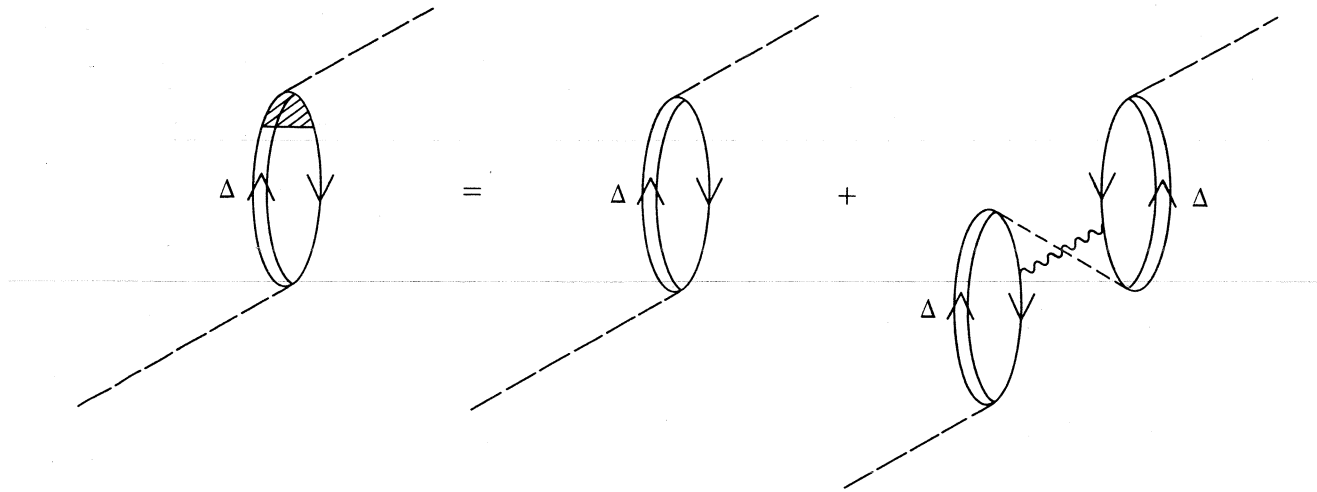


Figure 7. Illustration of vertex corrections in Fermi-liquid nomenclature. The dashed line represents the pion; the wavy line here represents a number of  $\omega$ -meson exchanges, the effect of which can be thought of as a hard-core repulsion of radius  $a \approx 0.4$  fm.

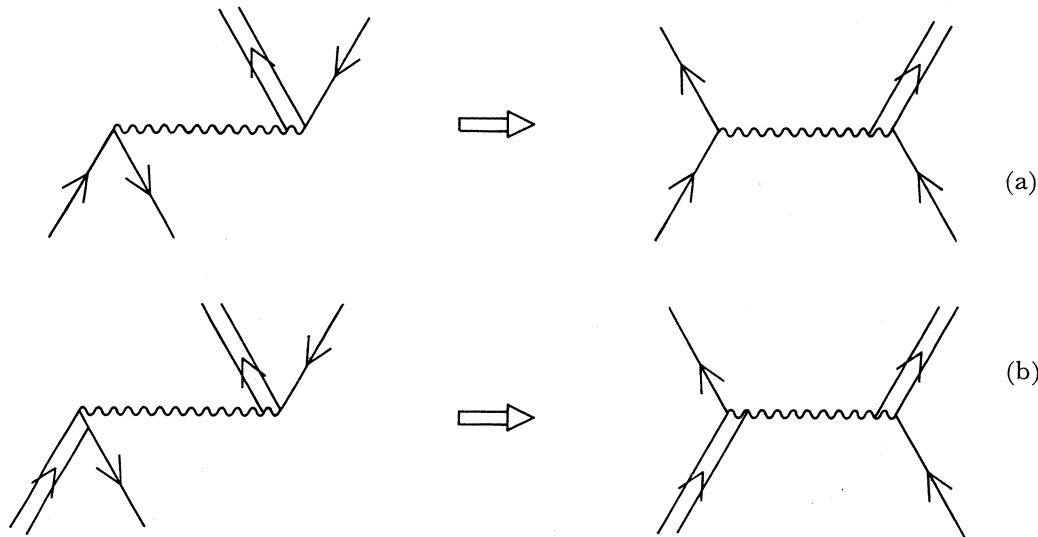


Figure 8. Forces reinterpreted in the particle-particle channel. Here the wavy line represents the complete (possibly  $\omega$ -dependent) interaction.

We can be reasonably sure that  $\rho$ -meson exchange also contributes to the force. The tensor coupling\* of the  $\rho$  meson to the nucleon is

$$\delta L = ig_\rho \left( \frac{1+K_v}{2m} \right) \bar{\psi} (\boldsymbol{\sigma} \times \mathbf{k}) \cdot (\boldsymbol{\tau} \cdot \boldsymbol{\rho}) \psi. \quad (28)$$

Here vectors in both ordinary and isospin space are indicated. Commonly accepted values of  $g_\rho^2$  are  $\sim 0.5$ ;  $K_v = 3.7$  is the isovector magnetic moment term in the electromagnetic current.

\*Exchanges invoking the vector coupling will simply modify slightly the hard-core repulsions.

The above  $\delta L$  for the tensor interaction of the  $\rho$  meson between nucleons is easily translated into an interaction between nucleon and isobar by introducing the transition spin and transition isospin,<sup>17</sup>  $S$  and  $T$ . These are  $4 \times 2$  matrices, since the lead from the two-component nucleon to the four-component isobar. Interaction are formally the same, the transition spins replacing  $\sigma$  and  $\tau$ . One easily finds the interaction from  $\rho$ -exchange in Figure 8a.

$$V_{\rho\text{-exchange}} = -\frac{f_\rho f_\rho^*}{m_\rho^2} \left\{ \frac{\frac{2}{3}(\sigma_1 \cdot S_2)k^2 - [(\sigma_1 \cdot k)(S_2 \cdot k) - \frac{1}{3}(\sigma_1 \cdot S_2)k^2]}{k^2 + m_\rho^2 - \omega^2} \right\} (\tau_1 \cdot T_2) \quad (28.1)$$

where

$$f_\rho = g_\rho (1 + K_\nu) m_\rho / 2m \quad (28.2)$$

and  $f_\rho^*$  is the  $\Delta N_\rho$  coupling constant.

If this potential from  $\rho$ -exchange were to be used directly in the spin, isospin sound, we would find contributions from the spin-spin and tensor interactions in Eq (28.1) canceling each other. This is because the spin, isospin-sound is established by the pionic  $(\sigma \cdot k)$  interaction operating on the vacuum, and the  $\rho$ -coupling goes as  $[\sigma \times k]$ . We now argue that the two invariants in Eq. (28) should be treated separately. The  $(\sigma_1 \cdot S_2)$  term contains a  $\delta(r)$  interaction which will be removed by the short-range repulsion due to  $\omega$ -exchange; i.e., if we write

$$\frac{(\sigma_1 \cdot S_2)k^2}{k^2 + m_\rho^2 - \omega^2} = (\sigma_1 \cdot S_2) - \frac{(\sigma_1 \cdot S_2)(m_\rho^2 - \omega^2)}{k^2 + m_\rho^2 - \omega^2} \quad (29)$$

we see that upon removal of the first term on the right-hand side, which is the  $\delta$  function, the remaining term is relatively innocuous, and has even changed sign. The tensor part of Eq. (28.1) is relatively unaffected by the short-range repulsion although when expressed in coordinate space it will be cut off at short distances.

The only question left concerns  $f_\rho^*$ . We claim that the tensor coupling between nucleon and isobar can reliably be calculated by using the quark model. This coupling involves matrix elements of  $\sigma_i \tau_j$ , in terms of quark spins and isospins, and the quark model has been particularly successful not only in calculation of nucleon spin but in predicting, in terms of them, the predominant  $M1$  excitation of the  $\Delta_{33}(1236)$  isobar in photoproduction. We use here just such matrix elements, although admittedly off-energy shell.

Calculation of this coupling is described by Haapakoski.<sup>12</sup> Of course, the pion coupling to quarks also involves matrix elements of  $\sigma_i \tau_j$ , so that ratios of nucleon isobar to nucleon-nucleon couplings will be the same for the tensor coupling of the  $\rho$  meson as for pions. We reiterate, however, that the quark model should be better in predicting the tensor coupling of the  $\rho$  meson between nucleon and isobar than in calculating pion couplings, because we are here using the quark model where it is strongest! The modification due to inclusion of  $\rho$ -exchange is tremendous. Figure 9 shows the (static) transition potential found by Haapakoski with and without inclusion of  $\rho$ -exchange.

Both Bäckman and Weise<sup>13</sup> and Bertsch and Johnson<sup>6</sup> find that inclusion of  $\rho$ - and  $\omega$ -exchange cuts down the isobar contribution drastically, sending the critical

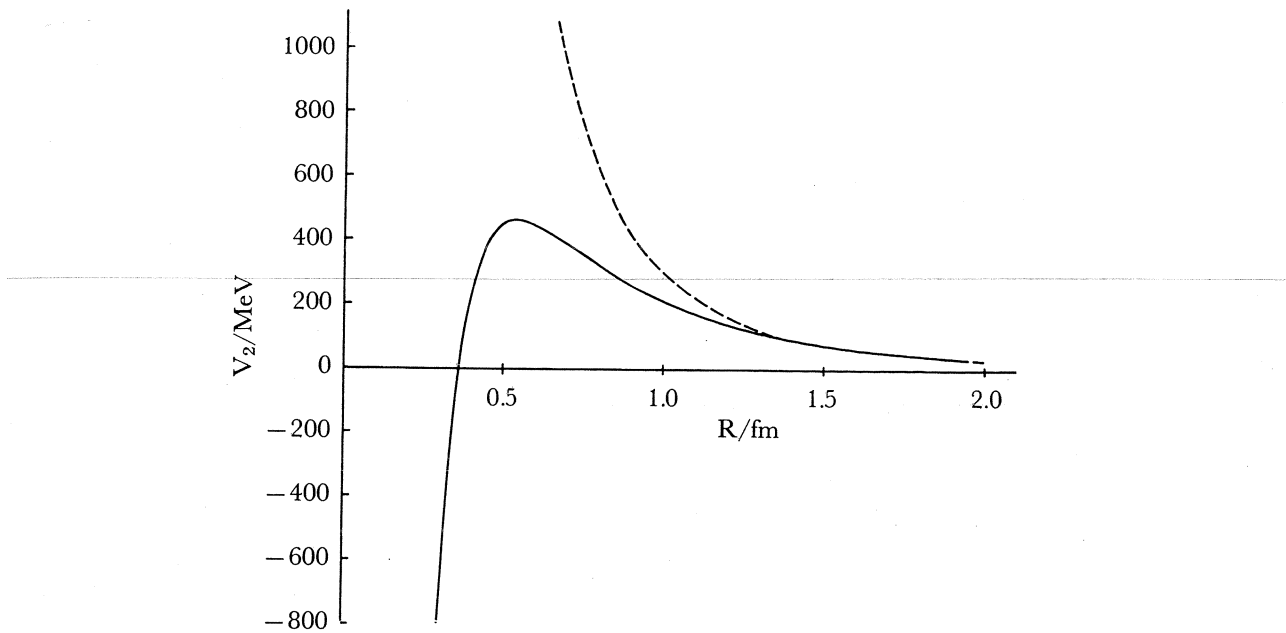


Figure 9. Solid line: the transition potential  $V$  including the  $\rho$ -contribution; dashed line: the  $\pi$ -contribution alone. (From Haapakoski.<sup>12</sup>)

Table 2

Threshold Values for  $\pi^-$  Condensation in Neutron Matter Including Isobars, With Nucleon-Nucleon Correlations and S-Wave Pion Interactions Taken Into Account

	$\rho_c/\rho_0$	$\omega_c[m_\pi]$	$k_c[m_\pi]$
OPEP only*	0.6	0.55	2.1
Isobar-nucleon corr. incl.**	2.1	1.1	2.9

\*One-pion-exchange isobar-nucleon interaction only.

\*\*Including isobar-nucleon correlations due to  $\rho$ -exchange supplemented by a short-range ( $d=0.5$  fm) cutoff.

density for condensation in neutron matter well above  $\rho_0$ . (These authors multiply the spin-spin and tensor interactions by a common correlation factor.)

Table 2 presents the results of Bäckman and Weise with inclusion of isobars. “OPEP” means that in the potentials (Figure 9) only the pion is included in the interaction. These calculations were made to compare with the results of Migdal et al.,<sup>8</sup> who did not put correlations into their calculations with isobars. The small difference between these results and those of Migdal et al. stems from the use here of chemical potentials  $\mu_n$  and  $\mu_p$  of Sjöberg as in Table 1, rather than those of the free Fermi gas.

We note in closing that the matrix element, Figure 8b, can be obtained by the above arguments by making the replacements

$$\sigma_1 \rightarrow S_1, \quad \sigma_2 \rightarrow S_2$$

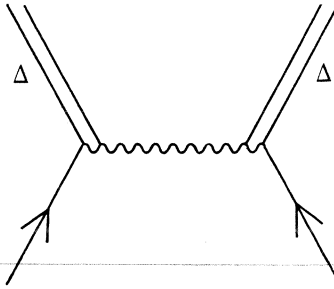


Figure 10. Interaction leading to the double- $\Delta$  component in the deuteron.  
Here the wavy line represents all possible interactions.

in both pion exchange and the tensor-coupling part of the  $\rho$ -exchange potential. A similar interaction (see Figure 10) leads to the double- $\Delta$  component of the deuteron wave function. With the above model for this transition matrix element, Haapakoski and Saarela (to be published) obtain a probability of  $\sim 0.5\%$  for this component which seems to be in accord with experiment. Without the many agencies cutting down the one-pion-exchange interaction, they obtain unreasonably large probabilities.

### IX. REFINEMENTS WHICH CAN AND SHOULD BE MADE

A. Inclusion of nucleon recoil in the Lindhard function which, for the large  $k_c$  encountered, changes  $U(k, \omega)$  roughly from  $\rho/\omega$ , Eq. (14), to

$$U(k, \omega) \cong \frac{\rho}{\omega + k_c^2/2m}$$

where  $m$  is the nucleon mass.

B. The values of  $\mu_n$  and  $\mu_p$  must be calculated including the internal degrees of freedom of the nucleon-nucleon interaction (see Figure 5). From the discussion following Figure 5 we see that this will increase  $\mu_n - \mu_p$  and raise the condensate density.

C. Because of the large values of  $k_c$ , form factors will have some influence in the  $NN\pi$  and  $\Delta N\pi$  interactions.

D. Relativistic effects in the isobar recoil must be taken into account; e.g., the factor  $k^2$  in Eq. (26) is modified when the relativistic Rarita-Schwinger isobar is used. (Barshay and Brown<sup>10</sup> found that inclusion of such factors gave large reductions in the calculated pion double-charge exchange.)

All these effects tend to raise the condensate density, so that the final  $\rho_c/\rho_0$  will be significantly higher than shown in Table 2.

### REFERENCES

1. A.B. Migdal, *ZhETF* **61**, 2210 (1971); *Sov. Phys. JETP* **34**, 1184 (1972).
2. R.F. SAWYER, *Phys. Rev. Lett.* **29**, 382 (1972); D.J. SCALAPINO, *Ibid.* 386.

3. R.F. SAWYER AND D.J. SCALAPINO, *Phys. Rev.* **D7**, 953 (1972).
4. G. BAYM, *Phys. Rev. Lett.* **30**, 1340 (1973).
5. G.E. BROWN, *Unified Theory of Nuclear Models and Forces*, Chap. IV, North-Holland, Amsterdam, 1971.
6. G. BERTSCH AND M. JOHNSON, *Phys. Lett.* **48B**, 397 (1974); and preprint.
7. G. BAYM AND E. FLOWERS, *Nucl. Phys.* **A222**, 29 (1974).
8. A.B. MIGDAL, O.A. MARKIN, AND I.N. MISHUSTIN, *ZhETF* **66**, 443 (1974).
9. W. WEISE AND G.E. BROWN, *Phys. Lett.* **48B**, 297 (1974).
10. S. BARSHAY AND G.E. BROWN, *Phys. Lett.* **47B**, 107 (1973).
11. M. ERICSON AND T.E.O. ERICSON, *Ann. Phys.* **36**, 323 (1966).
12. A.M. GREEN AND P. HAAPAKOSKI, in Fifth Int. Conf. on High Energy Physics and Nuclear Structure, Uppsala, June 1973, and T.F.T. Helsinki preprint; Talk at Symp. on Correlations in Nuclei, Balatonfüred, Hungary, Sept. 1973; P. HAAPAKOSKI, *Phys. Lett.* **48B**, 307 (1974).
13. S.O. BÄCKMAN AND W. WEISE, To be published.
14. S.O. BÄCKMAN, Private communication.
15. O. SJÖBERG, *Nucl. Phys.* **A222**, 161 (1974).
16. S. BARSHAY, G.E. BROWN, AND M. RHO, *Phys. Rev. Lett.* **32**, 787 (1974).
17. H. SUGAWARA AND F. VON HIPPEL, *Phys. Rev.* **192**, 1764 (1968).

# Comments on Charged Pion Condensation in Dense Matter

GORDON BAYM

*University of Illinois at Urbana-Champaign, Urbana, Illinois 61801*

I would like to add to Gerry Brown's talk some comments on the physics of the instability leading to pion condensation, and to remark briefly on the nature of the condensed state. Because pions are bosons, if they do appear in the ground state they will macroscopically occupy the lowest available mode, i.e., form a condensate as in ordinary Bose-Einstein condensation. Such a state corresponds to a classical or coherent excitation of the pion field in the medium, or alternatively, to a nonvanishing ground state expectation value of the pion field; in the normal ground state, with no pions, this expectation value vanishes.

The appearance of charged pions, or more precisely, pionlike modes of excitation in the ground state, leading to a nonvanishing expectation value of the charged pion field can actually take place through several different physical mechanisms. As Migdal<sup>1</sup> has shown, neutron star matter may possess a neutron hole-proton particle collective mode, or spin-isospin sound, with the quantum numbers of the  $\pi^+$ . Let us denote this mode, a form of zero sound, by  $\pi_s^+$ . Then in addition to the possibility  $n \rightarrow p + \pi^-$ , in which a neutron quasi particle turns into a proton quasi particle plus a  $\pi^-$ , condensation can occur via spontaneous appearance of a  $\pi^-$  plus the collective mode  $\pi_s^+$ . In addition, if the matter is initially in beta equilibrium, so that a small fraction of protons are initially present, then condensation can occur also through the mechanism  $p \rightarrow n + \pi_s^+$ . The existence of this additional mechanism for condensation means that matter in beta equilibrium can condense at a lower density than pure neutron matter; however, studies by Weise and Brown<sup>2</sup> indicate that with inclusion of short-range correlations between nucleons, matter in beta equilibrium does not condense at very different density than pure neutron matter.

The charged-pion condensed system is characterized by a nonvanishing expectation value  $\langle \Pi(\mathbf{r}, t) \rangle$  of the charged pion field. In the normal state this expectation value vanishes from charge conservation, as well as parity conservation, since the pion field is pseudoscalar. The  $\pi^-$  condensed phase is a state of broken symmetry with a complex parameter  $\langle \Pi \rangle$ , and it is thus superconducting. It is useful to compare this state with a neutral Bose superfluid such as liquid  $^4\text{He}$  and with a BCS superconductor. In  $^4\text{He}$  the nonvanishing complex order parameter is  $\langle \psi(\mathbf{r}, t) \rangle$ , where  $\psi$  is the  $^4\text{He}$  field operator. In a BCS superconductor one has pairing of particles of opposite spin and momenta, and  $\langle \psi_\uparrow(\mathbf{r}, t) \psi_\downarrow(\mathbf{r}, t) \rangle$  is the order parameter. One can equivalently regard the  $\pi^-$  condensed phase as arising from a pairing of neutron particles with proton holes, and proton particles with neutron holes, with order parameter  $\langle \psi n^\dagger(\mathbf{r}, t) \sigma \psi_p(\mathbf{r}, t) \rangle$ , the divergence of which is the nonrealistic source of the pion field  $\langle \Pi \rangle$ .

From another point of view one can look at the  $\pi_s^+$  mode in the normal state as the fluctuations in isospin space of the neutron isospin vectors. The neutrons normally point along the negative  $T_z$  axis; the mode  $\pi_s^+$  is a small oscillation about

zero of the angle  $\alpha$  that the vector makes with respect to the negative  $T_z$  axis. At the point of condensation this mode becomes "soft" and the system beyond this prefers a nonzero value of  $\alpha$ . The Hamiltonian is then diagonalized<sup>3,4</sup> by the nucleon state vectors that are linear combinations of neutrons and protons.

The equilibrium conditions<sup>5</sup> of the  $\pi^-$  condensed state are first that  $\langle \Pi^-(\mathbf{r},t) \rangle = e^{-i\mu_\pi t} \langle \Pi^-(\mathbf{r}) \rangle$  where  $\mu_\pi = \mu_n - \mu_p$  is the  $\pi^-$  chemical potential. Even though the pions may condense into a mode  $e^{i\mathbf{k}\cdot\mathbf{r}}$  with a nonzero momentum  $\mathbf{k}$ , or perhaps a more complicated mode with spatially varying modulus,<sup>6</sup> the spatial average of the electromagnetic current must vanish in the ground state. So also must the spatial averages of the baryon current, and the electronlike and muonlike lepton currents vanish. The net charge density associated with the condensed field (in the absence of the interactions dependent on  $\Pi$ ) is<sup>5</sup>  $-2\mu_\pi |\langle \Pi \rangle|^2$ ; since, generally,  $\mu_\pi > 0$ , this is a negative charge density. The overall system is electrically neutral.

By contrast, possible  $\pi^0$  condensation of dense matter is described by a non-vanishing real expectation value  $\langle \Pi_0(\mathbf{r}) \rangle$  of the neutral pion field. Because the order parameter is real, the state is therefore not superconducting. Rather, since the (non-relativistic) source of the neutral pion field is the divergence of the  $T=1$ ,  $T_z=0$  nucleon spin polarization, the neutral condensed mode  $\langle \Pi_0(\mathbf{r}) \rangle$  will have a finite wave vector, thus varying in magnitude in space, and leading to a spatially nonuniform spin-ordered phase, analogous to the state of electron particle-hole "pairing" produced by a Peierls' transition in a solid.

## REFERENCES

1. A.B. MIGDAL, *Phys. Rev. Lett.* **31**, 247 (1973).
2. W. WEISE AND D.J. BROWN, *Phys. Lett. B* **48**, 397 (1974).
3. R.F. SAWYER AND D.J. SCALAPINO, *Phys. Rev. D* **7**, 953 (1973).
4. G. BAYM AND E. FLOWERS, *Nucl. Phys. A* **222**, 29 (1974); C.-K. AU AND G. BAYM, *Nucl. Phys. A* **236**, 500 (1974).
5. G. BAYM, *Phys. Rev. Lett.* **30**, 1340 (1973).
6. R.F. SAWYER AND A.C. YAO, *Phys. Rev. D* **7**, 953 (1973).

# Nuclear Matter Calculations of Finite and Infinite Nuclear Systems From Relativistic Field Theory

A.K. KERMAN

*Massachusetts Institute of Technology, Cambridge, Massachusetts 02139*

## I. MOTIVATION

The central aim of these efforts is to perform calculations of nuclear properties in the region from saturation density to, say, twice that density with our current knowledge of finite nuclei. The main question, of course, is how to extrapolate this knowledge. We believe that the “standard” program in nuclear physics of taking the interaction that fits the two-body data, constructing from it an effective nucleon-nucleon interaction in the nuclear medium, and performing Hartree-Fock or shell-model calculations has had many successes but is probably not as reliable as we need for this extrapolation.

What we suggest is a new direction which can be put in perspective with the aid of the diagram in Figure 1. The claim we make is that one can do all the conventional calculations such as Hartree-Fock, Hartree-Fock-Bogoliubov, random phase approximation (RPA), etc., along this new route. We now sketch the route we have been pursuing.

## II. THE HARTREE APPROXIMATION

The key thrust of the effort is to develop a framework in which the meson field can be made self-consistent. What we are looking for are the equations of motion of single-hole states. We identify  $\langle p | \bar{\psi} \psi | p \rangle$  as the probability amplitude for destroying a particle in an occupied state. Then the property

$$\langle p | \psi(x) | P \rangle = e^{i(P-p)x} \langle p | \psi(0) | P \rangle, \quad (1)$$

i.e., Lorentz invariance, goes through as in the conventional equations. We obtain the Hartree approximation in our equations of motion by truncating intermediate-state sums to include only those states that have the same mass as the initial mass. For those situations in which the mass is much greater than the momenta (for example  $^{16}\text{O}$ ) one reduces the elements of the equations to functions of the three momenta. With these as the ingredients of our approach we claim we can make the “conventional” nuclear physics approximations and perform calculations. Furthermore, we find we can generate the equations without violating Lorentz invariance. In this systematic approach we can also get the Hartree-Fock equations, but we have not yet worked out the terms that result from exchange.

## III. ACTUAL CALCULATIONS

Since this is rather new territory we really don’t know what field theory to start with. For simplicity we start with the  $\sigma$  model and we express it in a manner that is

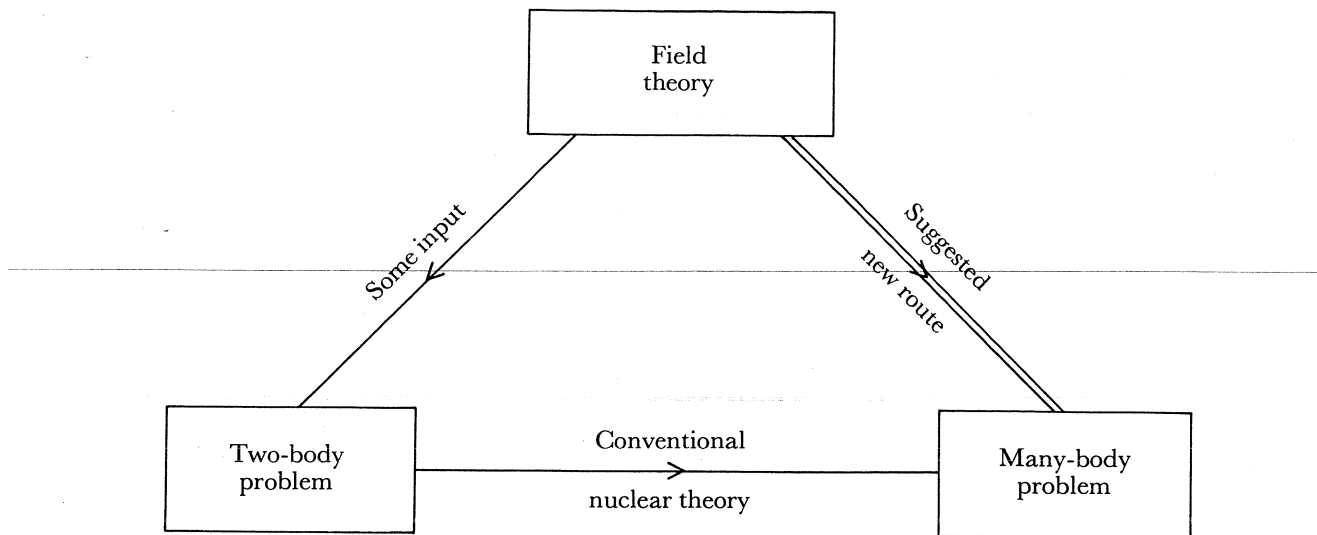


Figure 1.

general enough for finite systems. However, we know by experience that the exchanges of heavier mesons ( $\omega, \rho, \phi, \eta$ , etc.) are important, and in order to attempt to accommodate their effects here we attach a form factor to the nucleon. We then concentrate on looking at specific relativistic many-body effects. The  $\sigma$  model in the Hartree approximation takes the form

$$-(\nabla^2/\mu_\rho^2 - 1)\chi = \frac{1}{2}(3 - \chi)\chi^2 + \alpha\rho_F \quad (2)$$

where  $\chi(r)$  is the meson field expressed in units of the nucleon mass at ordinary vacuum. Here  $\rho_F$  signifies the nucleon density and is given in a Thomas-Fermi-type approximation by

$$\rho_F \sim \int^{k_F} dk \chi k^2 / \sqrt{k^2 + m^2} \quad (3)$$

for an infinite system and a sum over occupied states for a finite system.

L.D. Miller of MIT has iterated these equations for  $^{40}\text{Ca}$  and has obtained results analogous to those found at Stanford for the quark model of nucleons. Namely, all the particles accumulate in a dense shell at the nuclear surface with an abnormal state of the vacuum ( $-2m/g$ ) inside. Note that we have not yet put in vacuum polarization, however.

One may develop an energy density  $\Sigma$  in this approach,

$$\Sigma = -\chi^4 \ln \chi + (3\chi^2 - 1)(\chi^2 - 1) \equiv f(\chi), \quad (4)$$

where the second term is necessary to have chiral symmetry. Then, the implication of intermediate states whose mass is not equal to the initial mass is a type of RPA with mesons popping up at intermediate times. This, then, generates a correction to the energy density,  $\Delta\Sigma$ , where

$$\Delta\Sigma = \frac{3}{2} f'(\psi) \quad (5)$$

where

$$\psi = 1 + b(\chi^2 - 1). \quad (6)$$

This indicates a strong interplay between these states and those with the initial mass with delicate cancellations likely. Thus one is forced to conclude that it will probably be necessary to do Hartree-Fock and RPA together to accommodate these subtle interplays correctly.

It is appropriate to comment on an additional big problem that has been ignored here. One should include in (2) a Thomas-Fermi-type term for a sum over occupied but negative energy states. This leads to major difficulties, however.

#### IV. EXPERIMENTS TO DO

There are at least three types of experiments that one might speculate are worthwhile to do.

1. Search for stable nuclei near  $A = 250$ ,  $Z = 125$ . They may exist and not be seen naturally because nothing can decay through this region to feed these nuclei. For this region we don't have to wait for uranium on uranium.
2. Search for density isomers near  $^{208}\text{Pb}$ , for example, with binding energy of about 5 MeV/nucleon. As for the question of lifetimes, they may be comparable to fission lifetimes.
3. In fact, for these excitations, 2 MeV/nucleon, one may even see density isomers in collisions of rather light systems, say  $^{40}\text{Ar}$  on  $^{40}\text{Ar}$ .

# On the Possibility of Nuclear Shock Waves in Relativistic Heavy-Ion Collisions\*

J. HOFMANN, H. STÖCKER, W. SCHEID, AND W. GREINER

*Institut für Theoretische Physik der Johann Wolfgang Goethe Universität,  
Frankfurt am Main, Germany*

The possibility of compression of nuclear matter in the overlap region of two colliding nuclei has been discussed in recent papers.<sup>1,2</sup> In the second of these, the formation of  $(\frac{3}{2}, \frac{3}{2})$  resonances and higher nucleon states as a consequence of the thermal excitation of the nucleons during the collision process was suggested. We have generalized this model to include resonances of higher mass and have studied their influence on the compression effect.

Using a hydrodynamical model we first discuss the validity of hydrodynamics in nuclear dimensions. At high kinetic energy of the nuclei the nucleons of the individual nuclei have high relative momenta. Therefore we can disregard the Pauli principle and calculate<sup>3</sup> the mean free path of nucleons using the free nucleon-nucleon cross section  $\sigma \simeq 40$  mb. With  $\rho_0 = 0.17$  fm<sup>-3</sup> we thus find for the mean free path

$$\lambda = \frac{1}{\sigma \rho_0} \frac{\rho_0}{\rho} = \frac{1}{4.0 \times 17} \frac{\rho_0}{\rho} \simeq 1.47 \frac{\rho_0}{\rho} \text{ fm}$$

which yields  $\lambda = 1.47, 0.735, 0.368$  fm for  $\rho = \rho_0, 2\rho_0$ , and  $4\rho_0$  respectively. The validity of hydrodynamics is assured by the condition  $\lambda \ll R$ , where  $R$  is the dimension of the compression zone, i.e., of the nucleus. Therefore, the hydrodynamics should be better, the more the nuclear matter is compressed. This confirms the approximate applicability of hydrodynamics in superdense nuclear matter. The question arises, however, whether a shock can develop during the initial phase of a nucleus-nucleus encounter, when the densities are still small. Since the free nucleon-nucleon scattering cross section is mainly in the forward direction, one would naively expect a rather unperturbed interpenetration of the two colliding nucleon clouds, and therefore no initial compression. However, at 1 to 2 GeV/ $N$  most of the total nucleon-nucleon cross section is inelastic, i.e., the process  $N \rightarrow N^* \rightarrow N + \pi$  occurs within  $6 \times 10^{-24}$  sec, which immediately helps to scatter the pions and nucleons perpendicularly to the axis of collision, i.e., this helps to shock the matter. This is further supported by the fact that the nucleons of a nucleus exhibit short-range correlations with typical momenta up to 300 MeV/ $c$ . These also help to scatter the colliding nucleons perpendicularly to the collision axis, i.e., to shock nuclear matter. In a nucleus-nucleus collision there could eventually occur multiple nucleon-nucleon collisions, so that a sort of collective short-range correlation can lead to an enhancement of the scattering perpendicular to the direction of the colliding nuclei.

\*Work supported by the Bundesministerium für Forschung und Technologie and by the Gesellschaft für Schwerionenforschung. We acknowledge stimulating discussions with Professor E. Schopper.

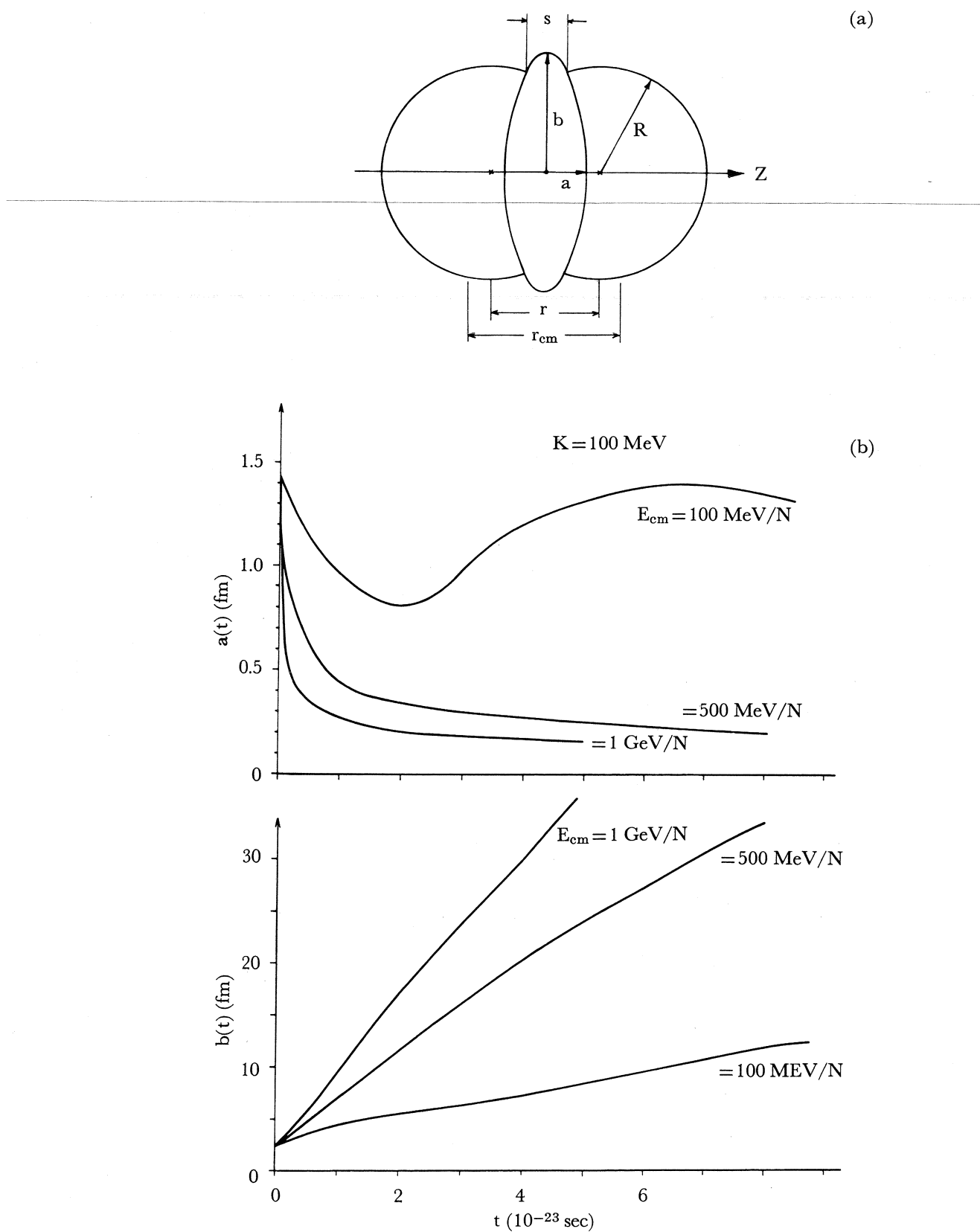


Figure 1. (a) The basic configuration of the model for the central collision of two identical nuclei with a compression zone (ellipsoid) in the middle. (b) The time dependence of  $a(t)$  and  $b(t)$  in  $^{238}\text{U}$ - $^{238}\text{U}$  collision at energies of 100, 500, and 1000 MeV/N. A compressibility constant  $K=100 \text{ MeV}$  has been assumed.

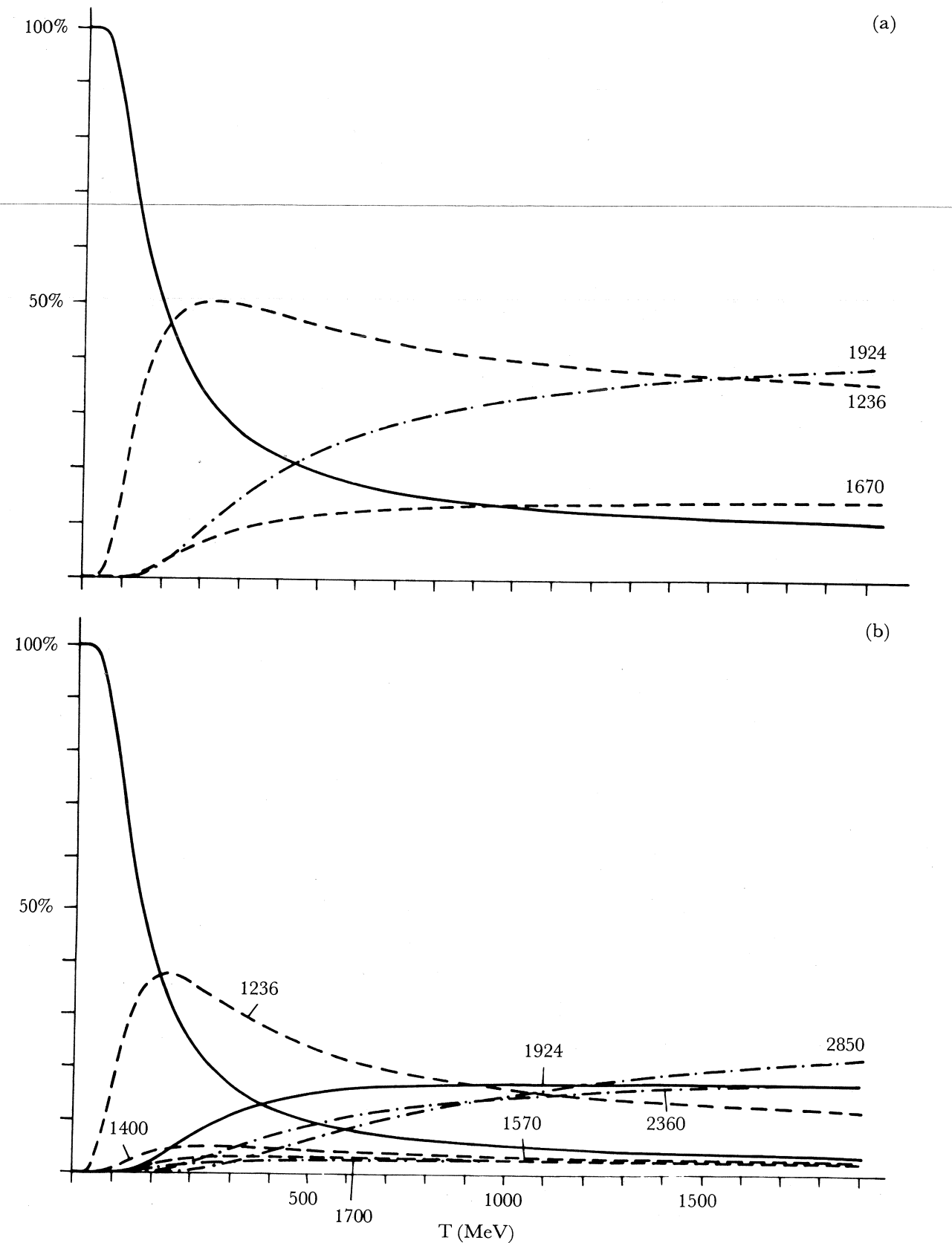


Figure 2. The composition of the isobaric gas as a function of temperature (a) for four isobaric phases and (b) for 10 isobaric phases. The solid curve is for nucleons in the ground state. The energies shown are the excitation energies of the nucleonic resonances.

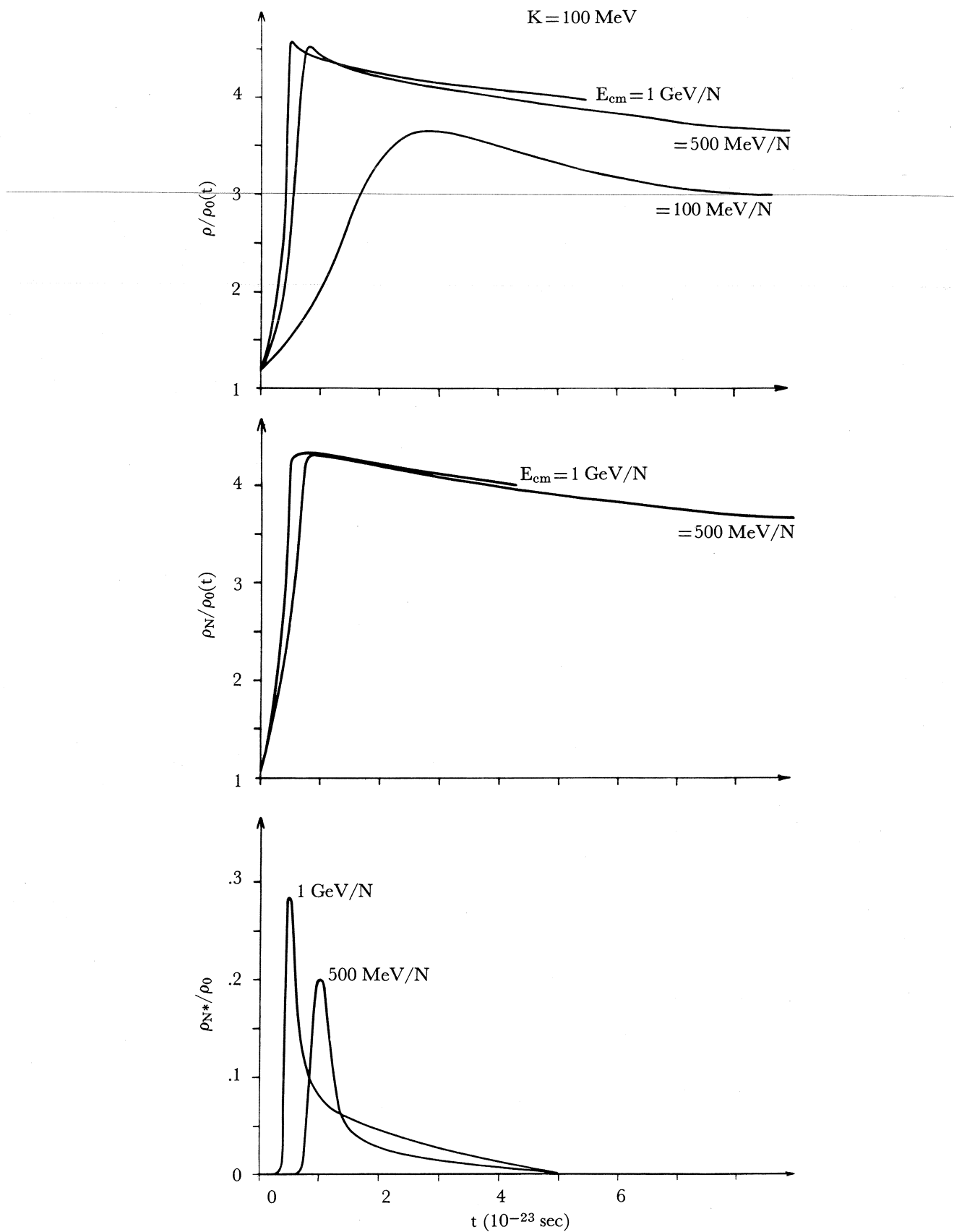


Figure 3. The time dependence of the total density  $\rho(t)$ , the nucleon density  $\rho_N(t)$ , and the  $N^*(\frac{3}{2}, \frac{3}{2})$  density  $\rho_{N^*}(t)$  for the collision described in Figure 1b.

In order to learn the essential features of the compression process, we restrict ourselves to the scattering of two identical nuclei whose volumes are divided into three parts: an ellipsoid with axes  $a(t)$  and  $b(t)$  sandwiched between two cutoff spheres with radius  $R$  and relative distance  $r(t)$  (Figure 1a). Only within this ellipsoid does compression occur ( $\rho > \rho_0$ ). Within the cutoff spheres the density is  $\rho_0$ . Choosing  $R = \text{const}$  during the collision, we are dealing with three degrees of freedom:  $a$ ,  $b$ , and  $r$ .

The exact solution of the full hydrodynamical problem, which would involve dividing the total volume into a great number of independent parts, is clearly very complicated. In contrast, the above described model<sup>1,2</sup> is mathematically much more feasible and contains the essential physical features; Figure 1b, showing the time dependence of  $a(t)$  and  $b(t)$ , indicates a push-out of nuclear matter perpendicularly to the collision axis. Figure 2 gives the composition of hadronic matter, calculated according to a Boltzmann distribution. The excitation energies of the various nucleonic isobars are indicated at the curves. Figure 3 shows the total density obtained  $\rho$ , the nucleon density  $\rho_N$ , and the  $N^*$  density  $\rho_{N^*}$  as a function of time for various collision energies.

The formation of such nuclear shock waves in relativistic heavy-ion collisions is a fundamental process because of its relation to the velocity of first sound in nuclear matter,  $c_s = \sqrt{K/9M}$ , and, through that, to the nuclear compressibility,

$$K = 9 \rho_0^2 d^2 W / d\rho_0^2$$

where  $M$  = nucleon mass and  $W$  = total nucleon binding energy. Shock waves serve as a generator of high nuclear densities which might be useful in searching for density isomers and for creating highly isobaric and hot nuclear matter.<sup>2</sup>

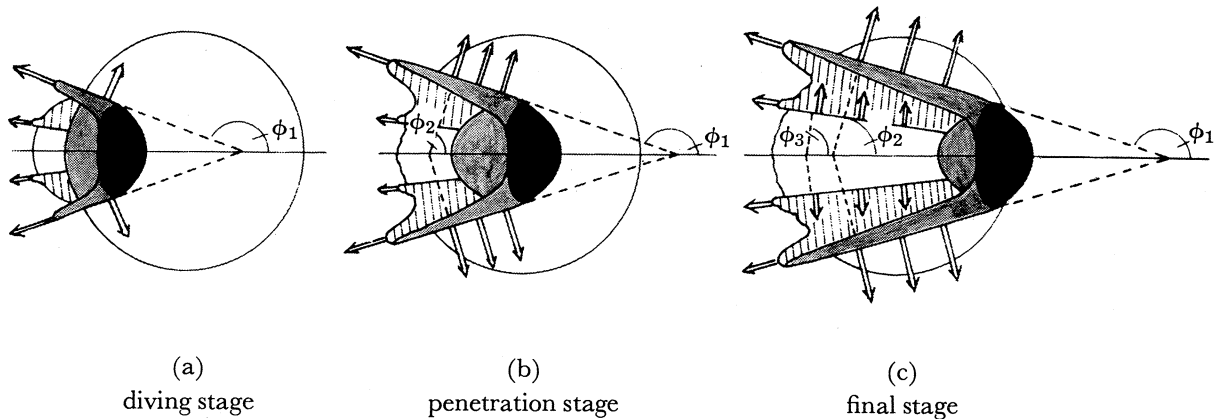


Figure 4. Schematic figure of the various stages in a central collision between an incident smaller (relativistically contracted) and a heavier target nucleus. The head-front shock is drawn very dark. The Mach-shock wave, which is traveling to the sides, also contains high density but not as high as the projectile head. A minor backward fragment ejection along the Mach-front is also indicated. This is expected especially in the diving stage, where it is easier to eject fast particles along the Mach-shock into free space. A secondary Mach-shock wave of intermediate density is also indicated.

More recently\* we investigated a signature of shock waves, namely *Mach cones*, which should occur if a smaller nucleus 1 ( $A_1$ ) travels through a bigger one 2 ( $A_2 > A_1$ ) with overshock velocity.<sup>5</sup> This process is illustrated in Figure 4 for a central collision of unequal fragments and various steps of interpenetration. In the initial phase a *splashinng tide wave* is expected at the backward angle  $\sin\phi_1 = v_s/v$  ( $v_s$  is the shock velocity and  $v$  the projectile velocity). This can be imagined as the initial Mach-shock traveling to some extent more easily into the matter-free exterior during the diving phase. There should also occur a shock wave in the light fragment caused by the heavy one. It will cause some destruction of  $A_1$ , but not its annihilation, and will lead in the lab system to a very smeared-out echo-Mach at angles around  $90^\circ$  or slightly in the forward direction.\*\* The penetrating core will, upon diving, deform for better traveling and cause in the second stage a strong shock at its head (*head shock*) and initiate a primary *Mach-shock wave* propagating in the direction  $\phi_2$  through  $A_2$ , determined by  $\cos\phi_2 = v_s/v$ . A strong disturbance of nuclear matter ( $\rho/\rho_0 \approx 2$  to 4) propagates with the shock velocity  $v_s$ . At the position  $\phi_1 = 90^\circ + \phi_2$ , where the Mach-front hits the surface  $A_1$ , some ejection of matter can be expected. Clearly,  $\phi_1$  and  $\phi_2$  are strongly correlated and therefore observable in experiments, as is the Mach-angle  $\phi_2$  itself, in which direction the by far major ejection of matter should occur. This process will continue up into the final stage for any impact parameter  $b < R_1 + R_2$ , for which also Mach-shock waves are generated. Even though the individual collisions with  $b \neq 0$  are expected to yield a very asymmetric Mach-distribution still peaking at  $\phi_2$ , the ensemble of all events should show only  $\phi_2$  and minor  $\phi_1$  as the dominant directions for fragment emission.

Behind the projectile a low-density channel ("drilled hole" or "dead-water region") collapses, which – contrary to the fragments emitted along  $\phi_2$  and  $\phi_1$  – leads quite plausibly to a rather isotropic distribution (thermal evaporation). Behind the primary Mach-shock wave, secondary and eventually further Mach cones can occur. They characterize lower-density zones in between the primary zone and the dead-water region and are well known in hydrodynamics (see, e.g., ref. 6).

As mentioned above, it is necessary to obtain expressions for the projectile velocity in nuclear matter and also for the shock velocity. The latter is dependent on the matter density  $\rho$ , which is most easily obtained in the model described in refs. 1 and 2. The relativistic shock-front velocity  $v_s$  is<sup>7</sup>

$$v_s = c \sqrt{\frac{pW(\rho)\rho}{[W(\rho)\rho - W(\rho_0)\rho_0][W(\rho_0)\rho_0 + p]}} \quad (1)$$

where the pressure  $p$  is given through the energy density  $W(\rho)$  via  $p = \rho^2 \times (\partial W / \partial \rho)_{\text{const. entropy}}$  [see Eq. (4)]. The Mach-angle  $\phi_2$  is then given by

\*The material that follows was added to the manuscript, but not presented orally. (See also ref. 4.)

\*\*If, however, the fragments were equal, Mach- and echo-Mach-shock would be equal in the center-of-mass system, and this would lead to a push-out of matter perpendicularly to the axis of motion, as discussed in ref. 1. This is important in Schopper's experiment<sup>4</sup> for  $^{16}\text{O}$ -Cl collisions. It produces a minor peak in the forward direction in the lab system which is expected to move towards larger forward angles as the projectile energy increases.

$$\cos\phi_2 = \frac{v_s}{v} = \frac{c}{v} \sqrt{\frac{p \cdot W(\rho)\rho}{[\rho W(\rho) - \rho_0 W(\rho_0)][\rho_0 W(\rho_0) + p]}} \quad (2)$$

and related to the compressed density  $\rho/\rho_0$  in the Mach-shock wave. This in turn is related to the dynamics of the model used and to the compression constant  $K$  of nuclear matter. The dynamical calculations are carried out with the energy density as a function of  $\rho$  given by

$$W(\rho) = Mc^2 - W_0 + \frac{K}{18\rho\rho_0} (\rho - \rho_0)^2 + \frac{e_T}{\rho}$$

with

$$\frac{e_T}{\rho} = \frac{1}{2} \left( \frac{2\pi}{3} \right)^{2/3} \frac{MK_B^2}{h^2} T^2 \rho^{-2/3} \quad (3)$$

where  $T$  is the temperature, and  $W_0 = 16$  MeV is the binding energy per nucleon at equilibrium. The pressure is given by

$$p = \frac{K}{18\rho_0} (\rho^2 - \rho_0^2) + \frac{2}{3} e_T. \quad (4)$$

By measuring the Mach-angle one can thus deduce the nuclear compression constant  $K$  from Eq. (2). It is essential to note, however, that in this step the specific model (3) enters via the pressure and via the dynamics, which determines the density  $\rho/\rho_0$ .

Indeed, the Mach-shock and head-shock waves and eventually also higher-order Mach-shocks should be observable by *analyzing the angular distribution of fragments occurring in the bombardment of heavy targets with light high-energy nuclei*. Particularly suitable would be detectors that do not register the very light fragment particles, especially pions, because of the above-mentioned isotropic background expected for them. The AgCl detectors used by Schopper et al.<sup>4</sup> and developed by Schopper, Granzer, et al.<sup>8</sup> fulfill this requirement. The distributions of the fragment tracks observed in star events by Schopper et al.<sup>4</sup> indeed show the structure predicted above. For  $^{16}\text{O}$  ions bombarded on Ag the peaks seen for various projectile energies are listed in Table 1.

From the 250-MeV data we deduce the nuclear compression constant  $K = 300$  MeV, and from it the sound velocity  $c_s = \sqrt{K/9M} = 0.19c$ , by applying the specific

Table 1  
Peaks for  $^{16}\text{O}$  Ions Bombarded on Ag

Projectile energy, GeV/N	Major peak ( $\phi_2$ )		Minor peak ( $\phi_{1\text{ theore}} = \phi_{2\text{ theore}} + 90^\circ$ )		$(\rho/\rho_0)_{\text{MS}}$	$(\rho/\rho_0)_{\text{HS}}$
	Exp.	Theor.	Exp.	Theor.		
2.1	53°	53°	145°	143°	3.0	5.4
0.87	45°	48°	133°	138°	3.0	4.1
0.25	20°	21°	110°	111°	2.9	3.0

model outlined in ref. 1. The data are in fair agreement with the assumption of a constant Mach-shock velocity of  $v_s = 0.57c$ . With this shock velocity  $v_s$  we predict the Mach angles given in Table 1, which obviously agree nicely with the observed values. It is worth while to note that the velocity of sound in a relativistic ideal gas comes out as  $c_s = c/\sqrt{3} = 0.577c$ . The 250-MeV/ $N$  data seem to give some evidence also for a secondary Mach-shock traveling with  $v_s^{(2)} = 0.33c$  and its satellite again shifted backward by  $90^\circ$ . For high projectile velocities the primary and secondary Mach-shocks indeed move together, as expected theoretically. In the next to the last column of Table 1 are listed the compression densities reached in the Mach-shock wave, which are obviously considerable but still smaller than those in the head-shock wave (last column). The former are obtained with Eq. (1), and the latter also with Eq. (1), assuming that the head velocity is identical with the projectile velocity.

One might think of target recoil effects as an alternative explanation of these observations. To that end we calculated the target recoil for two cases: pure Coulomb interaction, and Coulomb interaction with a hard core at  $R = R_1 + R_2$ . The true interaction of such highly energetic ions is expected to be between these two cases probably closer to the hard-core potential, because of the strong soft core occurring between relativistic nuclei due to the compression effects. In the first case the recoil peaks at  $90^\circ$ , in the latter case at  $35^\circ$ , but in both cases the recoil peak is independent of energy, contrary to observation. Furthermore, the obvious correlation between the major forward peak and the minor backward peak and the indicated occurrence of secondary Mach-shocks cannot be explained by recoil. One cannot, at this stage, rule out an energy-dependent nucleus-nucleus potential which could reproduce the major peak structure via the recoil effects. The interpretation of the experimental observations as a signature for nuclear head-shock and Mach-shock waves is, however, simpler and more natural. They seem to demonstrate, for the first time, that nuclear compressibility is of the order of  $K = 300$  MeV, that the nuclear sound velocity is approximately  $c_s = 0.19c$ , that the Mach-shock velocity  $v_s = 0.55c$  is nearly independent of projectile energy, and that shock waves exist even at very high energies of 2 GeV/ $N$ . The last contradicts, at least at these energies, the opinion of some workers<sup>9</sup> that nuclei might again become transparent, which we do not share because of short-range correlations and pion-exchange effects.<sup>2</sup> This all adds considerably to fundamental knowledge on the behavior and properties of nuclear matter.

## REFERENCES

1. W. SCHEID, H. MÜLLER, AND W. GREINER, *Phys. Rev. Lett.* **32**, 741 (1974).
2. W. SCHEID, J. HOFMANN, AND W. GREINER, in *Proc. Symp. Physics With Relativistic Heavy Ions* Lawrence Berkeley Lab., July 1974, p. 1, L. Schroeder, Editor, LBL Report 3675; J. HOFMANN, W. SCHEID, AND W. GREINER, Thermal excitation of nucleons in nuclear shock waves, Preprint, Institut für Theoretische Physik, Dec. 1974, to be published.
3. A.N. DIDDENS, in *Proc. 4th GIFT Seminar Theoretical Physics, Universidad de Barcelona, April 1973* p. 170, GIFT (Scientific Information Service, Facultad de Ciencias, Universidad de Zaragoza Zaragoza, Spain).

4. E. SCHOPPER, W. BAUMGARDT, AND J.U. SCHOTT, Search for shock waves in nucleus-nucleus collisions, to be published in *Phys. Rev. Lett.*; J. HOFMANN, H. STÖCKER, W. SCHEID, AND W. GREINER, Mach-cones of fast heavy ions in nuclear matter, to be published.
5. See also D.A. BROMLEY, in *Proc. Int. Conf. Reactions Between Complex Nuclei, Nashville, June 1974*, p. 603, North-Holland, Amsterdam, 1974.
6. W.D. HAYES AND R.F. PROBSTEIN, *Hypersonic Flow Theory*, Academic, New York, 1959.
7. L.D. LANDAU AND E.M. LIFSHITZ, *Fluid Mechanics*, Pergamon, New York, 1959.
8. E. SCHOPPER, F. GRANZER, G. HASSE, ET AL., *Photogr. Sci. Eng.* **17**, 409 (1973); and internal reports from the Institut für Kernphysik and the Institut für Angewandte Physik der Universität Frankfurt am Main.
9. P. J. SIEMENS, See paper in this volume.

# Shock Waves in Colliding Nuclei\*

PHILIP J. SIEMENS  
*The Niels Bohr Institute, Copenhagen, Denmark*

We consider the circumstances under which matter at high densities can be produced in heavy-ion collisions. We argue that laboratory energies of a few hundred MeV per nucleon will be suitable: the matter velocity will exceed the speed of sound, while the nuclear matter has sufficient stopping power to generate a shock front. A measure of the stopping power is the momentum transport length  $\lambda(p)$  shown in Figure 1; if  $\lambda(p)$  is comparable with or greater than the nuclear radius, the nuclei will interpenetrate instead of compressing. The hydrodynamic conservation laws can be written

$$\frac{1}{2} m(\mathbf{v}_0 - \mathbf{v}_s)^2 = \epsilon_s - \epsilon_0 = \frac{1}{2\rho_0} \frac{\nu-1}{\nu} p_s = \left(\frac{\nu-1}{\nu}\right)^2 \frac{1}{2} m(\mathbf{v}_0 \cdot \mathbf{n} - U)^2$$

where  $\epsilon_s, p_s, \mathbf{v}_s$  are the internal energy per nucleon, pressure, and mean velocity of the matter just inside the shock front,  $\epsilon_0$  and  $\mathbf{v}_0$  the internal energy and velocity of the cold, unshocked matter,  $\mathbf{U} = U\mathbf{n}$  is the shock-front velocity, and  $\nu = \rho_s/\rho_0$  is the compression ratio. In terms of dimensionless ratios,

$$\epsilon_s - \hat{\epsilon} = \frac{\nu_\infty - 1}{\nu_\infty - \nu} \left( \frac{\nu-1}{\nu_\infty-1} \frac{R_s}{\hat{R}} - 1 \right) (\hat{\epsilon} - \epsilon_0)$$

where the quantities with a caret (^) over them are computed for cold matter at density  $\rho_s$ ,  $\hat{R} = [\partial \ln(\hat{\epsilon} - \epsilon_0) / \partial \ln \nu]^{-1}$  measures the stiffness of the internucleon forces and the ratio  $R_s = \rho_s [\epsilon_s - \hat{\epsilon}(\nu)] / [p_s - \hat{p}(\nu)]$  describes how the energy converted to heat produces a thermal pressure which resists compression. There is a maximum compression given by  $\nu_\infty = 2R_s + 1$ .

\*Work done in collaboration with M.I. Sobel, J.P. Bondorf, and H.A. Bethe. A preprint of a more detailed paper can be obtained from the author.

Table 1  
 Model Predictions for the Maximum Compression

Degrees of freedom	Maximum compression $\nu_\infty$
nonrel. point particles	4
nonrel. translation + rotation	6
rel. translational motion	7
massless bosons	
Landau theory	$\left[ \frac{1}{3} - \frac{\partial \ln m^*(\nu)}{\partial \ln \nu^2} \right]^{-1} + 1$

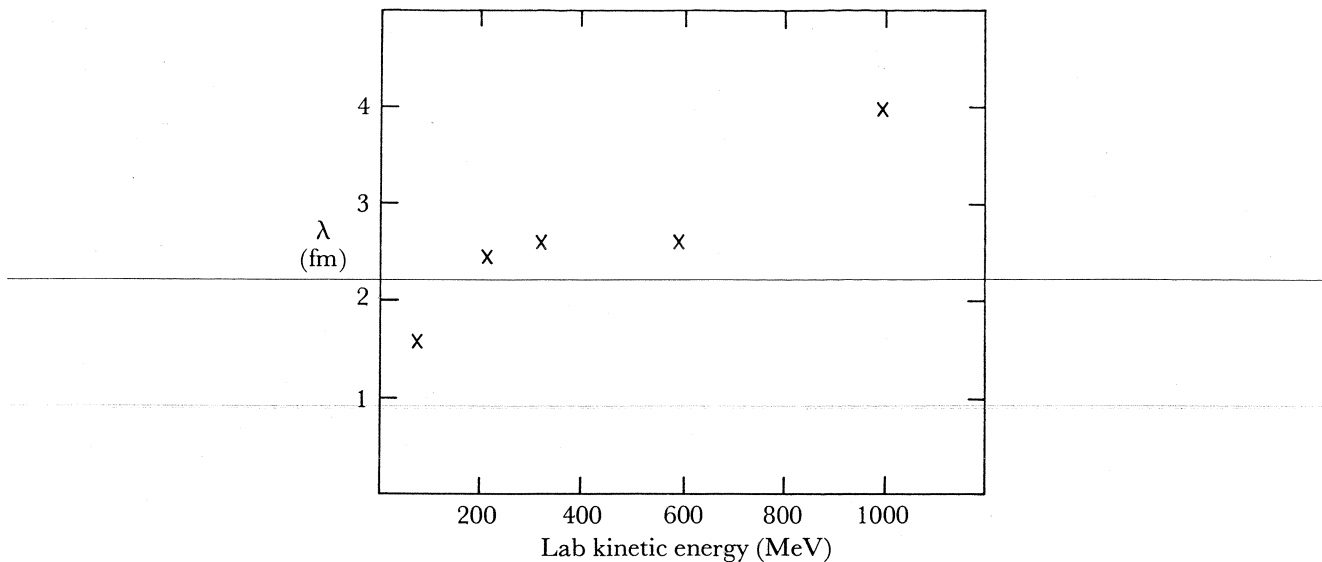


Figure 1.

Some values of  $\nu_\infty$  for different models are shown in Table 1. It is seen that  $\nu_\infty$  is determined by the kinematic character of the degrees of freedom; however,  $\nu_\infty$  is not a differential but an intergral quantity and can become very large when phase transitions introduce new degrees of freedom. A useful formula is

$$R_s = \frac{F(\nu, T_s) - \hat{\epsilon} - T_s \partial F(\nu, T_s) / \partial T}{\nu \partial [F(\nu, T_s) - \hat{\epsilon}] / \partial \nu}$$

where  $F(\nu, T_s)$  is the free energy of the fluid at temperature  $T_s$ . Under disintegration of the compressed matter, a mean asymptotic speed is attained

$$\langle v_{\text{asym}} \rangle = \int_{\nu_{\min}}^{\nu} c_s(\nu', S) d\nu' / \nu'$$

where  $c_s(\nu, S)$  is the speed of sound and the specific entropy  $S$  remains constant under the decompression, as long as the fluid is dense enough to be thermally equilibrated  $\nu \geq \nu_{\min}$ .

# Astrophysical Implications for Nuclear Interactions

MALVIN RUDERMAN

*Columbia University, New York, New York 10027*

---

## ABSTRACT

Over the past few centuries astrophysics has rarely told physicists anything about physics not already known from terrestrial experiments. However, because astrophysical environments do encompass extremes of pressure, temperature, and density that are quite inaccessible to direct observation, modern astrophysics has been very dependent upon medium energy nuclear physics for vital concepts and data.

1. In models of the early universe, present hydrogen, helium, deuterium, black-body photons, and an undetected neutrino background flux survive from a regime in which the temperature was between 100 keV and 1 MeV and the corresponding density was  $10^{-3}$  to  $1 \text{ g cm}^{-3}$ . Various data, especially those relating to the formation and destruction of deuterium, are important in determining the relevant initial conditions.

2. It seems likely that the elements beyond helium were made in explosive cobalt and silicon burning; these nuclei presumably fused up to iron and nickel in a second or so at a density of around  $10^{10} \text{ g cm}^{-3}$  and a temperature of at most a few MeV. A truly exotic feature is the intense flux of neutrons liberated by matter imploding toward a neutron star or a black hole. Such internal neutron fluxes may build transuranic elements, but only thorium and uranium have survived the  $5 \times 10^9$ -year age of the solar system. Most interesting is the possibility of a "stability island" with  $Z > 110$  with some nuclei surviving up to  $10^8$  years, long enough to survive in cosmic rays.

3. High energy collisions of cosmic-ray heavy nuclei (100 MeV to 100 GeV per nucleon) with interstellar protons probably generate many of the nuclei observed in cosmic rays. About half of Na, Al, S, Ar, Ca, Cr, and Mn probably come from such spallation. All of Li, Be, B, F, Cl, K, Sc, Ti, and V probably have a similar origin from the fragmentation of H, He, C, O, and Fe. One would especially like to know the fragmentation production of  $^{10}\text{Be}$  ( $\tau = 1.6 \times 10^6$  years),  $^{26}\text{Al}$  ( $\tau = 0.74 \times 10^6$  years), and  $^{36}\text{Cl}$  ( $\tau = 0.30 \times 10^6$  years) to give the lifetime of cosmic rays as a function of energy.

4. High energy heavy-ion collisions between heavy cosmic rays and interstellar heavy nuclei are extremely rare. The ratio of lead to hydrogen is of the order of  $10^{-9}$ , and of uranium to hydrogen of the order of  $10^{-10}$ . (The iron-hydrogen ratio is of the order of  $10^{-3}$ .) Thus the flux of residuals from high energy Pb-Pb collisions at the top of our atmosphere is only of the order of  $10^{-18} \text{ cm}^{-2} \text{ sec}^{-1}$ , and in the age of the solar system the incident matter from such collisions is  $< 0.1$  particle per  $\text{cm}^2$ .

5. Only in the case of the neutron star does there seem to be a possibility that astronomical observations may contribute some knowledge about medium energy

---

nuclear interactions not already well known to nuclear physicists. The equation of state of matter near nuclear densities and up to about 10 times greater is relevant for neutron stars between their minimum and maximum possible masses. Details of the nuclear force and especially technical problems involved in the computation of nuclear matter equations of state are especially important near the upper range. A comparison of the moments of inertia of such stars with that needed to explain the energy loss to its surrounding nebula of the Crab pulsar already gives a lower bound to the stiffness of nuclear matter at densities considerably greater than those found in nuclei. Various proposed equations of state can already be excluded. Present activity on this subject depends upon a more quantitative understanding of the phenomenon of pion condensation in superdense matter. Other details of nuclear matter in these density regimes probably have observational consequences for glitches, post-glitch healing (spin up and solid vs liquid cores), neutrino-antineutrino bursts during neutron star formation, and the heat capacity and cooling rate of newly formed neutron stars.

---

# Astrophysical Implications of Pion Condensation

RAYMOND F. SAWYER

*University of California at Santa Barbara, Santa Barbara, California 93106*

---

I shall report briefly on some consequences for neutron star structure of assuming a substantial softening of the equation of state in the region of densities from just above nuclear density to about ten times nuclear density, above which the short-range repulsion (in the models considered) restores the pressure to almost the values predicted in the usual models. The work to be described was done in collaboration with J.B. Hartle and D.J. Scalapino, and is based on a model of neutron star matter in the presence of pion condensation. However, the results describe qualitatively the possible implications of the existence of other forms of "abnormal" nuclear matter (or possible new phases which at high densities have lower energy than that of the conventional neutron gas with Reid potential interactions).

The link to heavy-ion reactions is somewhat tenuous. However, it is possible that theories which propose very radical softening of the equation of state of nuclear matter over a broad density region will run afoul of the usual interpretation of the energetics of the Crab nebula, which sets a minimum value of the moment of inertia of the Crab pulsar. Thus, not only has the experiment on the ground state of nuclear matter at high densities been performed, in neutron star interiors, but some of the data may already have been transmitted back to us.

It turns out that even a very generous estimate of pion-condensation effects does not put the theory in conflict with this single number. We do not know whether this would hold true, for example, for extensions of theories of the Lee-Wick type to neutral nuclear matter. In any case, in some of the models we have considered there are predictions of neutron star properties that could be tested at such time as only very rough observational data are obtained on the masses and radii of neutron stars.

Thus, in time astrophysics will probably yield real data (or at least some limits on various possible kinds of absurd behavior) on high-density nuclear matter. Conversely, if heavy-ion reactions can be analyzed in any way to give more information about the state of nuclear matter up to twice nuclear density (assuming that they do not yield up some spectacular new form of matter), this will be of great value to the development of the theory for even higher density, which must be pursued for the astrophysical applications.

Many nuclear and particle physics questions that arise in calculating an equation of state for pion-condensed matter will not be settled for some time. The critical density for the phase transition has been estimated to be anything from nuclear density to four times nuclear density, depending on detailed theoretical assumptions. The equation of state above the critical density is much more difficult to calculate than the critical density itself. Thus there is not now, nor will there soon be, an authoritative equation of state.

What we did was to take a fairly primitive form of pion-condensation theory basically that of Sawyer and Scalapino,<sup>1</sup> with some additions and deletions. This

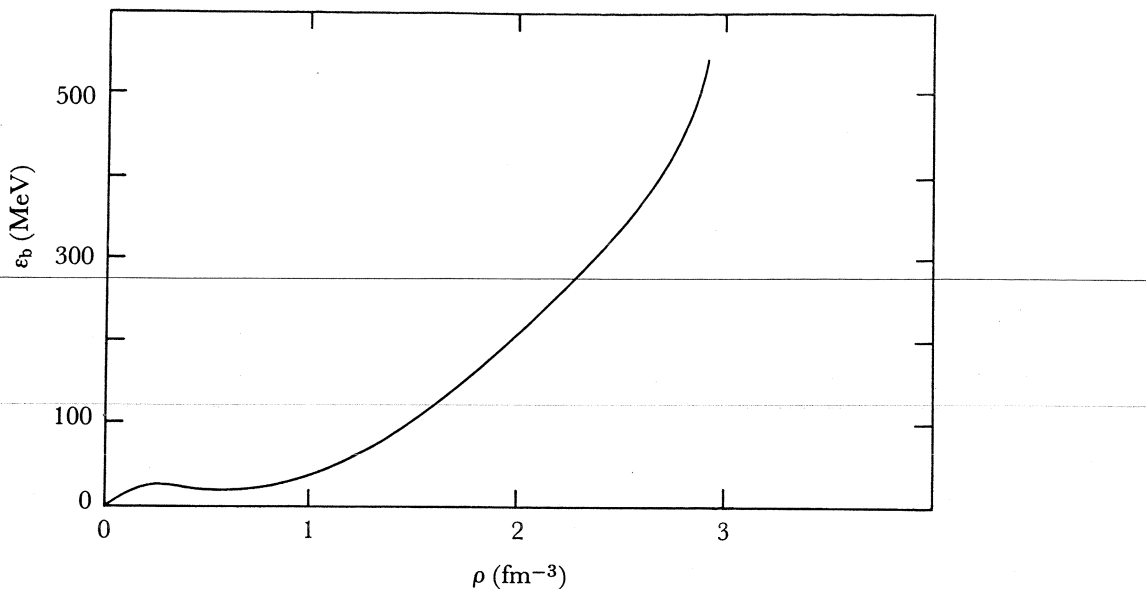


Figure 1.

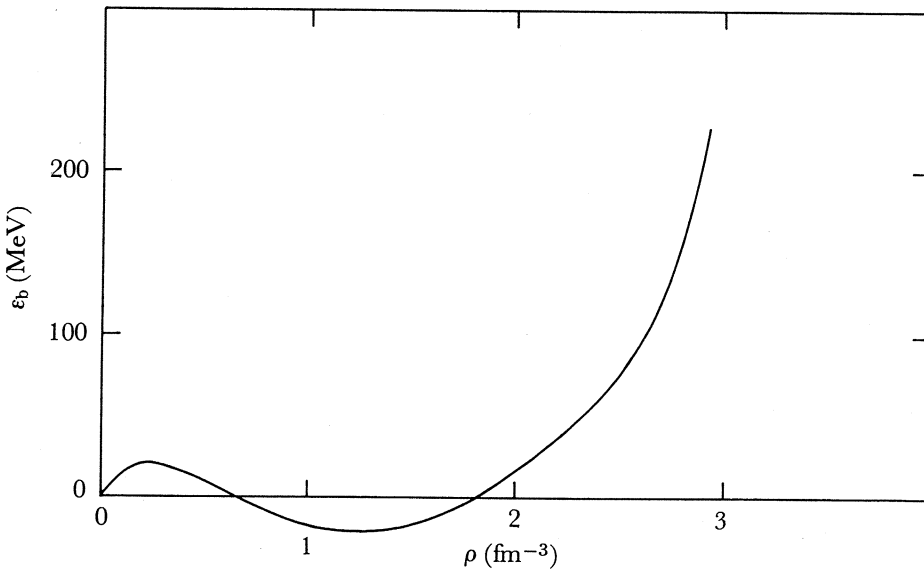


Figure 2.

gives a generous estimate of the effects of pion condensation, more generous than that which would be estimated from the work of Brown or of Baym reported in this volume. The purpose of the calculation is to put a bound on the potential effects of pion condensation; we do not claim that our results are definitive.

I shall not discuss the details of the model. It gives a critical density, for formation of a pion-condensed phase, of slightly above nuclear density. In the calculation of an equation of state we begin with an equation of state for neutron matter alone, in the presence of ordinary nuclear forces, and then add a pion-condensation term (which depends much less strongly on the details of the nuclear wave function). For

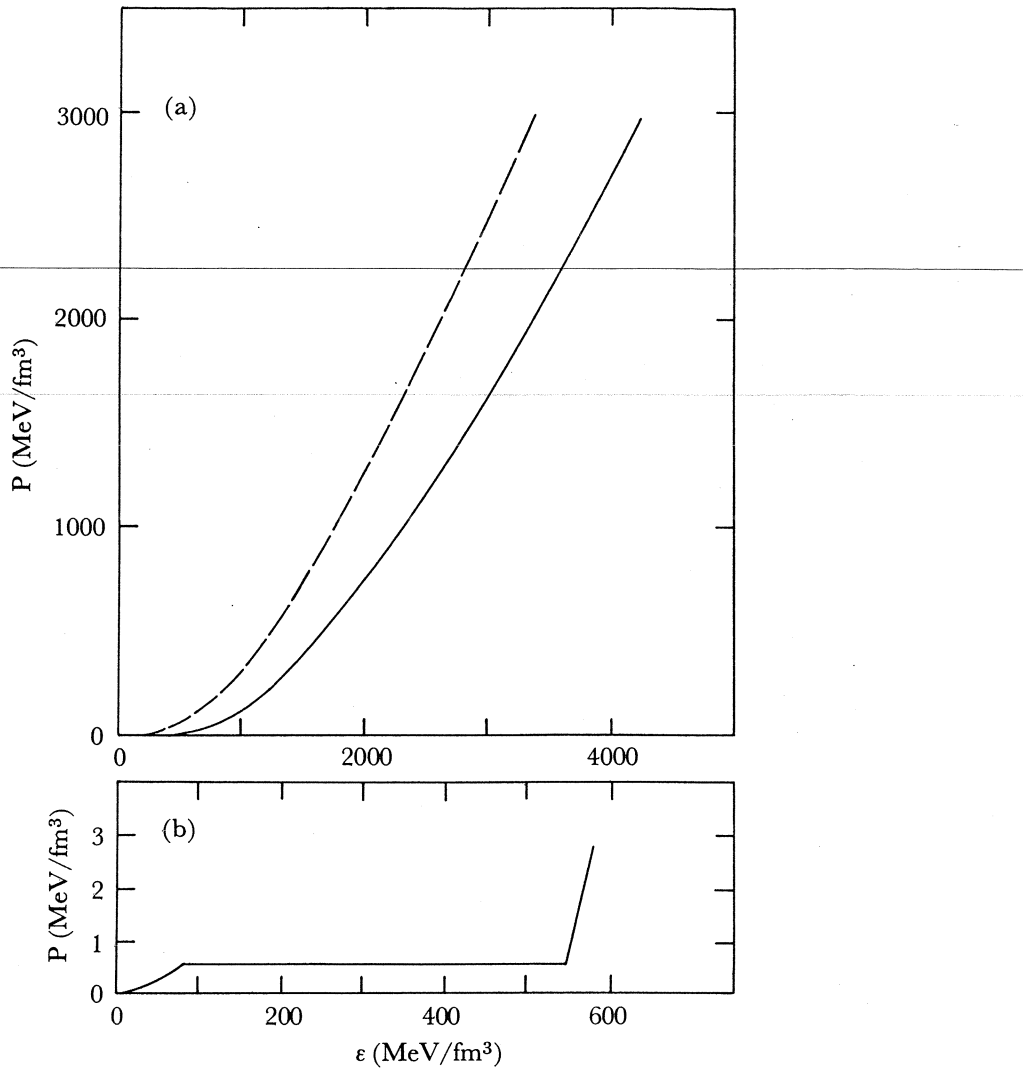


Figure 3.

the background equation of state we chose either of two due to Pandharipande.<sup>2</sup> Neutron star models based on these equations of state (without pion condensation) have been constructed by Baym, Pethick, and Sutherland.<sup>3</sup>

Pandharipande's equation of state ( $n$ ) is for pure neutron matter; the one he designates as ( $c$ ) includes some hyperons in the higher-density regions. We shall refer to the equation of state built on ( $n$ ) plus pion condensation as ( $n'$ ); that built on ( $c$ ) plus pion condensation as ( $c'$ ). For the discussion of the results I shall refer to figures from the paper of Hartle, Sawyer, and Scalapino.<sup>4</sup>

In Figure 1 we show the energy per baryon,  $\epsilon_b$ , as a function of the baryon density for the model ( $n'$ ). The flattening and slight dip at small  $\rho$  in the plot of  $\epsilon_b$  against  $\rho$  is the effect of pion condensation.

In Figure 2 we show the same plot for the model ( $c'$ ). Here we note that  $\epsilon_b$  becomes negative at high densities, with a minimum at about six times nuclear density. Thus this model predicts bound nuclear matter at very high density (as does the theory of Lee and Wick).

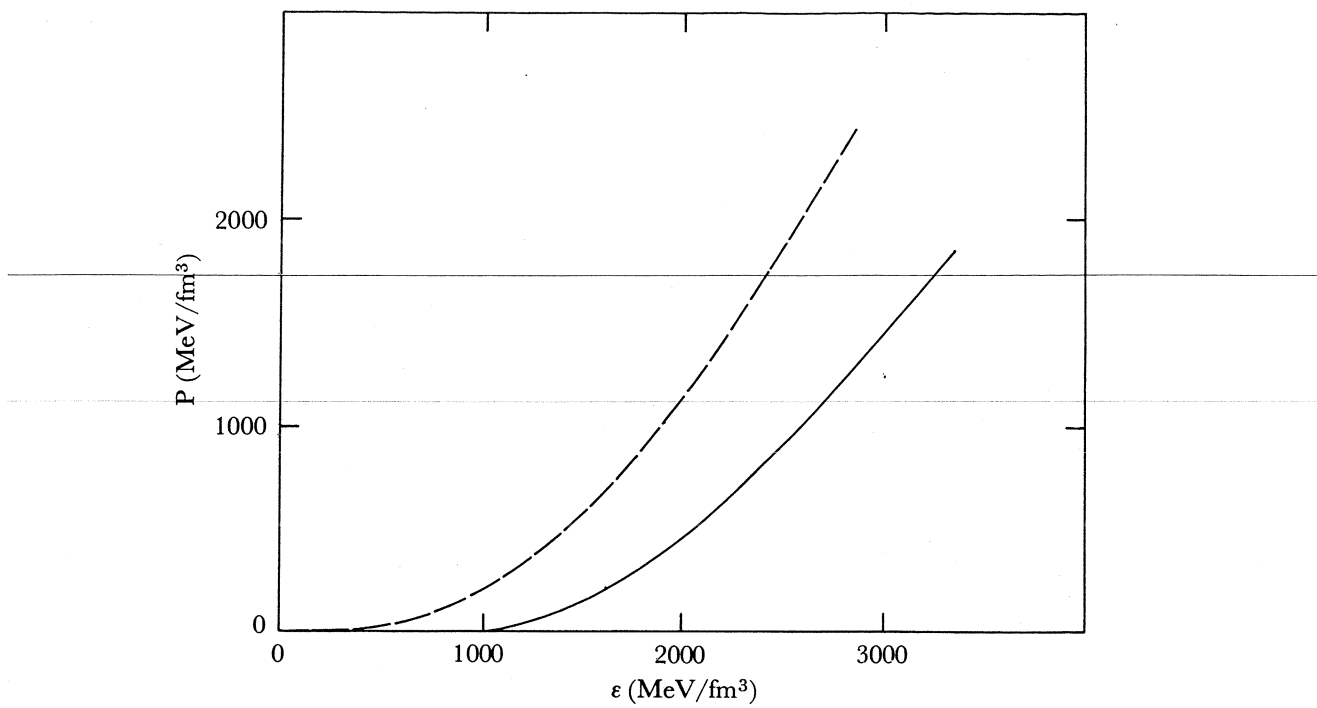


Figure 4.

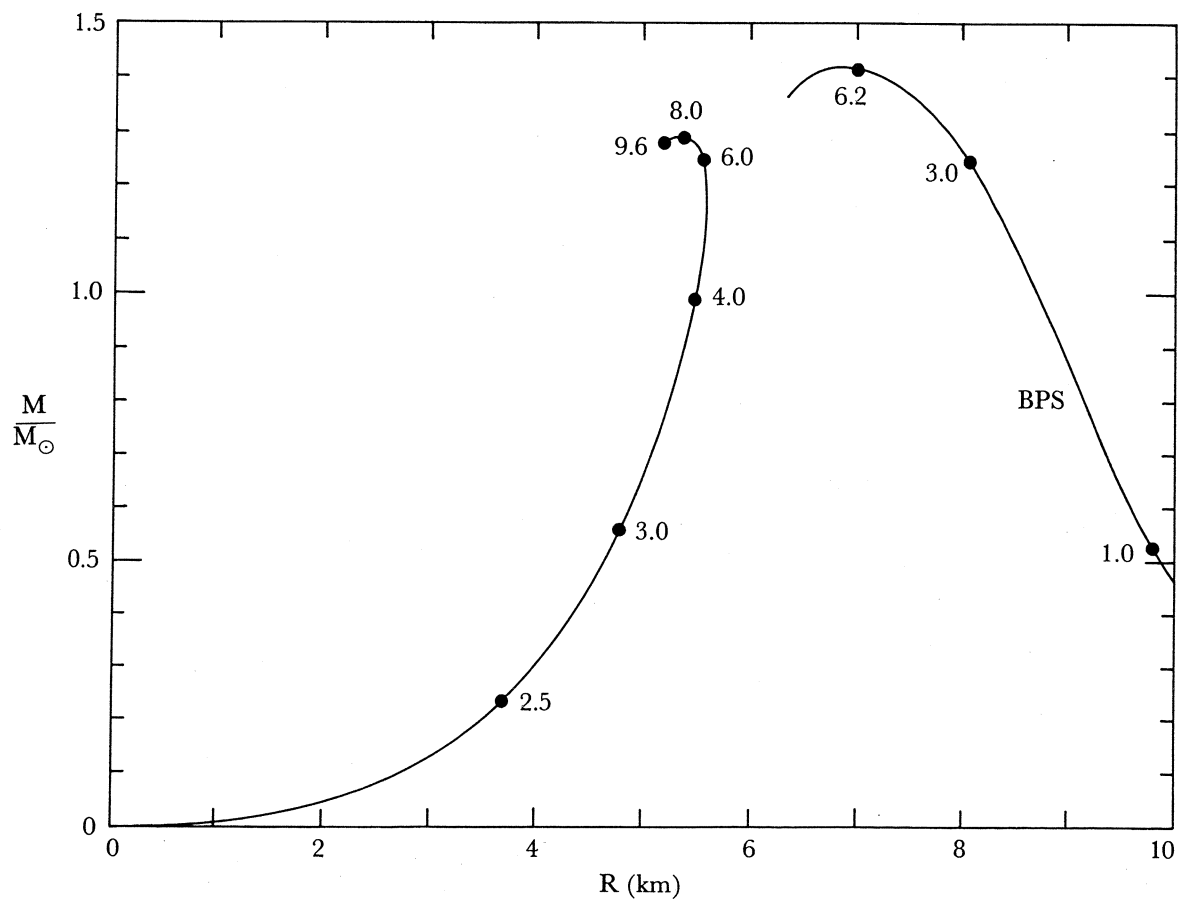


Figure 5.

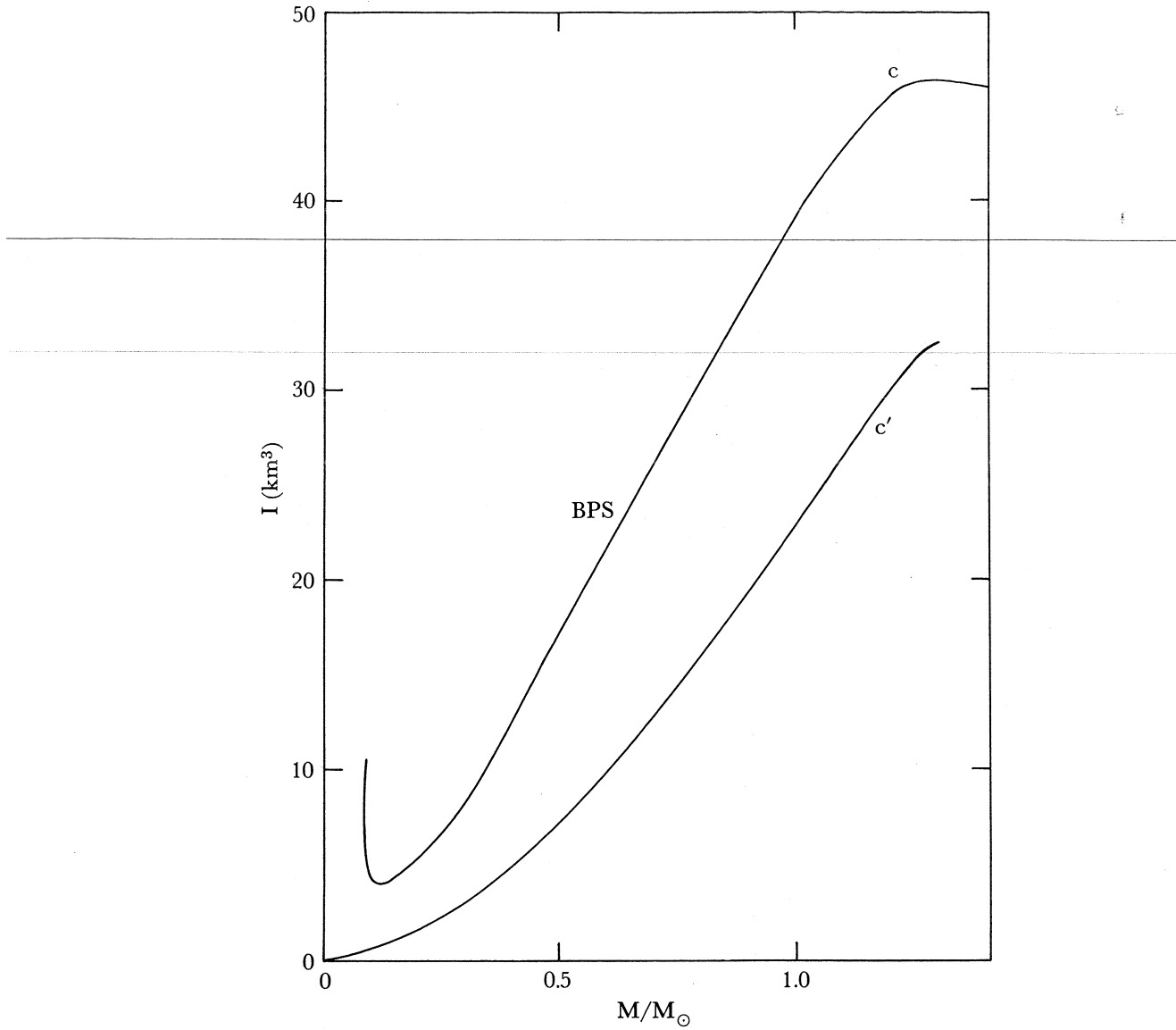


Figure 6.

Figure 3 shows the pressure as a function of energy density,  $\epsilon$ , for the ( $n'$ ) mode (solid curve) and the ( $n$ ) model (dashed curve). Since the calculation of pressure through differentiation of energy, gave a dip in the region of low density, the Maxwell equal area construction dictates a substantial density discontinuity at a particular pressure ( $\approx 0.5$  MeV/fm $^3$ ) in the equation of state, and a corresponding density discontinuity at some radius (quite near the surface for a massive star) in the neutron star built from this equation of state.

Figure 4 (solid line) shows the equation of state  $P(\epsilon)$  for the ( $c'$ ) model. In line with Figure 2, we terminate the curve at  $\epsilon = 1000$  MeV/fm $^3$ , the point of maximum binding, at which the pressure is zero. The dashed curve is the prediction of mode ( $c$ ) without pion condensation. If we build a star from matter obeying this equation of state ( $c'$ ) we will find that the lowest energy configuration with a given number of baryons begins with some very dense matter at the core, with the density declining

to 1000 MeV/fm<sup>3</sup> at the surface. This star will have a superdense surface, which could lead to interesting surface phenomena.

If the model (*c'*) were correct, nuclei of any size greater than some minimum could exist in this state. An agglomeration of nuclear matter as big as, say, a golf ball, would be stable. Clearly if there is a single branch of the mass-radius relation for a neutron star in this model, it will lead to  $R=0$  at  $M=0$ , in great contrast to the usual situation of increasing  $R$  for decreasing  $M$ .

The mass-radius relation resulting from solving the Tolman-Oppenheimer-Volkoff equations for model (*c'*) are shown in Figure 5. The curve on the left, passing through the origin, is the prediction of model (*c'*). The curve labeled BPS is the result of model (*c*) as calculated by Baym, Pethick, and Sutherland. The numbers along the curves refer to central density. The point of zero slope at the top of the curves is the point of transition to instability to gravitational collapse. We see that for the most massive neutron stars there is only a 25% or so reduction in radius due to pion condensation, and that the maximum mass is not greatly reduced. However, smaller-mass neutron stars are very different in the two models.

Figure 6 shows the moment of inertia predictions for model (*c'*) compared with those for the BPS model. For the larger stars we see that there is no drastic decrease in the moment of inertia.

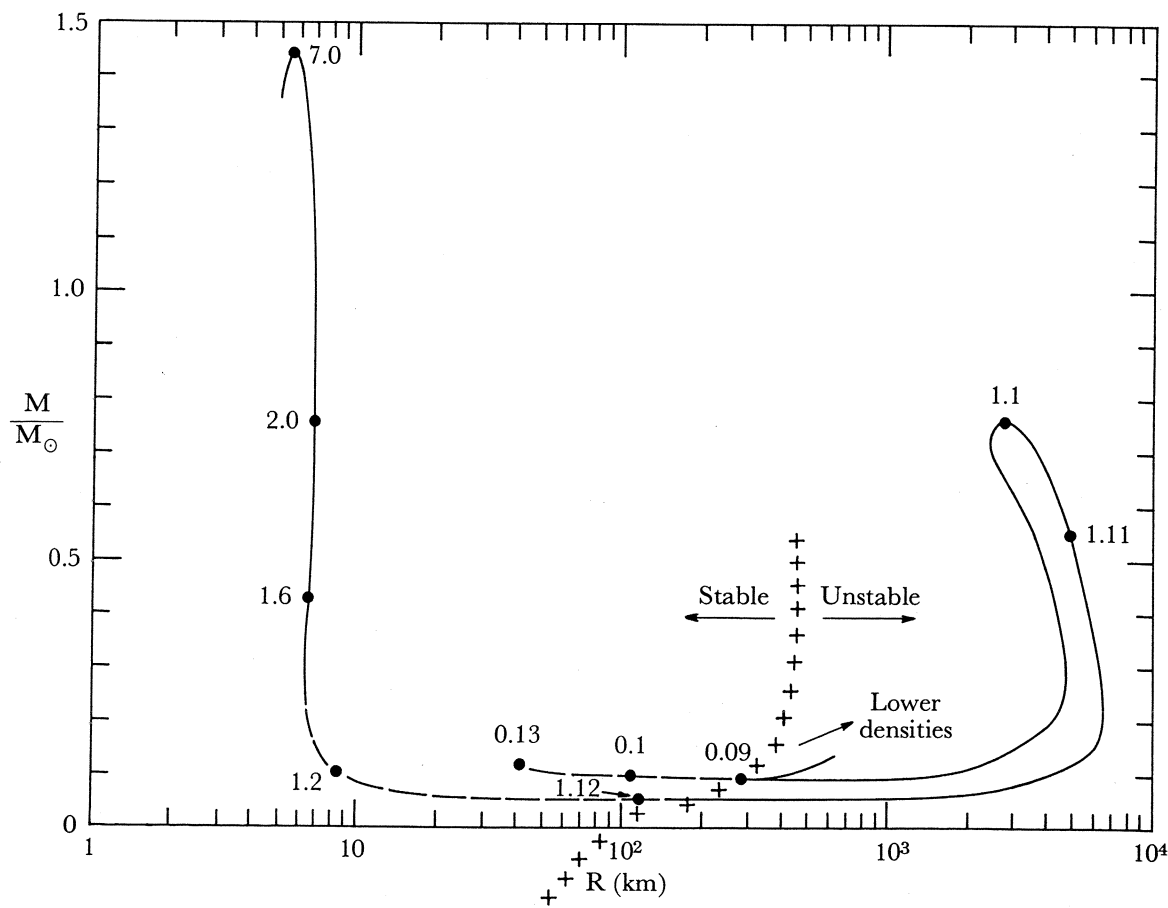


Figure 7.

Figure 7 shows the mass-radius relation for the ( $n'$ ) equation of state (in which there is no bound neutral nuclear matter at superhigh densities). The solid curves on the right are in a domain of instability. In this case the radius of the stable stars increases with decreasing mass, as in the usual theories, and the reduction of radii and of moment of inertia due to pion condensation is less, for the heavier stars, than in the ( $c'$ ) model. However, the large density discontinuity in the stars, which was responsible for the complex  $M(R)$  relationship, may lead to interesting mechanical properties which could be related to observable phenomena.

---

#### REFERENCES

---

1. R.F. SAWYER, *Phys. Rev. Lett.* **29**, 382 (1972); D.J. SCALAPINO, *Ibid.* 386; R.F. SAWYER AND D.J. SCALAPINO, *Phys. Rev. D* **7**, 953 (1973).
2. V. PANDHARIPANDE, *Nucl. Phys. A* **178**, 123 (1971).
3. G. BAYM, C. PETHICK, AND P. SUTHERLAND, *Astrophys. J.* **170**, 299 (1971).
4. J.B. HARTLE, R.F. SAWYER, AND D.J. SCALAPINO, *Astrophys. J.* **199**, 471 (1975).

## Round Table Discussion

A blue ribbon panel was convened for a round table discussion of speculative properties and applications of heavy isomers, abnormalities, superheavies, etc. Participants were O. Chamberlain, M. Goldhaber, L. Hand, A. Turkevich, and G.H. Vineyard, and L. Lederman was chairman of the session. Since they had been encouraged to indulge their fancies thoroughly, presuming that what resulted would be no more fantastic than the truth, the panelists expressed some unhappiness about the tape recorder that had been taking down the rest of the talks. Accordingly, it was turned off. The following summary has been pieced together from the editors' recollection of the discussion.

Vineyard noted that superdense nuclei might well be the basis for a new energy-producing reactor in which abnormal nuclei would grow heavier by swallowing neutrons while releasing large amounts of binding energy. It is to be hoped that this would be a "breeder" reactor, in which the swollen nuclei would eventually fission, and the fragments could start growing all over again.

Some of the more timorous participants were concerned that, once started, one of these abnormalities might not stop until it contained all matter. It was pointed out, however, that the Lee-Wick theory indicates that  $10^8$  or  $10^9$  of them have already been produced on the moon, and that the moon is still there, albeit with large holes.

It was decided that abnormalities are probably not responsible for the Schein cosmic-ray events, since those had a great many  $\gamma$  rays instead of the flood of  $\pi$ 's expected from collisions of abnormalities.

It is possible that abnormalities should have been produced in the usual stellar process of element formation, but that depends on how much more massive they are than normal nuclei.

Chamberlain agreed that heavy abnormal states were worth looking for, but warned against looking too specifically in regions suggested by the Lee-Wick theory or any particular theory. Rather, we should think of ways to conduct a very general search for new phenomena at high densities. He noted that Buford Price and his collaborators have a potentially powerful tool in their etched Lexan detectors, but warned that people would be suspicious of a new technique. He thought a more conservative approach might be to combine conventional instruments such as the magnetic spectrometer, pulse-height indicator, and time-of-flight meter to measure charge and mass for individual particles.

In the ensuing discussion, there was general agreement that one should look for a broad range of possible abnormal phenomena. Lederman noted that 5 years ago he had taken part in a discussion about the possibility of using the CERN ISR for  $U+U$  collisions to see what new phenomena might be produced.

Hand led off a discussion of ways to detect abnormal events, suggesting pion jets as an indicator of central collisions, even though Siemans expects them to go away at high energy. (Lederman noted that experimental techniques would be found - the AGS was built when the cloud chamber was the most sophisticated detector available.) Goldhaber noted that Heckman's central collision events did not look like those predicted by Greiner, but that this might be because the target was moving with a speed of only 0.1 Mach.

Turkevich pointed out vast possibilities for chemistry if superheavy elements exist, extending the periodic table by a factor of 10 or more. In particular, one might expect much more continuous changes in chemical properties from element to element than one finds now. If such materials could be mass produced, they would offer the possibility of custom tailoring materials with specified properties. As an example, he pointed out the search for a high temperature superconductor, which has been limited by the discontinuous chemical properties of existing elements.

---

# Search for Stable Strange Nuclei

JOHN P. SCHIFFER

*Argonne National Laboratory, Argonne, Illinois 60439*

*and*

*University of Chicago, Chicago, Illinois 60637*

The purpose of this talk is to examine the evidence for the existence of strange stable nuclei in the region indicated in Figure 1. One's first reaction is that if such nuclei existed in nature we would have seen them. I think this is wrong, that in fact we can set only poor limits. Mass spectroscopy comes to mind first; a comparison of chemical and physical methods should set a limit on strange isotopes. Table 1 shows that this limit is not very low. If one could tell mass spectroscopists to look for an anomalous isotope with a specific mass, one could get a better limit ( $\sim 10^{-9}$ ), but this is not practical since we have no idea what the mass should be.

Table 1

## Limit on Strange Isotopes From Atomic Weights Determined by Chemical Techniques

Example:  $^{209}\text{Bi}$

Physical value: 208.980401

Chemical value: 208.976

Would imply a concentration of  $^{166}\text{Bi}$  (with mass  $\sim 150$ ) of  $\gtrsim 6 \times 10^{-5}$

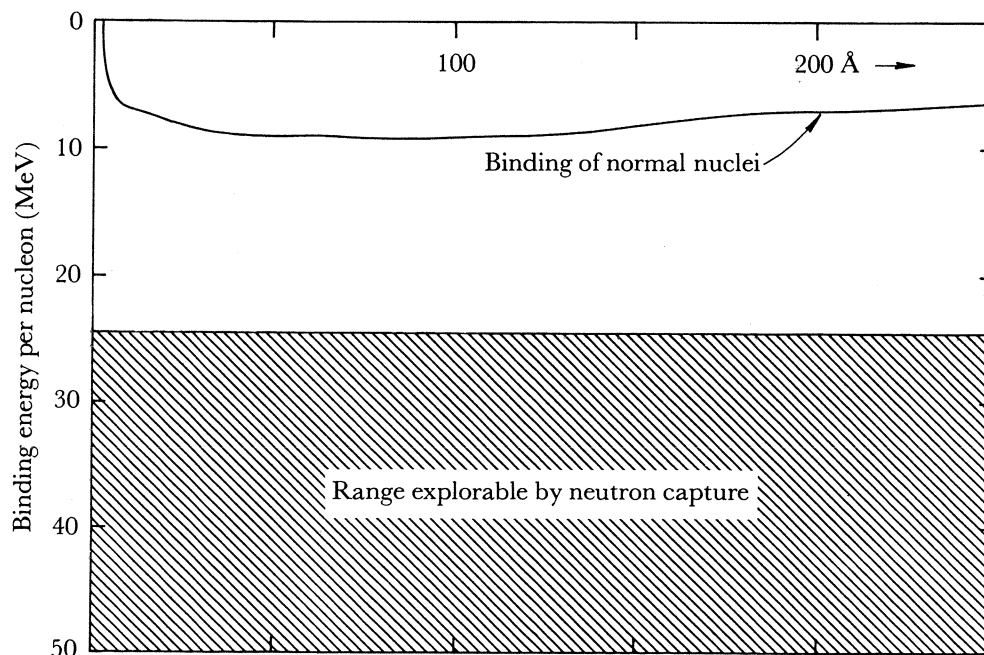


Figure 1.

Table 2

## Estimate of Neutron Capture by Collapsed/Abnormal Nuclei

ASSUMPTION: Level density high compared with thermal energies ( $D \ll 25$  MeV)(a) Pion emission possible:  $\Gamma \gg D$ 

Contribution of one resonance is

$$\sigma_i = \frac{\pi}{k^2} \frac{\Gamma_{ci} \Gamma_{ni}}{\Gamma_i^2/4} \approx \frac{4\pi}{k^2} \frac{\Gamma_{ni}}{\Gamma_i}, \quad \Gamma = \Gamma_n + \Gamma_c$$

(where  $\Gamma_c$  = capture width and  $\Gamma_n$  = neutron width).Now sum over all resonances with  $|E_0| \gtrsim \langle \Gamma \rangle_{Av}$ :

$$\sigma = \sum_i \sigma_i \approx \frac{\langle \Gamma \rangle}{D} \langle \sigma_i \rangle \approx \frac{2\pi}{k^2} \frac{\langle \Gamma_n \rangle}{D}.$$

(b) Only radiative capture possible, but since more energy is available than in normal nuclei:  $\Gamma_c \gg \Gamma_n$  with  $\Gamma < D$ 

This reduces to the same answer:

$$\sigma \approx \frac{2\pi}{k^2} \frac{\langle \Gamma_n \rangle_{Av}}{D}.$$

Best estimate for  $\Gamma_n/D$  is  $\approx k/\bar{k}$  (where  $\bar{k} \equiv \sqrt{2m(E+V)}/\hbar$  (Porter et al.<sup>2</sup>) with  $V$  perhaps 10 times larger than normal nuclei. This yields

$$\frac{\langle \Gamma_n \rangle}{D} \approx 1.6 \times 10^{-5} \quad \text{or} \quad \sigma_c \approx \frac{4\pi}{k\bar{k}} \approx 10^{-21} \text{ cm}^2.$$

N.B.: In normal nuclei where capture (fission) is "open" channel ( $\Gamma_c \gg \Gamma_n$ ), as in heavy nuclei  $\sigma_c \approx 10^{-22}$  to  $10^{-21} \text{ cm}^2$ .

Table 3

## Reactor Experiment With Carbon

Neutron flux	$\phi \sim 3 \times 10^{13} \text{ n/cm}^2\text{-sec}$
Efficiency $\times$ solid angle	$\Omega \times \epsilon \sim 0.4 \times 10^{-6}$
Observable rate ( $E_\gamma > 30$ MeV)	$N_0 \sim 2 \times 10^{-4}/\text{sec}$
Assumed cross section	$\sigma_c \sim 10^{-21} \text{ cm}^2$
Limit of observable sample	$N_0/\phi/\Omega/\epsilon/\sigma_c \sim 10^{10} \text{ atoms}$
In graphite sample: $\sim 10^{24}$ atoms	
Concentration: $\gtrsim 10^{-14}$	

As with quarks or magnetic monopoles, one would like to have an easily identifiable property for these anomalous nuclei. When Bodmer<sup>1</sup> suggested collapsed nuclei about two years ago, I thought about this problem, and the best I could come up with is the thermal-neutron capture cross section. The expectations are outlined in Table 2. Equipment developed by Bollinger, Thomas, and Specht at Argonne seemed ideally suited for this purpose, and a measurement they carried out about two years ago on carbon is outlined in Table 3.

The equipment used is shown in Figures 2 and 3. A restriction placed on the ratio of energy deposition in the inner and outer scintillators ( $C/A > 1/2$ ) reduced

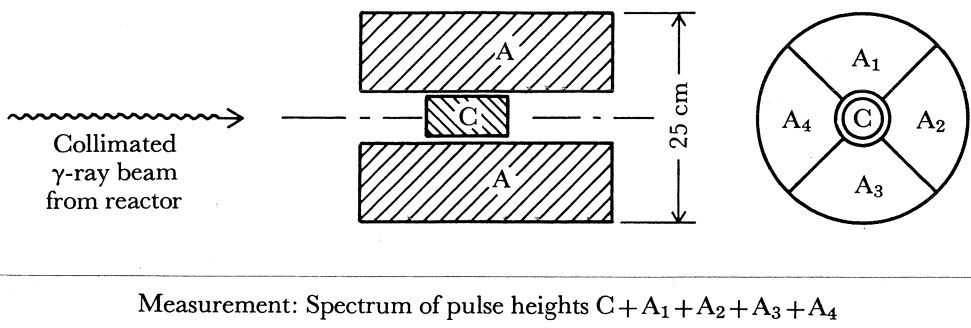


Figure 2. NaI detector system imbedded in 14-in.-thick lead and boron shield.

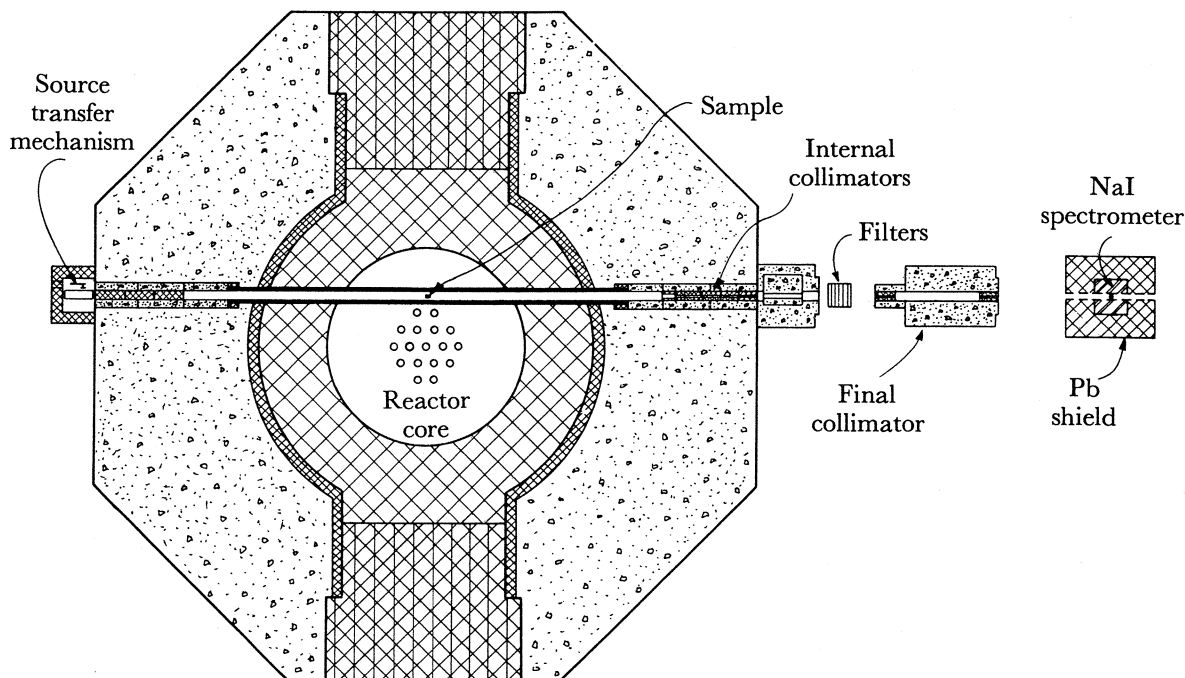


Figure 3. CP-5 reactor at Argonne.

the background to  $\sim 1$  ct/hr, as shown in Figure 4. An experiment lasting about a week yielded the results shown in Figure 5. The limits from these data lead to the value quoted in Table 3.

Perhaps a better candidate for such a measurement is radon, and by using the residue of xenon production we hope to make such a measurement with Friedman and Turkevich. This is outlined in Table 4.

Finally I would like to present some numbers on estimates of production of strange nuclei on the lunar surface in Table 5. This is a very low concentration, but

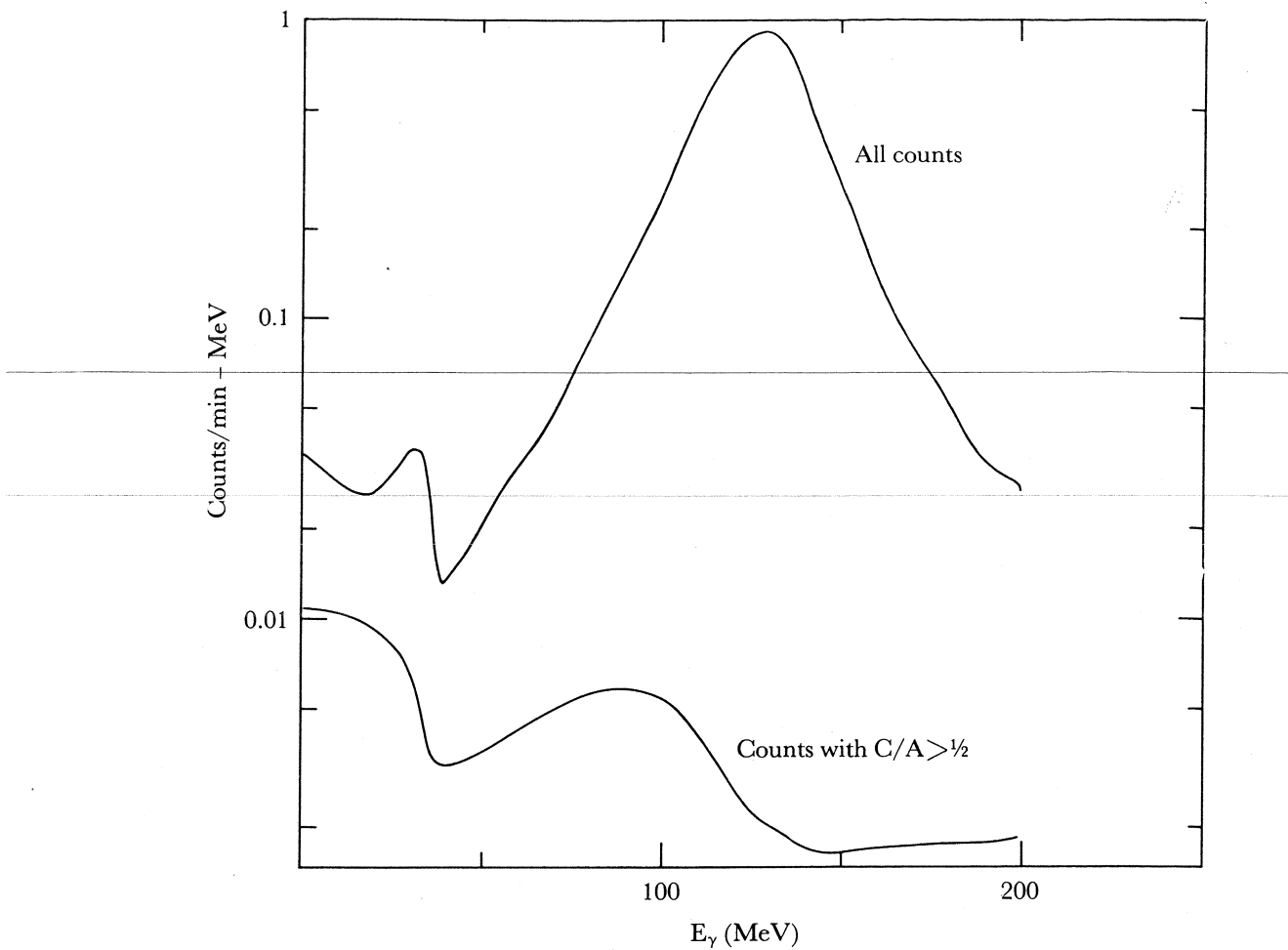


Figure 4. Background runs at reactor with and without restrictions.

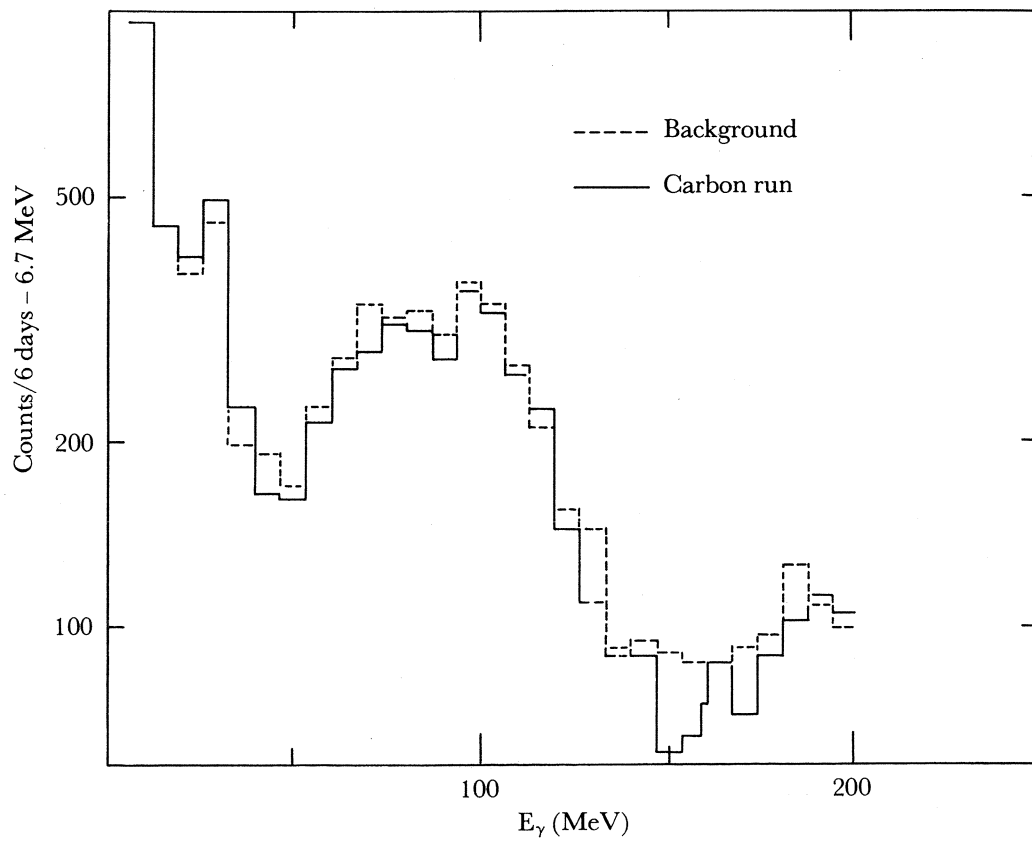


Figure 5. Data run at reactor.

Table 4

## A. CHARACTERISTICS:

Needed	Radon has
i. $A > 200$	$A \approx 220$ ; $Z = 86$
ii. Known chemistry	Noble gas
iii. Easy to collect from large sample	Like Xe, most primordial Rn should be in atmosphere, though depleted by $10^4$
iv. Has no stable or long-lived isotope	Longest-lived isotope has $\tau \sim 3.8$ days

## B. LIMIT OF ABNORMAL MATTER IN RADONLIKE MATERIAL

Xenon processed for radon	$\sim 2 \times 10^4$ liters
Air sample processed for Xe	$\sim 0.2 \text{ km}^3$
Atoms in air sample	$10^{34}$
Detectable level	$10^{10}$ atoms

Limit one could set for concentration in air:  $10^{-24}$ 

## Assumptions

- Almost all terrestrial primordial radonlike atoms are in atmosphere.
- Radon is lost from atmosphere at same rate as xenon.

Limit one could set on primordial concentration in terrestrial material:  $2 \times 10^{-31}$ 

Table 5

## Production of Abnormal/Collapsed Nuclei on Moon

Abundance of elements with $A > 150$	$\sim 3 \times 10^{-4}$
Flux of cosmic rays with $A > 150$ , $E > 1 \text{ GeV}/A$	$\sim 3 \times 10^8/\text{cm}^2/10^9 \text{ yr}$
Fraction of first interactions leading to A/C state	$10^{-5}$
Concentration on surface	$1/\text{cm}^2 (10^6/\text{cm}^2)^*$
Volume concentration, 1-m-deep mixing	$10^{-25} (10^{-19})$
complete mixing	$10^{-31} (10^{-25})$

\*Values in parentheses are based on the assumption that Si on Fe could produce these nuclei.

Table 6

## Capture by Tightly Bound Matter in Stars

## S-PROCESS

Integrated flux	$\sim 10^{27} n/\text{cm}^2$
Temperature	$\sim 10^8 \text{ }^\circ\text{K} \rightarrow \sigma_c \approx 10^{-23} \text{ cm}^2$
Time	$10^8 \text{ yr}$ , sufficient for $\beta$ decay
$\phi \times \sigma_c = 10^4$ captures	

But suppose these nuclei fission long before they reach  $A \approx 10^4$ 

- Fission after 100 captures:

 $2^{100} = 10^{30}$ -fold increase in such nuclei

- Fission after 1000 captures:

 $2^{10} = 1000$ -fold increase

## R-PROCESS

Integrated flux	$\sim 10^{34} n/\text{cm}^2$
Temperature	$10^9 \text{ }^\circ\text{K} \rightarrow \sigma_c \approx 3 \times 10^{-24} \text{ cm}^2$
Time	10 to 100 sec, not sufficient for $\beta$ decay
$\phi \times \sigma_c = 10^{10}$ captures	

(Conclusion: this process is not likely to form A/C)

it is possible that stellar processes could lead to a large enhancement, as shown in Table 6. Consider in particular the *S*-process, in which neutron capture is slow enough for  $\beta$  decay to take place. Here all depends on *when* fission is likely to occur, and very substantial yields from a few such nuclei *could* obtain.

#### REFERENCES

---

1. A. BODMER, *Phys. Rev. D* **4**, 1601 (1971).
2. H. FESHBACH, C.E. PORTER, AND V.F. WEISSKOPF, *Phys. Rev.* **96**, 448 (1954).

# Search for Ultradense Nuclei in Collisions of GeV/Nucleon Ar + Pb

P.B. PRICE

*University of California at Berkeley, Berkeley, California 94720*

We divide the task of creating abnormal nuclear states into two phases. First, we use the Bevalac to determine the optimum conditions for attaching high-energy heavy projectiles to heavy target nuclei, using Lexan plastic track detectors to identify heavy recoils ejected along the beam direction. Second, we measure some property of such high- $Z$  products that would indicate whether some of them could be stable ultradense nuclei. With Owen Chamberlain we might, for example, measure their mass defect with a combination of time-of-flight, magnetic analysis, charge, and range determinations. Or we might expose them to thermal neutrons and look for high-energy gamma rays from  $(n, \gamma)$  reactions.

In our first experiment, using  $5 \times 10^8$  Ar ions of initial energy 1.62 GeV/nucleon on a 5-cm-thick Pb target, John Stevenson and I have found no events with  $Z \gtrsim 21$  as of the half-way stage in our analysis.

Figure 1 is a sketch showing our system for detecting and determining the charge of high- $Z$  nuclei that recoil out of the Pb target. A stack of 1000 Lexan sheets, of total thickness 25 cm, is placed directly downstream from the Pb brick.

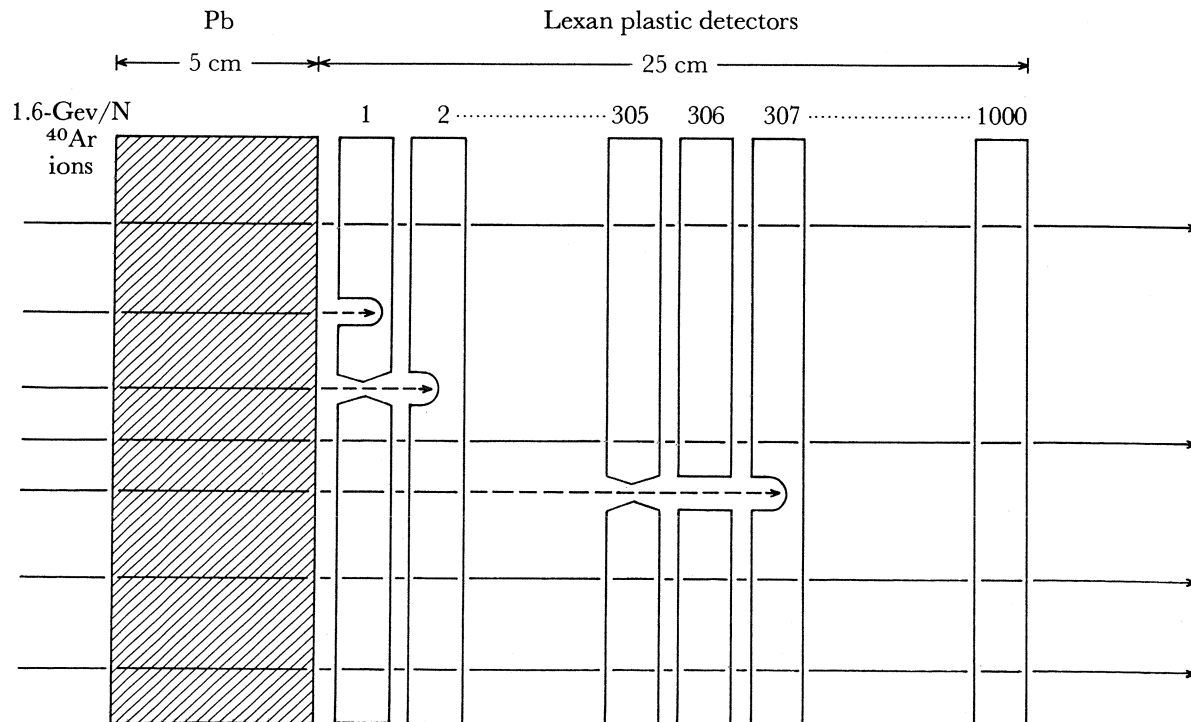


Figure 1.

Those Ar ions that emerge from the Pb without a nuclear interaction ( $\sim 50\%$  of them) have an energy of 1.11 GeV/nucleon; those that penetrate the 25 cm of Lexan without an interaction ( $\sim 12\%$ ) emerge with an energy of 0.65 GeV/nucleon. Lexan does not record tracks of relativistic particles with  $Z \lesssim 60$  and records tracks of Ar ions only in their last  $\sim 1$  mm of range. Tracks of highly ionizing particles are made visible by etching the Lexan in a strong solution of sodium hydroxide for several days at  $40^\circ\text{C}$ . Each track shows up as a pair of etch pits at opposite sides of a sheet. The length of an etch pit per unit etch time is roughly proportional to the square of the ionization rate. From a series of microscopic measurements of etch pit lengths one can determine the charge of the particle to within one unit of  $Z$ . One can selectively locate tracks of events with  $Z > 18$  by choosing the etch time so that at the end of their range the etch pits from opposite sides are connected in the form of a constricted cylinder. One can spot these holes by passing ammonia gas through the holes onto blueprint paper.

Figure 2 shows the distribution of ranges in the Lexan stack of recoils with  $Z = 20, 26, 32, 36, 52$ , and 100, calculated by assuming completely inelastic transfer of the appropriate number of nucleons from a Pb nucleus to an Ar projectile. Some of the high- $Z$  recoils will undergo a nuclear interaction before coming to rest. The velocity, range, and interaction probability decrease rapidly with increasing  $Z$ , as seen in Table 1.

Figure 3 shows our results thus far. The solid curve gives the number of nuclei with  $14 \lesssim Z \lesssim 18$  that come to rest per Lexan sheet (0.025 cm thick). The yield is surprisingly high in view of the observation by Heckman and co-workers of a Gaussian momentum distribution in the rest frame of the interacting projectiles. What we see is a continuous non-Gaussian tail extending to extremely large momentum losses, populating the velocity regime between that of the target and that of the projectile.

The dashed curve in Figure 3 gives the number of nuclei with  $Z \geq 18$  that come to rest per sheet, detected by the ammonia process. The etch time was chosen such that the efficiency for detecting Ar was  $\sim 10^{-3}$ . Nevertheless, the vast majority of

Table 1

Limits on Production of High- $Z$  Nuclear States  
(with  $\tau \gtrsim 10^{-10}$  sec at  $1.1 \lesssim E_{\text{lab}} \lesssim 1.6$  GeV/nucleon)

$Z$	Fraction stopping in Lexan	Detection efficiency	Fraction surviving interactions	Eventual upper limit on $\sigma$ , nb	Present limit on $\sigma$ , nb
18	supposedly none	$\ll 0.01$	$\sim 0.06$	—	—
26	0.8	$\sim 0.8$	$\sim 0.4$	50	140
32	0.5	1	$\sim 0.6$	40	80
36	0.36	1	$\sim 0.7$	45	70
52	0.07	1	0.96	180	200
100	0.008	1	1	1500	?
(Ar+Pb)					

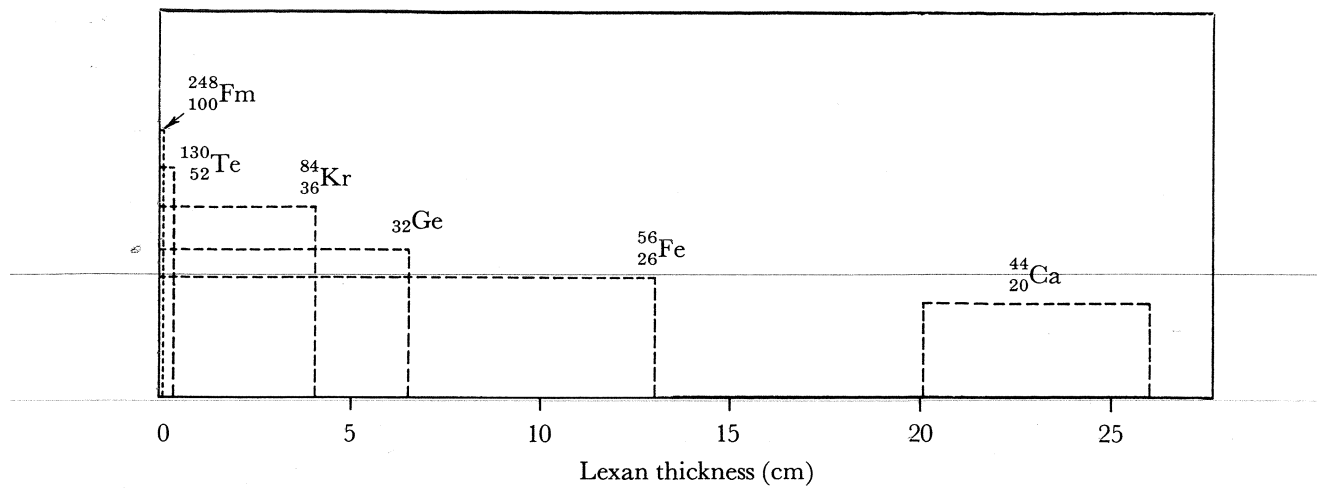


Figure 2. Range distribution of some inelastic recoils.

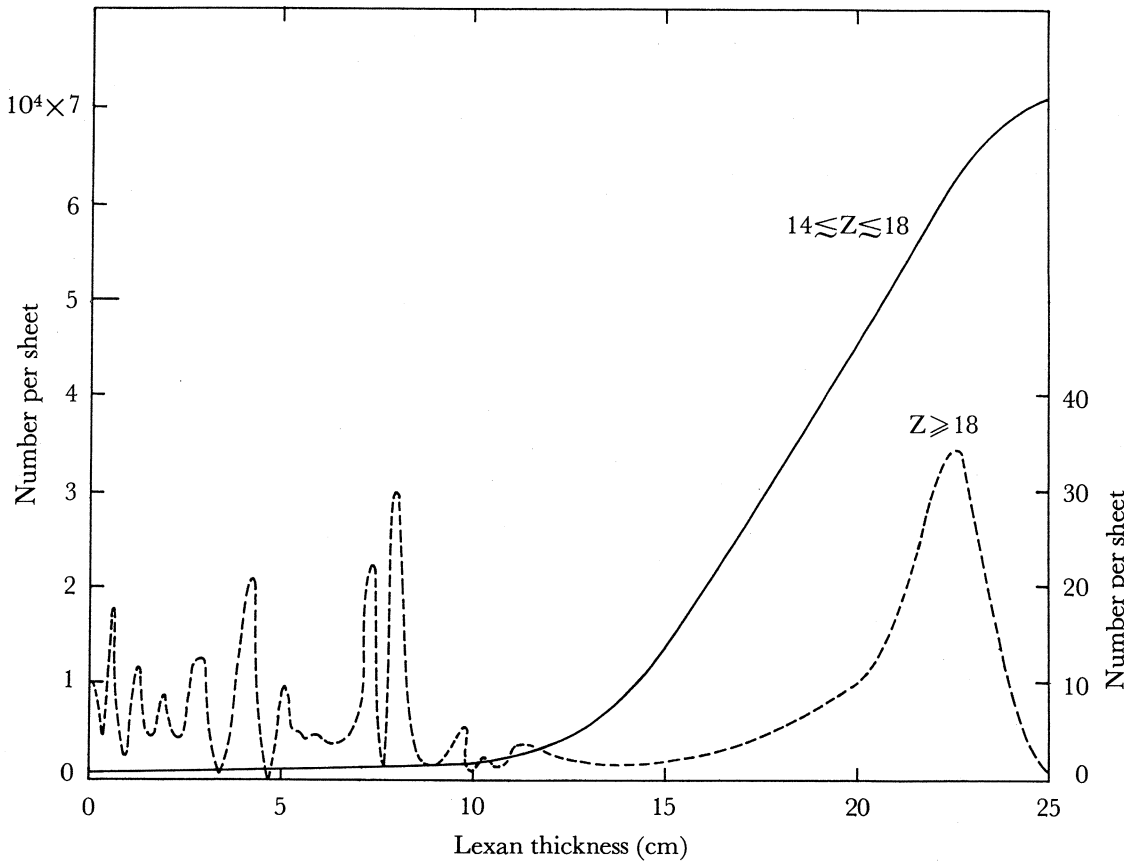


Figure 3.

these events are Ar. We have found less than ten with  $Z=19$  or 20 and none with  $Z \gtrsim 21$ .

Table 1 indicates the upper limits on cross section for production of high- $Z$  ejecta. The number varies somewhat with charge but is of the order of  $10^{-31} \text{ cm}^2$  now and will perhaps go down to  $5 \times 10^{-32} \text{ cm}^2$  in a few weeks, assuming that no high- $Z$  events are found.

One of the conclusions reached at this meeting is that 1 GeV/nucleon may be so high an energy that a shock wave is unlikely to be initiated in a nucleus-nucleus collision. We intend in the spring of 1975 to use lower bombarding energies (probably  $\sim 500$  MeV/nucleon), a higher flux of Ar ions, and if possible a beam of K ions, to continue our attempts to produce high- $Z$  nuclei that may possibly be ultra dense. We can probably detect such events at a production cross section as low as  $10^{-3}$   $\text{cm}^2$ , but if under optimal conditions they are indeed that hard to produce, it will be very difficult to design experiments that can establish whether they have normal or abnormal density.

---

# Ultrahigh Momentum Transfer Scattering of Protons by Heavy Nuclei\*

LAWRENCE E. PRICE

*Columbia University, New York, New York 10027*

L.M. Lederman and I are doing an experiment at Fermilab in the hope of getting an early look at the products of high energy uranium-uranium collisions. Lee and Wick have suggested such collisions, with the projectile having an energy of about 1 GeV/nucleon, as a favorable way of testing their suggestion of abnormal high-mass nuclear states. Other suggestions have also been made of possible stable super-heavy states that might be made this way.

Our thesis is that it just might be possible to produce the needed high energy uranium nucleus by hitting the uranium at rest with a 300-GeV proton at Fermilab. The rebounding uranium would then go on to hit another uranium in the same target and, one hopes, thus produce something new. The search for production of abnormalities could then be done with high sensitivity simply by putting a block of uranium in a quiet beam stop for, say, a year.

But in order to make an experiment out of this, it is necessary to know the flux of high energy uranums. This involves a calibration experiment, and it is the latter that we are currently doing. This is, of course, an interesting experiment in its own right, since it requires a very large momentum transfer to the nucleus, which must recoil elastically. In order to do a sensitive experiment, we are using dielectric track detectors, like those Buford Price has just described, but ours are synthetic fused silica instead of Lexan. The insensitivity of these detectors to lightly ionizing radiation allows them to be put into the proton beam without recording the protons. They have a threshold in  $Z$  of about 15.

A simple version of the setup, with a sheet of lead, and with three sheets of silica downstream and three upstream of the target for background determination, is currently about to be exposed to  $10^6$  protons at Fermilab. Results from this preliminary exposure will be used to design a more elaborate apparatus, with a large number of silica sheets for good range measurement and an ultimate exposure of  $10^{18}$  or  $10^{19}$  protons. This will give a sensitivity for the recoil process of about  $10^{-41}$   $\text{cm}^2$ . Thus, we are making a sensitive search for high momentum-transfer scattering, and perhaps providing a way to observe high energy uranium-uranium collisions.

---

\*Research supported by the National Science Foundation.

# The Bevalac, a High-Energy Heavy-Ion Facility – Status and Outlook

H.A. GRUNDER

*Lawrence Berkeley Laboratory, Berkeley, California 94720*

The very stimulating preceding discussions left it quite clear that experimental work in this new field is urgently needed. This state of affairs is most encouraging for an accelerator group in the process of developing the very beams needed. I shall describe what LBL has done, is doing, and could do with appropriate planning and support.

The high-energy heavy-ion facility commonly referred to as the Bevalac is a synchrotron with a  $\beta\rho$  of 9000 kG-in. or 230 kG-m having special injectors. As Figure 1 shows, the synchrotron has three injectors. The 50-MeV proton injector, originally from the BNL AGS, is a tool left over from the high-energy high-intensity days of that productive synchrotron. The 20-MeV linac is a proton linac designed so conservatively that it was possible to accelerate modest but useful beams of  $^{12}\text{C}$ ,  $^{14}\text{N}$ , and  $^{16}\text{O}$  as well as deuterons and  $\alpha$  particles in the  $2\beta\lambda$  mode. This was accomplished in 1971.

After our first trials, a suggestion made earlier by A. Ghiorso to inject from the SuperHILAC into the synchrotron was actively pursued. It should be explained why the SuperHILAC as injector to the Bevatron is a reasonable linkup. Heavy-ion linacs are expensive; hence, if a proper linac exists near by, it is advisable to make use of it. The SuperHILAC can accelerate particles with a minimum  $\epsilon$  ( $\epsilon$  = charge/mass) of 0.05 in the tank prior to a stripper and  $\epsilon = 0.167$  in the tank following the stripper. The acceptance of these relatively low charge states, with a judicious choice of other parameters, assures very high instantaneous beam fluxes – several microamperes on the heaviest ions up to several milliamperes of the lower-mass ions. Furthermore and most importantly, the SuperHILAC has a built-in macroscopic duty cycle (ignoring the 70-MHz rf structure) of 25 to 50%. The highest duty factor can be obtained when  $\epsilon$  is much larger than the minimum because then the electric gradient is much lower than the maximum.

If one keeps in mind that for injection purposes in our synchrotron a duty cycle of  $< 1\%$  is required, then it becomes apparent that a happy marriage can indeed be accomplished. The SuperHILAC operates with up to 36 pulses/sec, and it is planned to divert one pulse/sec into the transfer line connecting the SuperHILAC with the Bevatron. One pulse in 4 to 6 sec goes to the Bevatron; the others are used to facilitate tuning.

Another very important factor is the injection system at the SuperHILAC. The final element is a 750-kV air-insulated Cockcroft-Walton used for ions with  $\epsilon \geq 0.15$ . This low-voltage injector is adequate up to mass 40. For higher masses, a larger potential is needed to produce the injection velocities required by the first linac cavity. For this a 2.5-MV, compressed-gas-insulated, shunt-fed Cockcroft-Walton (often called a dynamitron) is used.

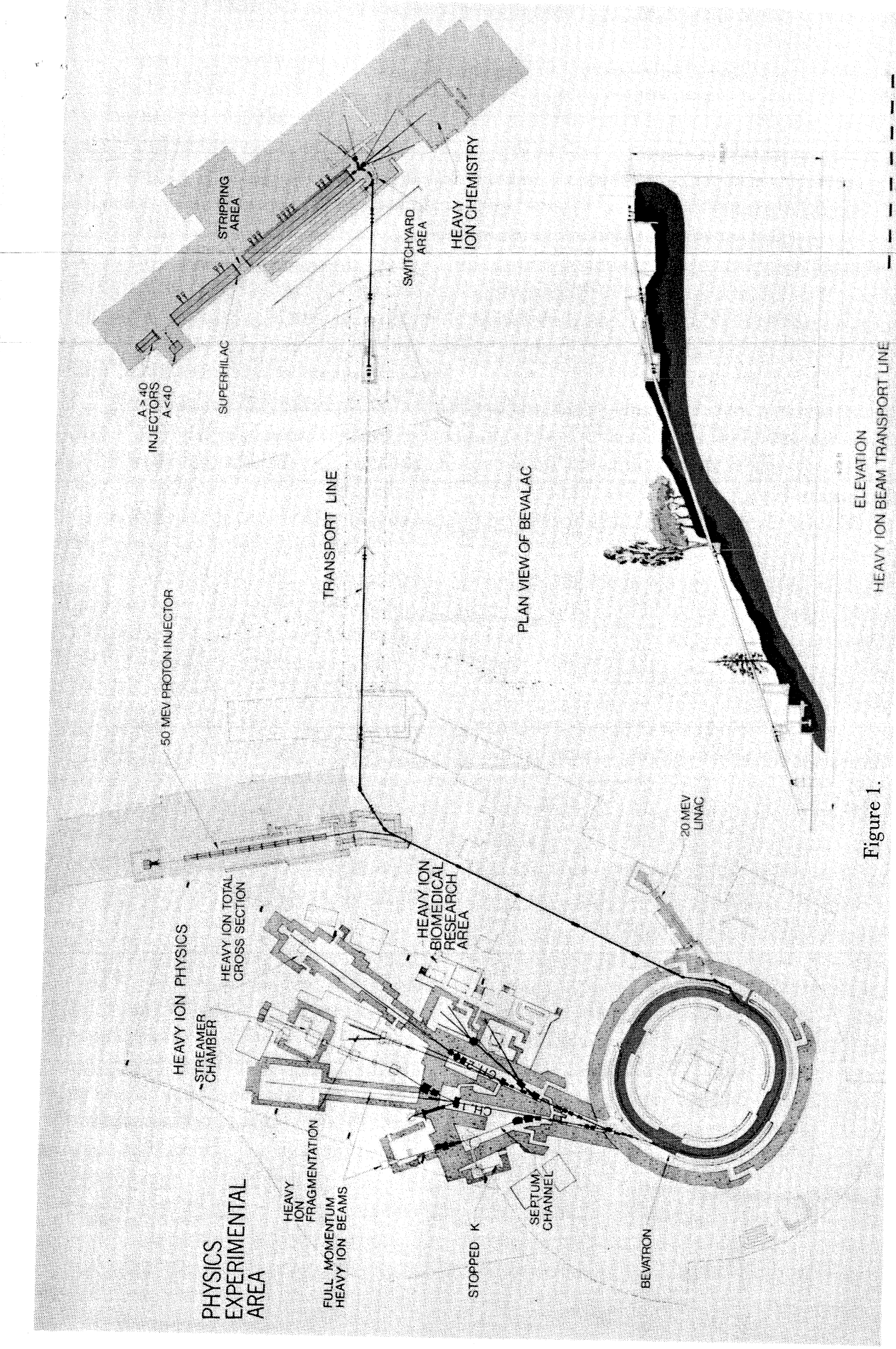


Figure 1.

# Developments at CERN

G. COCCONI

*Organisation Européenne pour la Recherche Nucléaire, Geneva, Switzerland*

At CERN, a group belonging to the Proton Synchrotron Division is preparing a proposal for a two-year study on polarized beam and light-ion acceleration in the PS (the final draft will be ready at the beginning of 1975). Injection into the PS of these particles is becoming compatible with that of ordinary protons because, within a year or so, completion of the new linac will leave free the 50-MeV linac that is now feeding protons into the PS. Another incentive for this project is that at CERN there is the possibility of transferring the particles accelerated in the PS to the intersecting storage rings (ISR) and eventually to the 400-GeV superconducting PS. This enlarges considerably the scope of the experimental program. In Table 1 are given the luminosities at present considered realistic for the PS and the ISR for fully stripped nuclei. No plans have yet been made for the acceleration of heavy ions. If approved soon, the project could lead to usable beams before 1980.

Table 1  
Luminosity of Fully Stripped Nuclei in PS and ISR

Accelerated particle	$\sigma_{\text{int}}$ , cm <sup>2</sup>	PS ( $\leq 28q/e$ GeV)		ISR [equiv. lab $E \leq 2000(q/e)^2/A$ GeV]
		Particles/pulse	Luminosity, cm <sup>-2</sup> sec <sup>-1</sup>	
$p^{\dagger}$	$10^{-25.5}$	$10^{12.5}$	$10^{31}$	$10^{5.5}$
$\bar{p}$	$10^{-25.5}$	$10^{10}$	$10^{27}$	$10^{1.5}$
$\alpha$	$10^{-24.5}$	$10^{9.5}$	$10^{26}$	$10^{1.5}$
$^{16}\text{O}$	$10^{-24}$	$10^9$	$10^{25}$	$10^1$

<sup>†</sup>Present performance.

# Heavy-Ion, $A > 200$ , Acceleration in the AGS

K. PRELEC AND A. VAN STEENBERGEN  
*Brookhaven National Laboratory, Upton, New York 11973*

## ABSTRACT

Acceleration in the AGS of  $\sim 10^9$  heavy ions per sec, with mass number  $A > 200$ , to kinetic energies of  $1 < T_N < 10$  GeV/nucleon is feasible without modification of basic AGS subsystems by using a (surplus) fast cycling synchrotron as a booster ring. This booster is required in order to obtain the fully stripped ion state, since partially stripped ion acceleration in a slow rise-time accelerator is impractical because of extreme vacuum pressure requirements. The fast cycling feature of the booster is essential in reducing transmission losses associated with electron capture or loss during acceleration and is beneficial in increasing the exit beam intensity.

## INTRODUCTION

Stimulated by the results of T.D. Lee's recent theoretical work<sup>1</sup> (in collaboration with G.C. Wick) implying the possible formation of abnormal nuclear states in collisions of very heavy ions,  $A > 200$ , with single-beam primary energies of  $T_N > 1$  GeV/nucleon, a study has been made of Hg-U acceleration in the AGS,<sup>2</sup> of which the results are reported here in condensed form.

In order to delineate directly the maximum energy capability of various accelerators the relationship between a particle's magnetic rigidity and its kinetic energy for various  $\epsilon$  ( $\equiv q/A$ ) ratios is useful (Figure 1). Figure 1 also indicates the relevance of the present study with regard to the eventual capability of the Bevalac (LRL) accelerator, since with a  $B\rho$  value of 23 Tm (Bevatron) a kinetic energy of  $\sim 2$  BeV/nucleon\* could be reached only when using the fully stripped ion state ( $\epsilon = 0.4$  for Hg,  $\epsilon = 0.38$  for U), which is not achievable with the Bevalac heavy-ion injector.

Because of the very active ongoing particle physics program using the 30-BeV proton beam from the AGS, the constraint was adopted that no significant change in any of the AGS subsystems would be acceptable in order to accelerate heavy ions in the AGS. An examination of the simplest accelerator combination, i.e., a Van de Graaff-AGS system, indicated that with a source comprising a 0.1-emA,  $U^{6+}$ , 10-MV single-stage Van de Graaff unit, a beam output from the AGS could be  $10^9$  particles/sec,  $U^{22+}$ ,  $T_N \lesssim 2$  BeV/N; however, even for an  $\epsilon^{-1}$  particle transmission ratio (due to electron capture or loss in the accelerator) a vacuum pressure of  $< 2 \times 10^{-11}$  Torr would be required, in addition to significant complexities of the rf acceleration system, since a frequency "swing" of a factor of  $\sim 40$  would be involved. Alternatives involving a tandem stage as an AGS heavy-ion injector were ruled out for similar reasons. Subsequently, a more detailed study of ion electron capture or

\*Suggested optimum energy before this meeting.

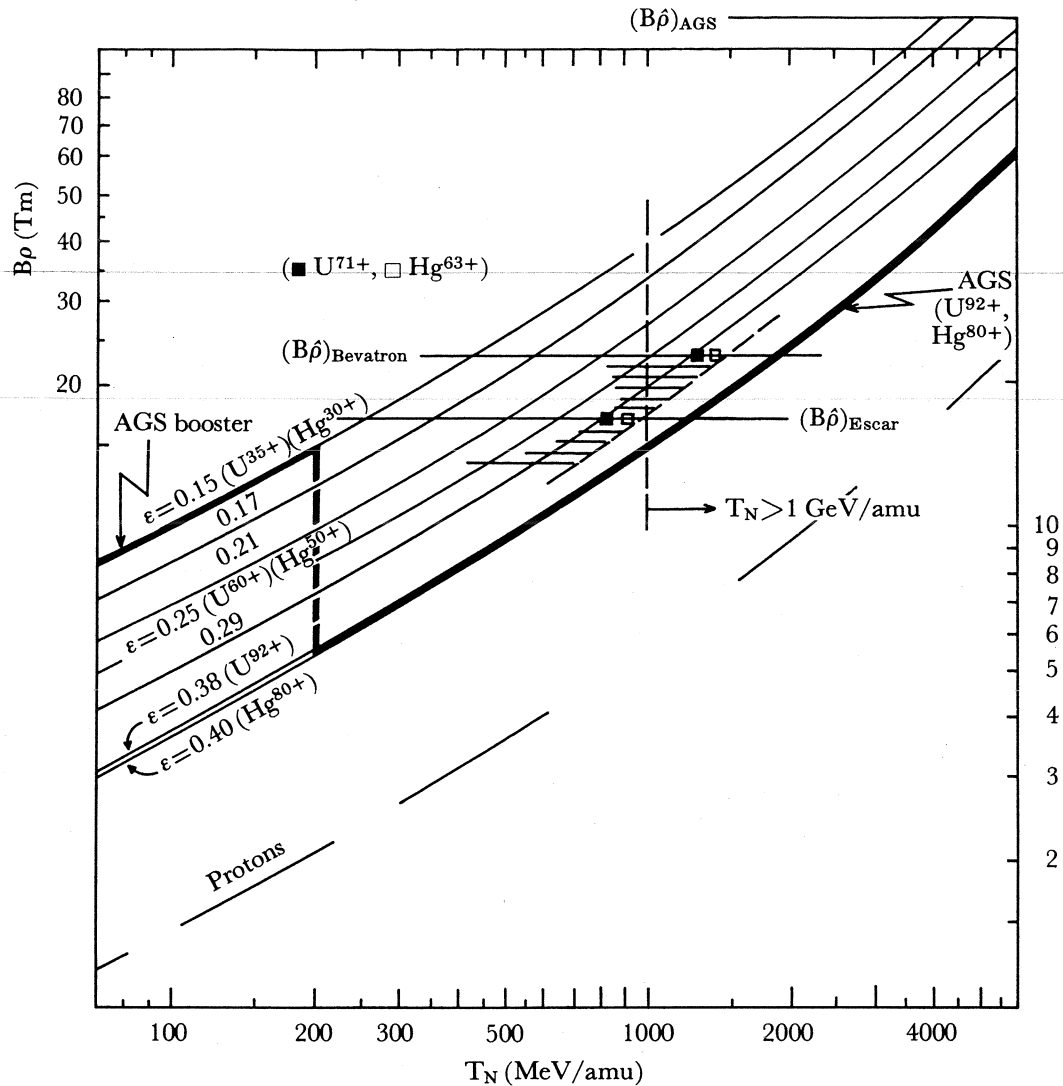


Figure 1. Magnetic rigidity versus particle energy.

electron loss cross sections versus particle energy for various ion charge states led to the following approach for achieving heavy ions,  $A > 200$ ,  $T_N > 2 \text{ GeV}/N$ , intensity  $\sim 10^9$  ions/sec: (a) Use fully stripped ions in the slow rise-time ( $\sim \text{sec}$ ) large  $B\rho$  accelerator, (b) obtain the fully stripped state ion (for U with  $E > 100 \text{ MeV}/N$ ) with a *fast* rise-time booster synchrotron, and (c) use the highest charge state in the booster (commensurate with a reasonable magnitude of the pre-accelerator stage) in order to sustain minimum transmission loss in the booster for a given vacuum pressure. The further justification for this approach will become evident below.

#### PARTICLE LOSS DURING ACCELERATION

Ion collisions with the rest gas molecules within the accelerator vacuum envelope lead to capture or loss of one or more electrons and consequently to loss of orbit stability in the accelerator and therefore result in particle loss during the acceleration process. In simplified form:

$$dN_{\text{charge exchange}} \propto N\sigma(\beta)\beta c dt n_g$$

resulting in

$$N/N_0 = \exp(-10^{27} P_{\text{vac}} \int \sigma \cdot \beta dt)$$

where  $\sigma = \sigma_{\text{capture}} + \sigma_{\text{loss}}$ , total charge-exchange cross section.

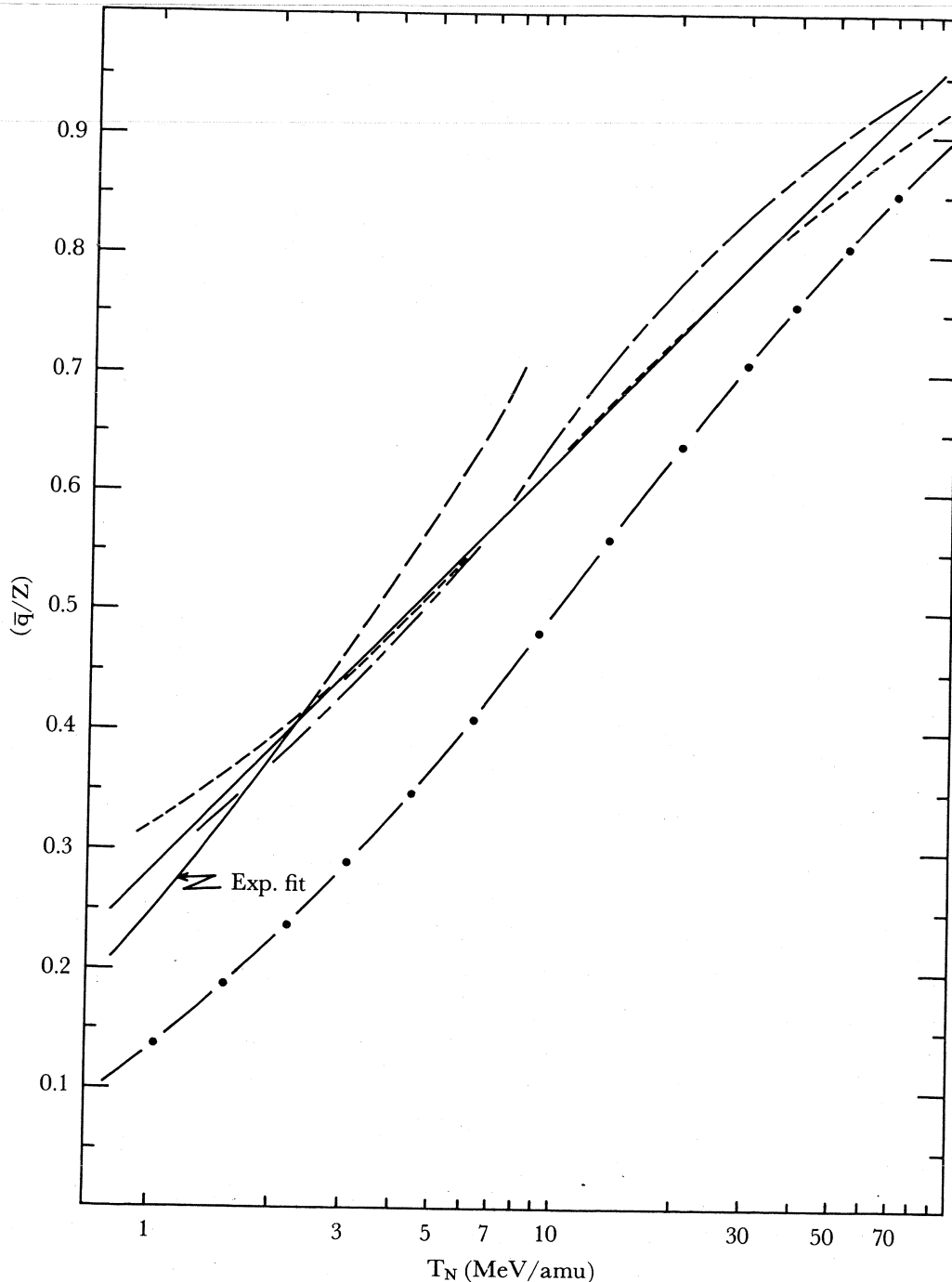


Figure 2. Extrapolation of  $(\bar{q}/Z)$  versus  $T_N$  for U and a gaseous stripper ( $N_2$ ). *Exp. fit*:  $(\bar{q}/Z) = 0.48(\beta/\alpha)Z^{-0.55}$ , good fit to experimental data with  $T_N < 3$  MeV/amu (ref. 7); —:  $(\bar{q}/Z) = \log(v/0.9Z^{0.4})/(\log 7)Z^{0.3}$  (ref. 5); -·-:  $(\bar{q}/Z) = 1 - C(0.71Z^a)^{\beta/\alpha}$  (ref. 6) with  $C = 1.1$ ,  $a = 0.67$ ; -·-·-: same, but with  $C = 1.007$ ,  $a = 0.064$ ; -·-·-·-: same, but with  $C = 0.87$ ,  $a = 0.066$ .

Table 1

## Pre-accelerator-Booster-AGS System

Specul sour						
SOURCE						
equiv. volt. source	MV ion	10.8 238U	10.8 238U	10.8 238U	20 238U	4 238U
	$q$	11+	11+	11+	11+	11+
	emA	1	1	1	1	—
post strip intensity emit.	$q$ eA $\mu$ rad-m	30+ $0.4 \times 10^{-3}$ $15\pi$	30+ $0.4 \times 10^{-3}$ $15\pi$	30+ $0.4 \times 10^{-3}$ $15\pi$	38+ $0.52 \times 10^{-3}$ $11.2\pi$	20+ $0.27 \times 10^{-3}$ $25\pi$
BOOSTER						
structure		“old CEA”	“old CEA”	“new CEA”	“new CEA”	“old CEA”
$T_{\text{inj}}$	MeV/amu	0.50	0.50	0.50	0.925	0.184
$\beta_{\text{inj}}$		0.0325	0.0325	0.0325	0.044	0.020
$B_{\text{inj}}$	gauss	306	306	459	494	279
$n_{\text{inj}}$	turns	3	3	3	3	2
$N_{\text{capt.}}$	particles/pulse	$(4.6 \times 10^9)$	$(4.6 \times 10^9)$	$(3.4 \times 10^9)$	$(2.5 \times 10^9)$	$(2.5 \times 10^9)$
$N_{\text{sp. ch.}}$	particles/pulse	$2.1 \times 10^9$	$2.1 \times 10^9$	$2.1 \times 10^9$	$1.8 \times 10^9$	$1.5 \times 10^9$
rep. rate	Hz	15	15	30	30	15
$V_{\text{max rf}}$	kV	236.4	236.4	205.0	235.8	236.4
rf	MHz	1.03–13.56	1.03–19.71	1.41–18.57	1.92–24.62	0.63–13.56
harmonic	$h$	24	24	24	24	24
accel. range	$\omega t$	$\pi/8$ –1.75	$\pi/8$ – $\pi$	$\pi/8$ – $\pi$	$\pi/8$ – $\pi$	$\pi/8$ –2.5
$*P_{\text{vac}} \leq$	Torr	$1 \times 10^{-9}$	$8 \times 10^{-10}$	$1 \times 10^{-9}$	$3.8 \times 10^{-9}$	$5 \times 10^{-10}$
$T_{\text{eject.}}$	MeV/amu	100	260	100	200	100
$B_{\text{max}}$	tesla	(0.759)	0.759	0.669	0.765	(0.759)
$*N_{\text{out}}$	particles/cycle	$8 \times 10^8$	$8 \times 10^8$	$8 \times 10^8$	$7 \times 10^8$	$5 \times 10^8$
post strip. inten.	$q$ particles/cycle	92+	92+	92+	92+	92+
emit.	$\mu$ rad-m	$4.8 \times 10^8$	$6.4 \times 10^8$	$4.8 \times 10^8$	$5.6 \times 10^8$	$3 \times 10^8$
AGS						
$\beta_{\text{inj}}$		0.428	0.622	0.428	0.566	0.429
$B_{\text{inj}}$	gauss	449	752	449	650	449
$n_{\text{inj}}$	turns	1	1	1	1	—
	cycles	4	4	6	6	4
$N_{\text{capt.}}$	particles/pulse	$1.5 \times 10^9$	$4.1 \times 10^9$	$2.3 \times 10^9$	$2.7 \times 10^9$	$0.9 \times 10^9$
$N_{\text{sp. ch.}}$	particles/pulse	$1.2 \times 10^{11}$	$3.9 \times 10^{11}$	$1.2 \times 10^{11}$	$2.8 \times 10^{11}$	$1.2 \times 10^{11}$
rep. rate	cps	1	1.25	1	1.25	1
rf	MHz	1.9–2.5	—	1.9–2.5	—	1.9–2.5
$V_{\text{max rf}}$	kV	~75	—	~75	—	~75
rf	MHz	2.5–4.2	2.8–4.2	2.5–4.2	2.5–4.2	2.5–4.2
$V_{\text{max rf}}$	kV	avail.	avail.	avail.	avail.	avail.
harmonic	$h$	12	12	12	12	12
$**P_{\text{vac}} \leq$	Torr	$1.3 \times 10^{-8}$	$1 \times 10^{-7}$	$1.2 \times 10^{-8}$	$0.7 \times 10^{-7}$	$1.3 \times 10^{-8}$
$N_{\text{out}}$	particles/pulse	$1.3 \times 10^9$	$3.7 \times 10^9$	$2.1 \times 10^9$	$2.4 \times 10^9$	$8 \times 10^8$
	particles/sec	$1.3 \times 10^9$	$4.6 \times 10^9$	$2.1 \times 10^9$	$3 \times 10^9$	$8 \times 10^8$
$**T_{\text{out}}$	GeV/amu	2	2	2	2	2

\*In booster,  $N/N_0 = 1/e$ ; in AGS,  $N/N_0 = 0.9$ .\*\*Maximum value in AGS  $\simeq 12$  GeV/amu, at lower cycling rate.

*Pre-accelerator:* Ion source,  $U$ ,  $q=11+$ , 1 emA, 600 kV Cockcroft-Walton structure;  $\simeq 10$ -m section Sloan-Lawrence or helix structure, exit energy  $\simeq 0.75$  MeV/amu.

*Booster:* Reduced radius ( $\simeq 20$  m rather than 36 m), "CEA" fast cycling (30 Hz) synchrotron. Frequency range of system 1.7 to 24 MHz,  $\hat{V}_{rf} \simeq 240$  kV/turn.  $P_{vac} \simeq 4 \times 10^{-9}$  Torr. Ion charge state  $\simeq 35$ . Exit energy  $\sim 200$  MeV/amu.

*AGS:* Rf requirements within range of existing system.  $P_{vac} \simeq 10^{-7}$  Torr ( $\simeq$  present value). Ion charge state 92. Extracted beam energy 1 to 10 GeV/amu. Intensity  $\simeq 10^9$  particles/sec.

## CONCLUSIONS

Although a number of facets of the acceleration of very heavy ions,  $A \geq 200$ , to very high energy in the AGS have not been explored here, such as shielding, longitudinal parameters of the heavy-ion beam (the exit beam momentum spread will be comparable with present proton-beam momentum spread), possibility of multiple charge-state acceleration, etc., a basic set of parameters for the acceleration of ions,  $A \geq 200$ , has been arrived at, even though the limited input of electron-capture and electron-loss cross section of very energetic heavy ions in the accelerator rest gas makes it difficult to determine with precision the accelerator transmission efficiency or accelerator vacuum pressure requirement. If heavy ions,  $A \geq 200$ , with kinetic energies  $\geq 2$  BeV/nucleon are required for experimental verification of possible formation of abnormal nuclear states, or other phenomena requiring the simultaneous impact of many energetic nuclei, the fast rise-time booster-AGS combinations, as indicated here, would constitute a unique facility for heavy-ion acceleration to very high energies, without compromising the AGS 30-BeV proton physics facility.

## REFERENCES

1. T.D. LEE, *Abnormal Nuclear States and Vacuum Excitations*, CO-2271-27, Jan. 1974.
2. K. PRELEC AND A. VAN STEENBERGEN, *Search for the "Abnormal Nuclear State" - Uranium Ion Acceleration in the AGS*, BNL Accelerator Dept. Informal Report, BNL 19407, Aug. 1974.
3. H.D. BETZ AND CH. SCHMELZER, UNILAC Bericht 1-67, Heidelberg, 1967.
4. K. PRELEC, PPA Tech. Note A-507, 1969.
5. I.S. DMITRIEV AND V.S. NIKOLAEV, *Sov. Phys. JETP* 20, 409 (1965).
6. CH. SCHMELZER, Special problems in heavy ion acceleration, in *Linear Accelerators*, p. 1036, P.M. Lapostolle and A.L. Septier, Editors, North-Holland, Amsterdam, 1970.
7. H.D. BETZ, *Rev. Mod. Phys.* 44, 465 (1972).
8. L.M. WELSH ET AL., *Phys. Rev.* 158, 85 (1967).

# The PPA as a Relativistic Heavy-Ion Accelerator

MILTON G. WHITE  
*Princeton University, Princeton, New Jersey 08540*

Before I speak about the PPA I would like to urge everyone who is as excited as I am about the possible significance of relativistic heavy-ion research to support the Bevalac, the only living example of an accelerator capable of producing very heavy ions with 1 to 2 BeV/ $N$  energy. With moderate expenditures it should be capable of accelerating uranium to an energy sufficient to test the imaginative suggestion by T.D. Lee that nuclei with sufficient density will collapse to a totally new state of matter. Such nuclei, if found, would have a profound effect on the development of fundamental physics and possibly even have areas of practical application.

The various speakers at this workshop reiterated that our present theoretical understanding of nuclear matter is incapable of predicting with certainty what will happen when two heavy nuclei collide with relativistic center-of-mass energy. Thus even if abnormal states, in T.D. Lee's sense, are never found, experiments to look for them are practically certain to reveal much of great value about nuclear matter. Most members of this workshop urged that abnormal states, and Greiner's shock waves, be looked for with whatever ions become available and at energies now, or soon to be, in hand.

Having made this plea for support of the only operating accelerator capable of producing abnormal states of nuclear matter, I will remind you of another existing accelerator, which, before being closed down for lack of funds, also accelerated ions of N, Ne, and Ar to energies close to the presumed optimum of about 500 MeV/ $N$  in the center-of-mass. The Princeton Particle Accelerator (PPA) managed to exist for one year after government funding ceased, with the help of private funds, largely from an anonymous source and the Fannie E. Ripple Foundation. We not only ex-

Table 1  
Acceleration of Heavy Ions in the Princeton Particle Accelerator  
(as of April 1972)

Charge state from ion source	Injection charge state after stripping	Energy/nucleon, MeV	Actual current, particles/sec at $4 \times 10^{-8}$ Torr	Predicted* current, particles/sec at $10^{-9}$ Torr
N <sup>2+</sup>	N <sup>5+</sup>	279	$4 \times 10^7$	$1.6 \times 10^9$
N <sup>2+</sup>	N <sup>6+</sup>	530	$10^7$	$10^9$
Ne <sup>2+</sup>	Ne <sup>6+</sup>	425	$10^5$	$\sim 10^7$
Ar <sup>4+</sup>	Ar <sup>12+</sup>	293	10	$\sim 10^4$

\*Limited only by current from PIG ion source up to space-charge limit of the PPA. Figures quoted are for present ion source. See text.

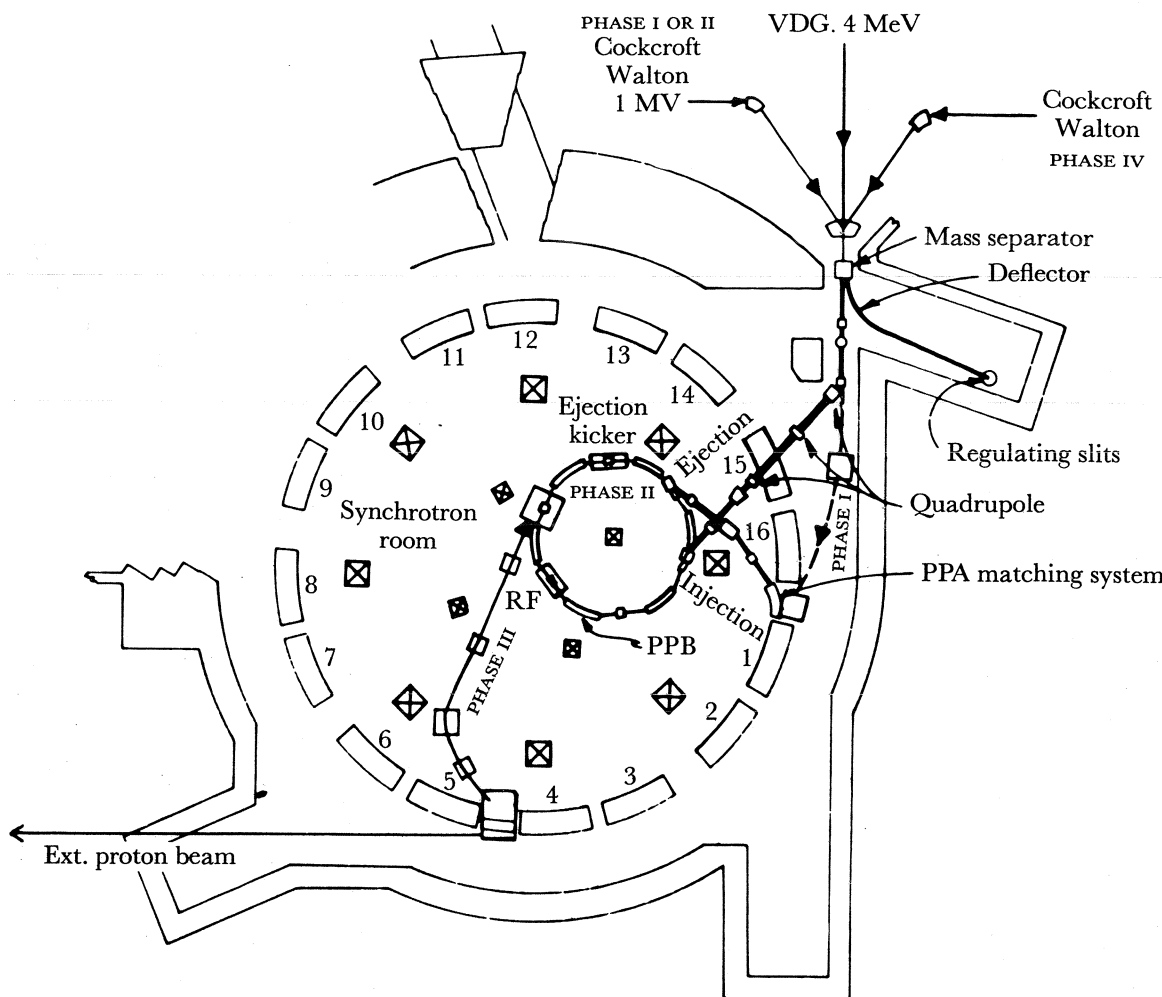


Figure 1. Proposed booster-injector/heavy-ion storage ring for the PPA.

isted but succeeded in converting<sup>1</sup> our 3-BeV proton synchrotron to the acceleration of N, Ne, and Ar.<sup>2</sup> The energies and beam currents shown in Table 1 were ion source limited and with a better source could all run as high as  $2 \times 10^{12}$  particles/sec, the space-charge limit. At a pressure of  $10^{-9}$  Torr the PPA, because of its 20-Hz pulse rate (and hence  $\frac{1}{40}$ -sec rise-time) should be capable of accelerating *any* ion in *any* charge state to the maximum magnetic field without significant beam loss due to charge changing collisions with the residual gas. This gives the PPA a substantial advantage over all slow cycling synchrotrons since ion source and stripping problems become much simpler. For this reason PPA currents should exceed those from slow machines by nearly a factor of 100.

Before closing down on April 9, 1972, the beams of N and Ne were used for a number of experiments, largely in the area of cancer radiation therapy, since that was the chief interest of our supporting foundation. Some physics experiments were also carried out. The accelerator is still completely intact and fully operable, though no doubt some electronic components have deteriorated and would require repairs were we to operate again. Most of the PPA buildings, comprising about 100,000

square feet, are temporarily occupied by various rent paying activities. The space can be recovered on suitable notice.

The PPA interest in heavy ions goes back to June 1968 when a proposal<sup>3</sup> for a high current booster synchrotron was submitted to the AEC. The booster proposed was a fast cycling synchrotron (75-MeV proton energy) which was also designed to accelerate heavy ions to sufficient energy for stripping to moderately high charge states. Since the PPA rise-time is only  $\frac{1}{40}$  second, a  $10^{-9}$ -Torr vacuum in the main ring would be sufficient for efficient acceleration of even partially stripped ions. To achieve the maximum energy possible obviously requires complete stripping. If carbon stripping foils are used it is probable that an energy of about 100 MeV/ $N$  would be necessary to fully strip uranium. The plan we proposed was to use the booster, on successive cycles, as an accelerator and as a temporary storage ring in the following manner (see Figure 1). Uranium ions, accelerated by a 750-keV Cockcroft-Walton, enter the booster as  $U^{7+}$ . After acceleration to 0.65 MeV/ $N$  the ions are extracted, stripped to  $U^{30+}$ , and injected into the PPA, which accelerates them to 80 MeV/ $N$ . After extraction and stripping, one hopes, to  $U^{92+}$ , the ions are next stored in the booster, now at its top field, or possibly in a separate dc storage ring where they are held until the PPA field has been recycled to a low value, whereupon the ions are extracted from the storage ring, reinjected into the PPA, and given the final acceleration to 800 MeV/ $N$ . The current attainable was estimated at  $1 \times 10^1$  particles/sec from existing ion sources, but the PPA space-charge limit was calculated to be around  $1 \times 10^{12}$  particles/sec. The cost in 1968 dollars was estimated at about 5 million. Needless to say our proposal received little support in view of the changing climate for funding of accelerators. Unfortunately we were regarded as competing with elementary particle research; therefore, no support came from the community.

In 1973 a group of nuclear physicists from Rutgers, Bell Telephone Laboratories, University of Pennsylvania, and Princeton looked into the possibility of purchasing a 20 to 25-MV, heavy-ion, tandem electrostatic accelerator for joint use by the four institutions as a nuclear physics research tool. When it was recognized that to reach 10-MeV/ $N$  uranium ions would definitely require a booster accelerator, it was natural to consider the PPA as a possibility, even though it was capable of going to far higher energy. A fairly detailed study was made of the PPA as a high quality medium energy, heavy-ion accelerator. Our conclusions were that with care an energy spread of  $\Delta E/E = 10^{-4}$  or better could be achieved, and beam currents, using present-day ion sources, of  $10^{10}$  to  $10^{11}$  particles/sec for most ions appeared well within reach. These properties are thus quite suitable for most proposed low energy heavy-ion nuclear research. In a separate study we also examined the feasibility of using the 20 to 25-MeV tandem to reach the highest possible uranium energy. In brief, we found that starting with  $U^-$  at ground potential and stripping three times before injection we could reach  $U^{55+}$  with an attenuation of  $5 \times 10^{-3}$ . Alternatively starting with  $U^{6+}$  in the 20-MV terminal and stripping three times also yields  $U^{53+}$  with an attenuation of  $5 \times 10^{-3}$ . The final PPA  $U^{54+}$  energy is about 510 MeV/ $N$ . The estimated intensities are about  $6 \times 10^7$  particles/sec/ $\mu$ A of  $U^-$  and  $1 \times 10^1$  particles/sec/mA of  $U^{6+}$  in the two cases, respectively. To reach 800 MeV/ $N$  for

uranium would require complete stripping to  $U^{92+}$ . To accomplish this requires either much better ion sources, much higher tandem voltage, or possibly a double acceleration in the PPA as proposed by us earlier. A storage ring, as described above, seems entirely feasible as a way to use the PPA in a two-step process.

In closing I would like to express my hope that the funding agencies will again demonstrate their willingness to support pioneering research even at a time when economic, societal, and political pressures are all in the direction of "relevance" to today's problems and towards immediate payoff. It could be that relativistic heavy-ion research will be relevant to tomorrow's problems.

#### REFERENCES

1. M.G. WHITE, M. ISAILA, K. PRELEC, AND H. ALLEN, *Science* **174**, 1121-3 (1971).
2. M.V. ISAILA, W. SCHIMMERLING, K.G. VOSBURGH, M.G. WHITE, R.C. FILZ, AND P.J. McNULTY, *Science* **177**, 424-5 (1972).
3. M. ISAILA, J. KIRCHGESSNER, K. PRELEC, F.C. SHOEMAKER, AND M.G. WHITE, *Particle Accelerators* **1**, 79-92 (1970).



## PARTICIPANTS

DR. MICHEL BARANGER  
Massachusetts Institute of Technology

DR. MARCEL BARDON  
National Science Foundation

DR. GORDON BAYM  
University of Illinois at Urbana-Champaign

DR. HENRY G. BLOSSER  
Michigan State University

DR. ARNOLD BODMER  
Argonne National Laboratory

DR. D. ALLAN BROMLEY  
Yale University

DR. GERALD E. BROWN  
Niels Bohr Institute

DR. OWEN CHAMBERLAIN  
University of California

DR. GEORGE CHAPLINE  
Lawrence Livermore Laboratory

DR. CHELLIS CHASMAN  
Brookhaven National Laboratory

DR. GEOFFREY F. CHEW  
University of California at Berkeley

DR. GUISEPPE COCCONI  
European Organization for Nuclear Research (CERN)

DR. GORDON T. DANBY  
Brookhaven National Laboratory

DR. HERMAN FESHBACH  
Massachusetts Institute of Technology

DR. ALFRED GOLDHABER  
State University of New York at Stony Brook

DR. MAURICE GOLDHABER  
Brookhaven National Laboratory

DR. WALTER GREINER  
Institut für Theoretische Physik der Goethe Universität

DR. HERMAN A. GRUNDER  
University of California at Berkeley

DR. LOUIS N. HAND  
Cornell University

DR. HARRY H. HECKMAN  
University of California at Berkeley

DR. ARTHUR K. KERMAN  
Massachusetts Institute of Technology

DR. LEON M. LEDERMAN  
Columbia University

DR. BENJAMIN W. LEE  
Fermi National Accelerator Laboratory

DR. TSUNG DAO LEE  
Columbia University

DR. ALFRED W. MASCHKE  
Brookhaven National Laboratory

DR. L. DUDLEY MILLER  
Massachusetts Institute of Technology

DR. JOHN W. NEGELE  
Massachusetts Institute of Technology

DR. LAWRENCE PRICE  
Columbia University

DR. P. BUFORD PRICE  
Lawrence Berkeley Laboratory

DR. LAZARUS G. RATNER  
Argonne National Laboratory

DR. R. RONALD RAU  
Brookhaven National Laboratory

DR. WILLIAM RODNEY  
National Science Foundation

DR. MALVIN RUDERMAN  
Columbia University

DR. RAYMOND SAWYER  
University of California at Santa Barbara

DR. GERTRUDE SCHARFF-Goldhaber  
Brookhaven National Laboratory

DR. W. SCHEID  
Institut für Theoretische Physik der Goethe Universität

DR. JOHN P. SCHIFFER  
Argonne National Laboratory

DR. LEE SCHROEDER  
Lawrence Berkeley Laboratory

DR. ROBERT SERBER  
Columbia University

DR. FRANK C. SHOEMAKER  
Princeton University

DR. PHILIP J. SIEMENS  
Niels Bohr Institute

DR. ANTHONY TURKEVICH  
University of Chicago

DR. ARIE VAN STEENBERGEN  
Brookhaven National Laboratory

DR. JAMES P. VARY  
Brookhaven National Laboratory

DR. GEORGE H. VINEYARD  
Brookhaven National Laboratory

DR. MORTON S. WEISS  
Lawrence Livermore Laboratory

DR. JOSEPH WENESER  
Brookhaven National Laboratory

DR. MILTON G. WHITE  
Princeton University

DR. GIAN-CARLO WICK  
Columbia University

DR. CHIEN SHIUNG WU  
Columbia University

